SISSA, International School for Advanced

Studies

PhD course in Functional and Structural Genomics

Academic Year 2011/2012

Reprogramming fibroblasts to Neural-Stem-like cells by structured overexpression of pallial patterning genes

THESIS SUBMITTED FOR THE DEGREE OF "DOCTOR PHILOSOPHIAE"

ACADEMIC YEAR 2011/2012

Candidate:
Marilena Raciti

Supervisor:
Prof. Antonello Mallamaci

To my beloved granny Sarina

I, Marilena Raciti, declare that the experimental data reported in this thesis are original and generated by me myself during my PhD work at SISSA. The experimental data employed for the compilation of this thesis have been supplemented with additional data kindly provided by the colleagues listed below:

- Marilena Granzotto, FACS analysis (IRCCS Burlo, Institute for Maternal and Child Health, Laboratory of Immunology, Trieste, Italy)
- Giada Cellot and Enrico Cherubini, electrophysiological recordings(SISSA-ISAS, Trieste, Italy)
- Mihn Do Duc, transplantation(SISSA-ISAS, Trieste, Italy)
- Cristina Fimiani, RT-PCR profiling(SISSA-ISAS, Trieste, Italy).

Index

ABSTRACT

In this study, we assayed the capability of four genes implicated in embryonic specification of the cortico-cerebral field, *Foxg1*, *Pax6*, *Emx2* and *Lhx2*, to reprogramm mouse embryonic fibroblasts toward neural identities. Lentivirus-mediated, TetON-dependent overexpression of Pax6 and Foxg1 transgenes specifically activated the neural stem cell (NSC) reporter Sox1-EGFP in a substantial fraction of engineered cells. The efficiency of this process was enhanced up to ten times by simultaneous inactivation of Trp53 and co-administration of a specific drug mix inhibiting HDACs, H3K27-HMTase and H3K4m2-demethylase. Remarkably, a fraction of the reprogrammed population expressed other NSC markers and retained its new identity, even upon transgenes switching off. When transferred into a pro-differentiative environment, Pax6/Foxg1-overexpressing cells activated the neuronal marker Tau-EGFP. Frequency of Tau-EGFP cells was almost doubled upon delayed delivery of Emx2 and Lhx2 transgenes. A further improvement of the neuron-like cells output was achieved by tonic inhibition of BMP and TGFb pathways. These Tau-EGFP cells showed a negative resting potential and displayed active electric responses, following injection of depolarizing currents.

CHAPTER 1. INTRODUCTION : CENTRAL NERVOUS SYSTEM PATTERNING

During early embryogenesis, the ectoderm is induced to form the nervous system and the epidermis. A portion of the dorsal ectoderm is specified to become neural ectoderm, and its cells become distinguishable by their columnar appearance. This region of the embryo is called the neural plate. The process by which this tissue forms a neural tube (fig.1), the rudiment of the central nervous system, is called neurulation, and an embryo undergoing such changes is called a neurula. Rostral and caudal neural tube will form the brain and the spinal cord, respectively.

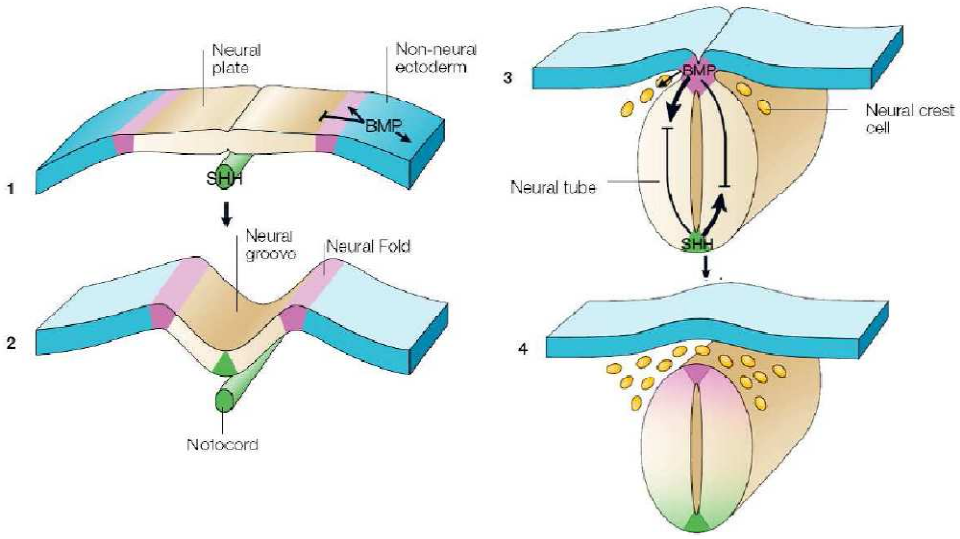

Figure 1. Schematic view of the neural tube formation and the signaling sources involved.
1) opened neural plate; 2) neural grove formation; 3) closed the neural tube; 4) delaminating neuralcrests.

1.1. Neurulation and primaryRostro/Caudal Patterning

The embryonic precursor of the brain is a planar sheet of pseudostratified neuroepithelium produced during gastrulation, known as the neural plate. The neural plate is induced by the underlying mesoderm. The neuroepithelial cells acquire distinct properties depending on the positions within the CNS primordium to yield divergent neuronal cells types at specific

locations. The neural plate is subdivided into molecularly distinct domains with characteristic locations.

Primary determination of the neural plate and of its main subdivisions is promoted to large extent by a wide set of factors, released by the underlying mesoderm. For example, the inhibition of ectodermal BMP signaling promoted by Cerberus, Chordin, Noggin, Follistatin allows general neuroectoderm to revert to its neural ground state. Inhibition of Wnt8a signalling and activation of Fgf signalling contribute to neural induction as well. This model, developed originally for Xenopus laevis, seems to be basically valid for all vertebrates(fig.2).

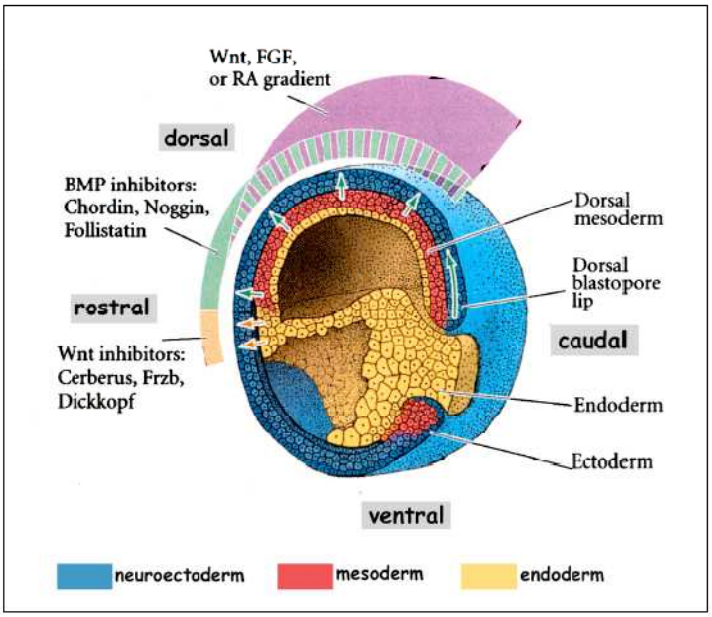

Figure 2. Model of determination of the neural plate in Xenopus laevis(adapted from Gilbert, Developmental Biology).

As mentioned above, the process of neurulation converts the neural plate into the neural tube (E7.5 in mouse).

The early mammalian neural tube is a straight structure. However, even before the posterior portion of the tube has formed, the most anterior portion of the tube is undergoing drammatic changes. In this region, a series of ring-like constrictions mark the approximate boundaries between the primordia of the major brain regions (or primary vesicles) **(Fig.3)**: forebrain (prosencephalon), midbrain (mesencephalon), and hindbrain (rhombencephalon).

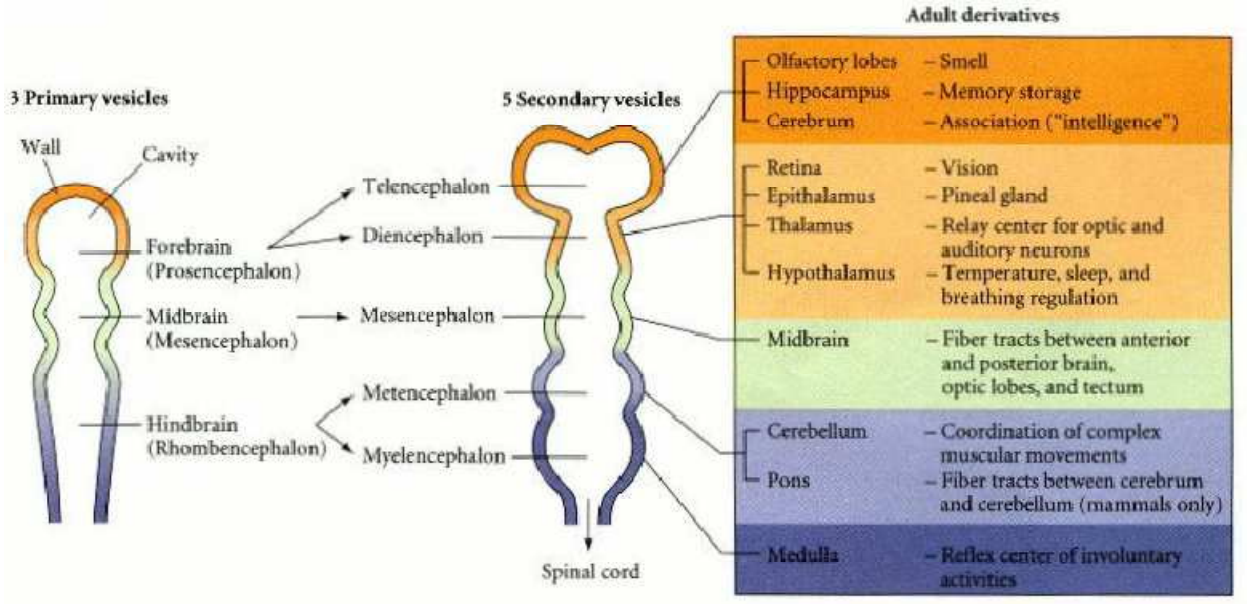

Fig. 3.Early human brain development. Left: primary brain vescicles. **Right**: adult derivative formed by the walls and cavities of the brain(adapted from Gilbert, Developmental Biology).

The prosencephalon becomes subdivided into the anterior telencephalon and the more caudal diencephalon**(fig.3).**As a result of early R-C and D-V patterning events , the dorsal telencephalon (the pallium) will give rise to the archicortex (subiculum, hippocampus and dentate gyrus), the paleocortex (olfactory piriform cortex and enthorinal cortex) and the neocortex**(fig.4)**. The ventral telencephalon (or subpallium) is further subdivided into two main domains, called basal ganglia: the more ventrally located is the medial ganglionic eminence (MGE), precursors of the globus pallidum, the more dorsal is the lateral ganglionic eminence (LGE), which generates the striatum. A third eminence called caudal ganglionic eminence (CGE) supplies for the amigdala **(Fig. 4).**

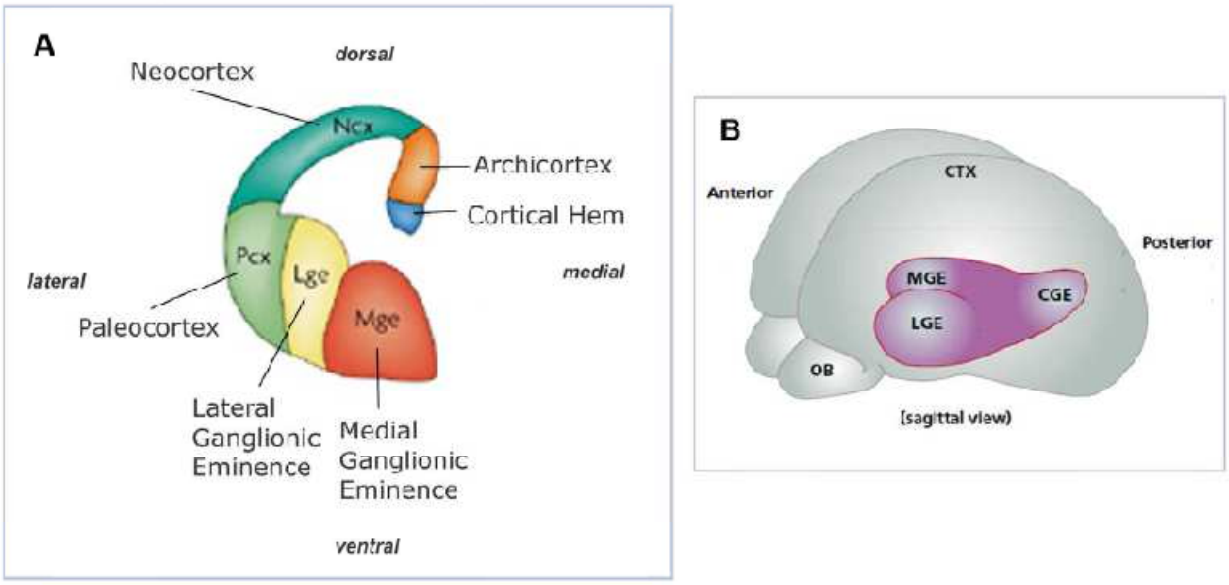

Figure 4. (A) Schematic view of a coronal section through the developing mousetelencephalic vesicle at E12. (B) Sagittal view of the embryonic vertebrate telencephalon as a transparent structure to reveal the ganglionic eminences CGE, caudal ganglionic eminence; CTX, cortex; LGE, lateral ganglionic eminence; MGE, medial ganglionic eminence; OB, olfactory bulb. Images modified from Molyneaux, Nature Reviews Neuroscience 8, 427-437 (June 2007) | doi:10.1038/nrn2151 **(A)** and Corbin,Nat Neurosci. 2001 Nov;4 Suppl:1177-82**(B).**

The diencephalon will form the thalamic and hypothalamic brain regions that receive neural inputs from a variety of structures, including the retina. Indeed, the retina itself is a derivative of the diencephalon. The mesencephalon does not become subdivided, and its lumen becomes the cerebral aqueduct. The rhombencephalon becomes subdivided into a posterior myelencephalon and a more anterior metencephalon **(fig.3).**

1.2.Anterior-Posterior Patterning in the Neural Tube: organizers, transcription factors and small molecules

The first and most evident process occurring in the mouse developing nervoussystem from E8.5 is the regionalization along the antero-posterior axis (A/P). By E10.0 forebrain, midbrain, hindbrain and spinal cord domains are formed. The patterning of this region is associated with precise antero-posterior expression domains or gradients of several regulatory genes coding for transcription factors.

The regionalization process bases on the activity of primary and secondary “organizers”. The early patterning of anterior and posterior neural tissues is mediated troughsignals released by the primitive node or organizer, known as Hensen’s node in chick, and Spemnann organizer in frog. In general, the so called neural-plate organizers are signaling center located in different positions and established to maintain and further refine positional cell identities along the A/P axis of the neural plate [1]. They produce signals that influence cellular fate, histogenic organization and growth of adjacent tissue in a position-specific manner.

Patterning starts when markers expressed throughout the early neural plateultimately become restricted to anterior domains of the central nervous system andmolecules, including the Wnts, fibroblast growth factors (FGFs) and retinoids (RA), startto function at this stage of development to induce posterior character in the neural plate[2].

The early R-C patterning of the anterior neural tissue (also known as “anteriorneural induction”) starts at E7 and is mediated by antagonistic signals coming from 2 important primary organizers: the primitive node(Hensen’s node in the chicken) and the anterior visceral endoderm (AVE), required for neural induction and maintenance[3].

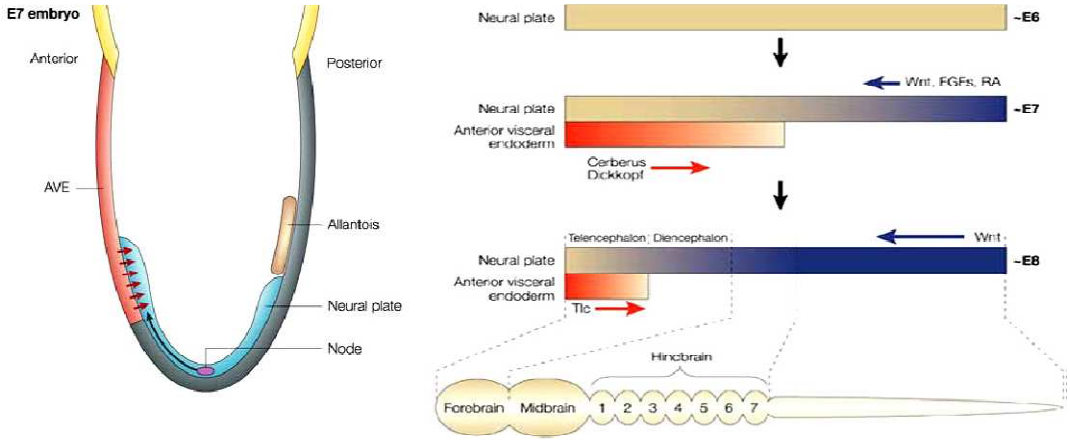

Figure7.Anterior- posterior patterning of the telencephalon, neural induction.

Signals that come from the node establish gross anterior pattern (black arrow). The anterior visceral endoderm (AVE), together with the early node, acts to induce and/or maintain anterior neural character. The AVE is located beneath the future neural plate and expresses molecules, such as cerberus and dickkopf (red arrows), that inhibit factors that would otherwise act to posteriorize the neural plate (Wnts, FGF, RA).(Adapted from Rallu et al.,Nature Reviews Neuroscience 3, 943-951 (December 2002) | doi:10.1038/nrn989).

The AVE is an extra-embryonictissue that underlies the neural plate and secrete antagonists of Wnt factors, fibroblast growth factor (Fgfs) family members as well as retinoicacid [4,5] (**fig.7**). Among them, major roles are played by Cerberus and Dickkopf,that act to maintain and stabilize the anterior neural plate character[6] **(**See **Fig. 8).**

As a consequence of the Wnt signalling, two different domains are defined alongthe anteroposterior axis by the expression of two homeobox genes: *Otx2* and *Gbx2***(fig.8A).**TheOtx-expressing region, rostrally located, will give rise to the forebrain and midbrain,whereas the Gbx2-expressing region, at caudal position, will develop into hindbrain andspinal cord. The boundary between them corresponds anatomically to the isthmus, anarrowing of the neural tube at the border between mesencephalon and metencephalon.

Canonical Wnt signaling represses *Otx2* expression, whereas induces *Gbx2* **(Fig. 8A).** Wnts induce also the expression of other two genes, *Irx3* and *Six3,* confining *Six3* to the anteriormost neural territory and promoting posterior expression of *Irx3,* at levelscaudal to the presumptive zona limitans intrathalamica (ZLI), subsequently placed between thalamus and prethalamus. Upon anterior neural induction, two sources of Fgf molecules are established at the borders of the anterior neural field **(fig.8).**The ANB activity is at least partly carried by the secreted frizzled-related proteins (sFRP), such us TLc, acting as a Wnt antagonist. This suggested a general model, in which the default forebrain identity is posterior (diencephalic) and anterior telencephalic identity is achieved through antagonization of Wnt signaling by the AVE and ANR patterning centers.

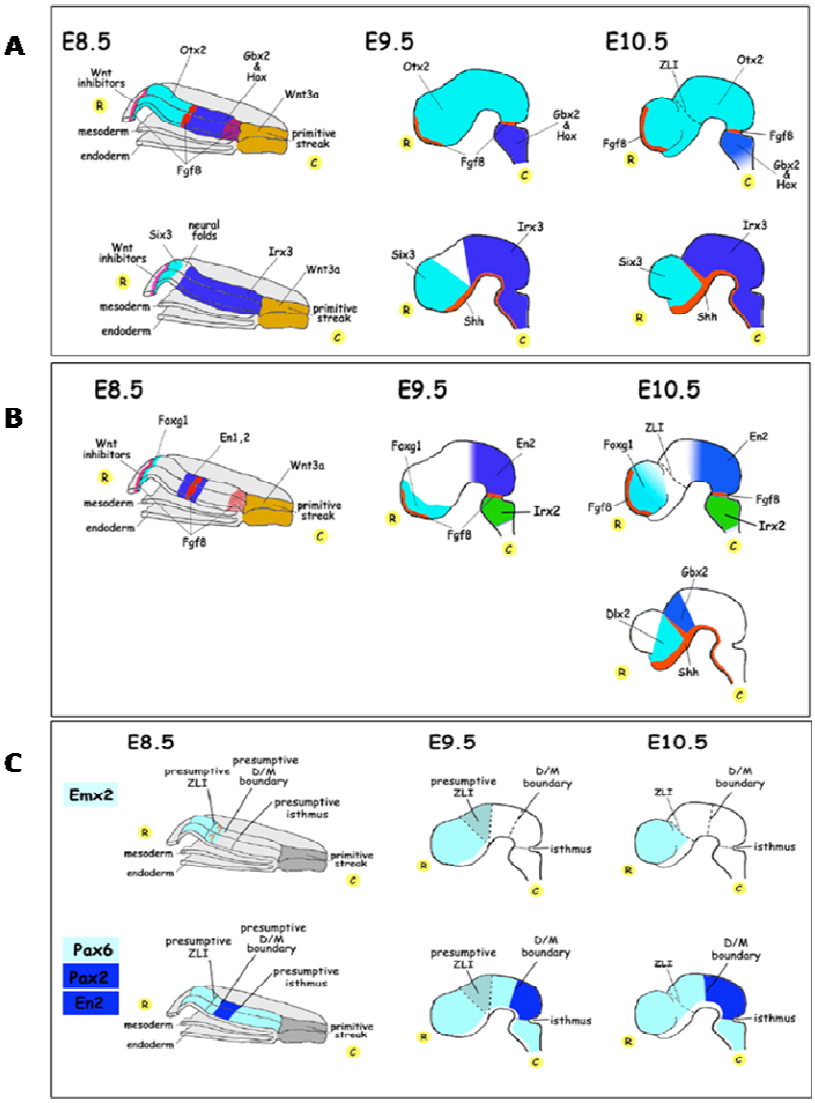

Figure 8. Schematic expression domains of the principal transcription factors involved in the antero/posterior patterning of the mouse central nervous system at E10.5. Images adapted from Mallamaci A, unpublished.

These “secondary organizers” are located at the junction between the anterior neural and non-neural ectoderm (anterior neural ridge or **ANR**)and at the boundary between midbrain and hindbrain fields, (i.e. at the isthmus), respectively. Both are crucial to subsequent patterning of the anterior brain.

The Anterior Neural Ridge is necessary for forebrain induction and maintenance. Ablation of the ANR in mice prevents the expression of the telencephalic markers Foxg1 and Emx1 [7].

The ANR stimulates the expression of *Foxg1,* a key transcription factor implicated in R/C specification of the telencephalic field, via Fgf8 secretion. The ANB activity is responsible for Fgf8 induction in the ANR , which in turn induces and/or maintains Foxg1.

The ZLI, deriving from the collapse of the region between Six3 and Irx3 domains**(Fig.8A),**releases molecules of the Sonic hedgehog (Shh) family [8] and splits theanterior neural plate into two distinct domains, able to differentially respond to *Fgf*signaling, expressing either Foxg1 or En2[9]. Remarkably, signalscoming from the ZLI induce expression of *Gbx2* and *Dlx2* in the thalamus and theprethalamus, respectively**(Fig.8).**

Recent data suggest that in mammals also the Fgfs, secreted by the ANR, actively estabilish the telencephalic identity: when Fgf receptors are deleted the telencephalon does not form[10].

1.3.Dorsal-Ventral Patterning in the neural tube

The polarity of the neural tube is induced by signals coming from itsimmediate environment. The dorsal pattern is imposed by the epidermis, while the ventral pattern is induced by the notochord **(Fig.9).**

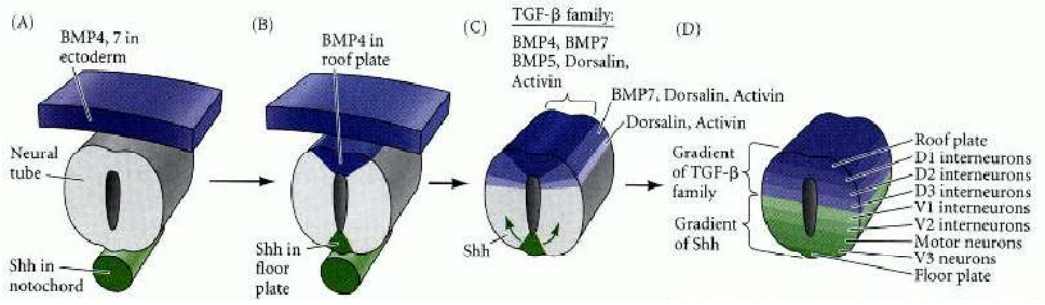

Figure 9. Dorsal-Ventral specification of the neural tube. (A)Two signalling centers influence the newly formed neural tube : the roof of the neural tube is exposed to BMP4 and BMP7 from the epidermis,while the floor is exposed to Shh protein from the notochord.
(B) Secondary signaling centers within the neural tube. The roof plate cells express and secrete BMP4, the floor plate are a source of Shh protein .
(C) BMP4 establishes a cascade of TGF factor, diffusing from the roof plate to the ventral neural tube. Sonic hedhog proteins spread dorsally as a gradient from the floor plate cells.
(D) The several spinal cord neurons identities are established by the exposure to BMP4/Shh gradients of paracrine factors. (Adapted from *S. Gilbert*).

1.3.1.Dorsal patterning of the neural tube

The dorsal fates of the neural tube are established by proteins of the TGF-β superfamily, especially the bone morphogenetic proteins 4 and 7, dorsalin, and activin[11,12]. Initially, BMP4 and BMP7 are found in the epidermis.As the notochord establishes a secondary signaling center (the floor plate cells) on the ventral side of the neural tube, the epidermis establishes a secondary signaling center by inducing BMP4 expression in the roof platecells of the neural tube. The BMP4 protein from the roof plate induces a cascade of TGF-β superfamily proteins in adjacent cells **(Fig.9C).**

Different sets of cells are thus exposed to different concentrations of TGF-β superfamily proteins at different times (the most dorsal being exposed to more factors at higher concentrations and at earlier times). The temporal and concentration gradients of the TGF-β superfamily proteins induce different types of transcription factors in cells at different distances from the roof plate, thereby giving them different identities.

1.3.2.Ventral patterning of the neural tube

The specification of the ventral neural tube appears to be mediated by external tissues.One agent of ventral specification is the **Sonic hedgehog protein**, originating from the notochord.

Another agent specifying the ventral neural cell types is retinoic acid, which probably comes from the adjacent somites [13].

Sonic hedgehog establishes a gradient, and different levels of this protein cause the formation of different cell types. Sonic hedgehog is initially synthesized in the notochord.The secreted Sonic hedgehog induces the medial hinge cells to become the **floor plate** of the neural tube. These floor plate cells also secrete Sonic hedgehog, which forms a gradient highest at the most ventral portion of the neural tube [14,15]. Those cells adjacent to the floor plate that receive high concentrations of Sonic hedgehog become the ventral (V3) neurons, while the next group of cells, exposed to slightly less Sonic hedgehog, become motor neurons **(Fig.10).** The next two groups of cells, receiving progressively less of this protein, become the V2 and V1 interneurons.

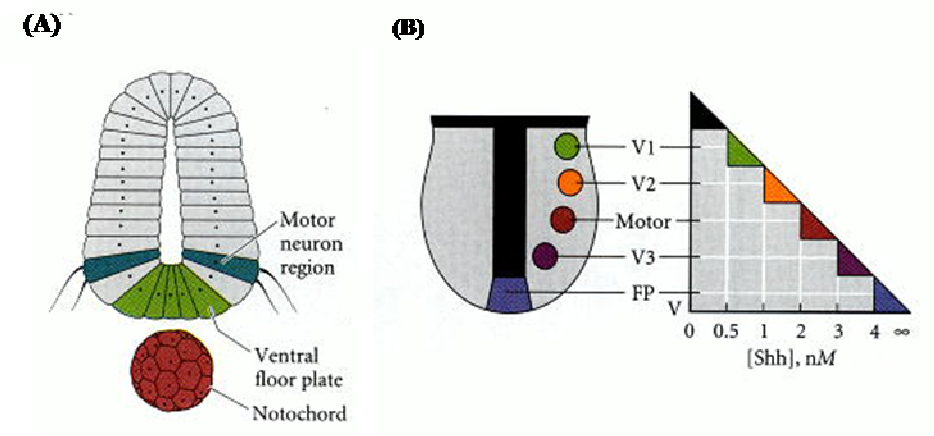

Figure 10.Induction of the ventral neural tube. (A) Cells closest to the notochord become floor plate neurons (in green);motor neurons originates from the ventro-lateral sides. (B) Relationship between Sonic hedgehog concentration and generation of different neuronal types *in vitro*.(Adapted from *S.Gilbert*).

1.3.3. Dorso-ventral specification in the telencephalon: Small Molecules and Transcription Factors.

The expression of transcription factors and secreted morphogenes along the D-V axis elicits the early partitioning of the telencephalon that will end up with the specification of pallial and subpallial structures.

Among these factors, major roles are played by the dorsalizing Zinc-finger transcription factor Gli3 and the ventralizing Winged helix transcription factor Foxg1 (**Fig. 11A).** The dorsalizing effect of Gli3 is counteracted by Sonic hedgehog protein (Shh), secreted by the ventral midline: the telencephalon of $Shh^{-/-}$ mice is reduced in size and ventral cell types lost. However, rescue of $Shh^{-/-}$ phenotype in double $Gli3^{-/-}$ $Shh^{-/-}$ mice [16] suggests that the Shh role in this process passes simply through inhibition of Gli3 activity.

The earliest site of Shh expression appears at E7.5; as neurulation progresses it is initially expressed by both prechordal plate and anterior mesoderm **(Fig. 12A),** then by the ventral hypothalamus and finally by the ventral telencephalon itself, from the medial ganglionic eminence together with the preoptic area[17]. Gli3 is induced by BMPs and is initially expressed

broadly throughout the telencephalic anlage and then is progressively downregulated in the ventral portion of it. Shh signaling neutralize the repressive form of Gli3, blocking the conversion from the activator (Gli3) to the repressor (Gli3R) and, as a consequence, promoting Fgf expression.

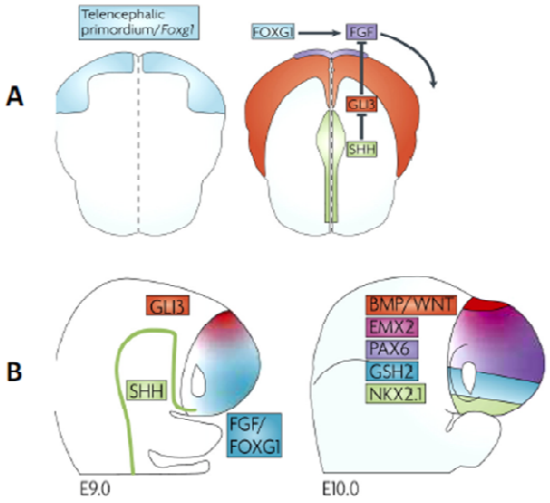

Figure 11. Dorso-ventral patterning of the forebrain.
The region that will become the telencephalon is defined by expression of Foxg1. Foxg1 (directly) and Shh (indirectly, via Gli3) promote Fgfs expression in the ANR. This patterns the nascent telencephalon. Dorsal view E8,E9 **(A).** Subsequently the dorsal telencephalon, expressing Gli3 at E9, is split, by E10, into a BMP and Wnt expressing medial region and a more lateral cortical regionex pressing countergradients of Emx2 and Pax6. The ventral telencephalon is subdivided into medialNkx2.1-expressing domains and lateral Gsh2-expressing domains (partially overlapping at E10).Sagittal view E9, E10 **(B).**

In absence of *Gli3*, the development of the dorsal telencephalon is disrupted[18].

Hence, Shh promotes ventral identity by preventing dorsalization of the telencephalon, rather than by directly promoting ventral cell character.

Ventral specification also requires the inhibition of dorsal signals by BMP antagonists, such as noggin (NOG) and chordin (CHRD). The ventralizing signal in the forebrain is probably mediated by a Foxg1/Fgf pathway. Foxg1 induction inside the anterior neural plate depends on signals that initially regulate antero-posterior patterning. Fgfs secreted by the ANR serve as major telencephalic patterning signals throughout the forebrain development. Remarcably, when three Fgf receptors are deleted, the telencephalon is no longer specified [10].

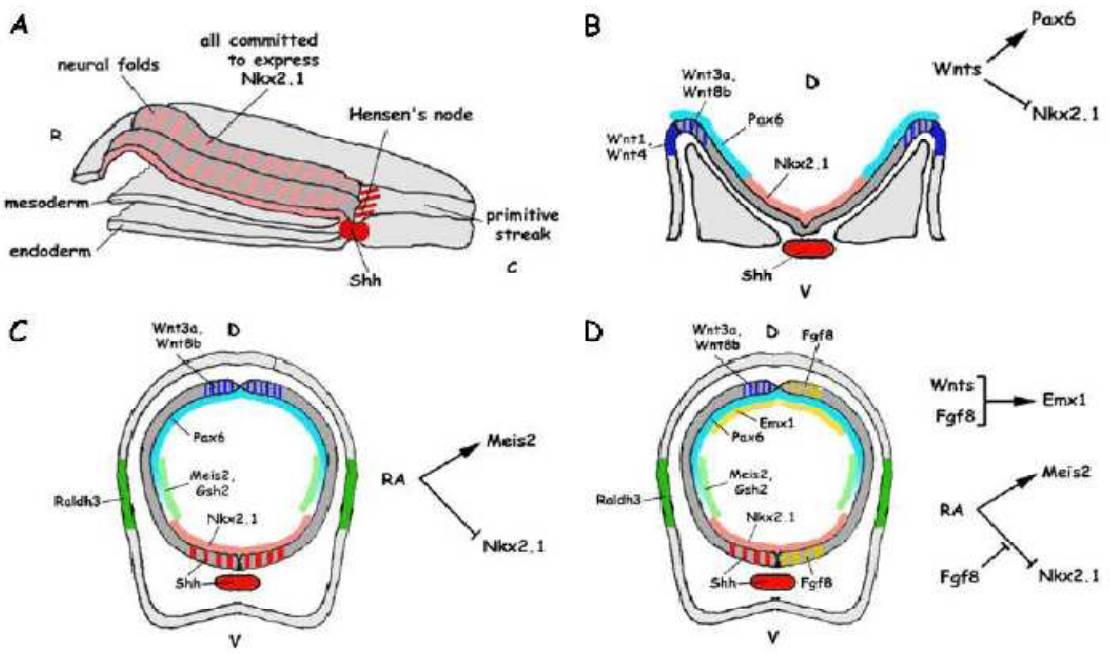

Figure12. Schematic view of early phases in dorso/ventral patterning of the rostral neural plate in the chick embryo. Image adapted from Mallamaci A, unpublished.

Forkhead box G1 (*Foxg1*) expression define the region that will become the telencephalon. Morever, Foxg1 promote Fgf expression, necessary to form all regions of the telencephalon. Disruption of *Foxg1* expression results in a loss of ventral cell types [19].

Mash1 and *Ngn1/Ngn2* are proneural genes, that play important roles in thedevelopment of the ventral and dorsal telencephalon, respectively. However they do not act as “master genes”, but simply link regional patterning to activation of specific neuronogenetic pathways in these structures [20,21].

- ***Molecular mechanisms mediating Forkhead box G1 role in D-V specification***

Foxg1(Forkhead box G1, formerly known as Bf-1) is expressed in the anterior neural plate cells from E8.5[22,23], slightly before the neural plate bends to form the head folds.

It is necessary for the expression of Fgfs from the ANR[19] and in turn Fgf8 induces Foxg1 expression[7,24], forming a positive feedback loop. In Foxg1$^{-/-}$ mice the formation of the subpallium is abolished(Xuan et al., Neuron, Voli. 14, 1141-1152, June, 1995).

Remarkably, recent data in zebrafish suggest that Foxg1 could integrate signals from Shh, Wnt and Fgf8 pathways, so having a pivotal role in D-V forebrain specification.

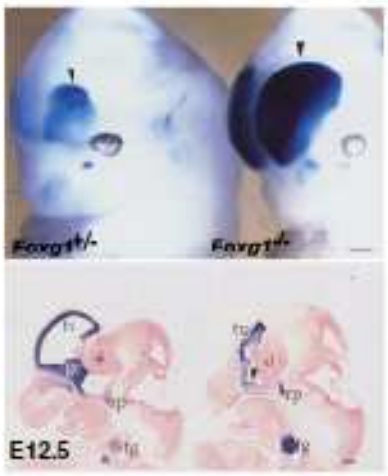

Figure 13.Forebrain development impairment in Foxg1-/- .
Foxg1 knockouts display a smaller size of the telencephalic emispheres, if compared to heterozygous mice. The ventral telencephalon formation is heavily impaired, but also the dorsal telencephalon size is reduced. X-Gal histochemistry identifies structures that normally express Foxg1(Modified by Xuan et al.,Neuron,Volume 14, Issue 6, June 1995, Pages 1141–1152).

In fact, Foxg1 could also act as a Wnt/β-catenin antagonist, as well as downstream effector of Shh to specify the subpallial identities [25]. As a result of early R-C and D-V patterning events, the prosencephalon will be subdivided in pallial territories and subpallial territories, characterized by the expression of specific set of TFs. The subpallium will give riseto the medial ganglionic eminence (MGE) and to the lateral ganglionic eminence (LGE) , expressing respectively the TFs Nkx2.1 and Gsh2.

Regarding the molecular mechanism, FoxG1 usually acts as a transcriptional repressor in both direct andindirect ways[26–30].

Moreover, this factor can also inhibit TGFβ signalling by binding to Smadand FoxO transcription factors[27,31]**(fig14).** It was shown that mouse Foxg1 proliferation-promoting effect ismediated by mechanisms based on protein-protein interactions and isnot dependent from its DNA-binding ability [27,32]. In contrast, Foxg1 requires an intact DNA-binding domain to inhibit or delay the neuronal differentiation of telencephalic precursor cells[32].

Foxg1 exerts its transcriptional repressor activity, at least in part, through the recruitment transcriptional co-repressors of theGroucho/Transducin-like enhancer of split (TLE) and AT-richinteraction domain (ARID) families [30,33,34].

In turn,TLE and ARID co-repressors, recruit chromatin-modifying enzymes (i.e. histone deacetylases) to the transcription factor complex [35]. In some cases, the co-repressor itself havedemethylation activity[36].

Specific TLEs are required for the activity of FoxG1 during forebrain development. In this regard, it was shown that when transfected in primary neural progenitors,FoxG1 acts as a repressor of cortical neurogenesis but this function can be enhanced by TLE1 or inverted by TLE6 [37].

Foxg1 plays also a crucial role in ventral telencephalon formation. To carry out this function, Foxg1 physically interacts with another member of the TLE family ,TLE2. Either FoxG1 or TLE2 knockdown abolishes or reduces the development of this region. The interaction between Foxg1 and TLE2 is mediated by aconserved Foxg1 N-terminal eh1 motif , whereas the C-terminal domain,which has previously been suggested to contain a TLE binding motif,is not required[38]. However, the C-terminal domain isnecessary for the functional synergybetween FoxG1 and TLE2, eitheralone or in combination with the N-terminal domain[38].

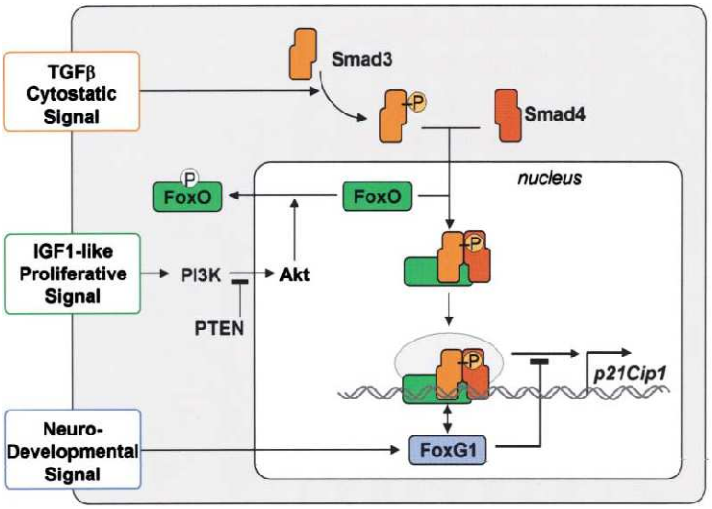

Figure 14. Model of FoxO Factors as a Node for Integration of TGF-_/Smad, PI3K/Akt, and FoxG1 Pathways. There are three pathways converging on FoxO to regulate the expression of *p21Cip1* and cell proliferation. **TGFβr**eceptor activation leads to Smad3 phosphorylation (P) and assembly of a Smad3- Smad4 complex in the nucleus. This complex associates with FoxO proteins and activate*p21Cip1*.
IGF-1-like proliferative signals induce the PI3K/Akt pathway that in turn phosphorylates FoxO. This mechanism exclude FoxO from the nucleus (Brunet et al., 1999) and prevent Smad-FoxO dependent gene activation. FoxG1 binds to the FoxO-Smad complex, inhibiting its transcriptional activity (Adapted Joan Seoane et al.,**Cell, Vol. 117, 211–223, April 16, 2004).**

- ***Other "Master genes" involved in dorso-ventral patterning of telencephalon***

  Wnt and BMP expression (promoted by Gli3) are required for the expression of the *empty spiracle* homologs*Emx1* and *Emx2*, confined to the primary proliferative layer of the cortex (**Theil et al., 2002**). Other transcription factors act subsequently to form specific subdivisions, such as *Pax6, Gsh2* and *Nkx2.1*, crucial for the proper morphogenesis of the lateral cortex, striatum and anlage of globus pallidus respectively **(Fig. 15).**

In the absence of any of them, the corresponding morphogenetic field is shrunken and the adjacent ones substantially enlarged [39–41].

Pax6 and *Gsh2* play complementary roles reciprocally compartmentalizing and establishing pallial and subpallial identities. In *Pax6* null mice, there is a dorsal expansion of markers of ventral progenitors, such as *Mash1*, *Gsh2* and *Dlx2*, whereas in *Gsh2*$^{-/-}$it is the opposite [20].

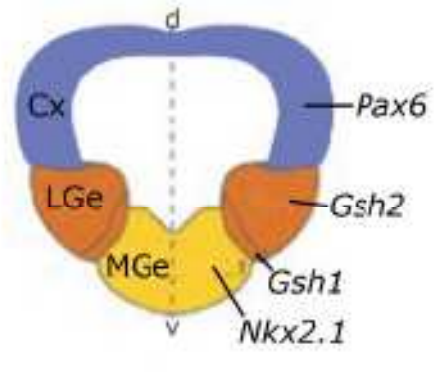

Figure 15. Schematic representation of main transcription factors involved in regionalization of early cortical primordium. Corolan section of mouse telencephalon at E10.

In summary, the coordinate action of different signals including BMP/Wnt, RA,Fgf8 and Shh and the differential activation their targets in space and time establish theside where the pallium will develop and regulates its size.

Some of these signalling systems and their targets are subsequently involved in furthersubdivision of the pallial anlage, in a process termed cortical regionalisation andarealization.

1.4.Cortical specification and Arealization.

The so-called arealization is a process that largely relies on the interplay between factors intrinsic to the cortical primordium and influences coming from subcortical structures.

In particular, several experimental evidences suggests that cortex-autonomous molecular cuesdrive the early phases of arealization, independent of information delivered later by thalamic afferents.

Cortical arealization starts at early stages (E10.5 in mouse), with the specification of a primitive molecular protomap, set up according to specific positional and temporal cues.

The codification of these signals initiates intrinsically to the cortical field, resulting from the interplay between soluble factors, secreted at the borders of this field, and transcription factors expressed along tangential gradients within it. Subsequently, (E13.5 in mice) thalamo-cortical axons (TCA), relaying sensory information from distinct nuclei of the dorsal thalamus to

different cortical regions, promote further inter-regional diversification, so leading to the properly called cortical arealization.

The process of areal pattering depends on setting up rostrocaudal and mediolateral gradients of TF expression, which are modulated by diffusible signals released by patterning centers at the edges of the cortical field.

Hence, there are two main classes of molecules that play a crucial in the regionalization of the early cortical primordium:

- secreted ligands (SLs), expressed at the borders of the cortical field **(Fig.17a)**,
- and TFs, gradually expressed within the proliferative layers of this field **(Fig.17b)**.

Three specialized sources of SLs (also knownas"organizers") may be found at the borders of the cortical field: the caudomedial cortical hem (between the hippocampal field and the choroidal field), the rostromedial commissural plate (between rostromedial cortex and septum) and the lateral cortical antihem (between the paleocortical and the striatal anlagen)(see **fig. 16).**

The cortical hem is a source of Wnts (2b, 3a, 5b, 7a, 8b)[42]and Bmps (2, 4, 6, 7)[43], expressed in nested domains which may include part of the adjacent cortical field. The formation of the cortical hem is dependent on LIM-homeodomain factors, in particular *Lhx2* and *Lhx5*; loss of *Lhx2* expands dramatically the hem and choroid plexus at the expense of the cortex [44]**(Fig.19).**

The commissural plate is an anterior patterning center for arealization placed at the rostromedial pole of telencephalon. It is the derivative of the anterior neural ridge (ANR) and express Fgfs (8, 15, 17, 18).

Finally, the antihem (on the lateral side of the cortical field, at the pallial–subpallial boundary), express an heterogeneous mix of SLs including Egf-like molecules (TGFα, Nrg1, Nrg3), the Wnt-chelating protein Secreted frizzled-related protein 2 (Sfrp2) and Fgfs (7, 15),antagonizing Wnt signaling coming from the hem[45].

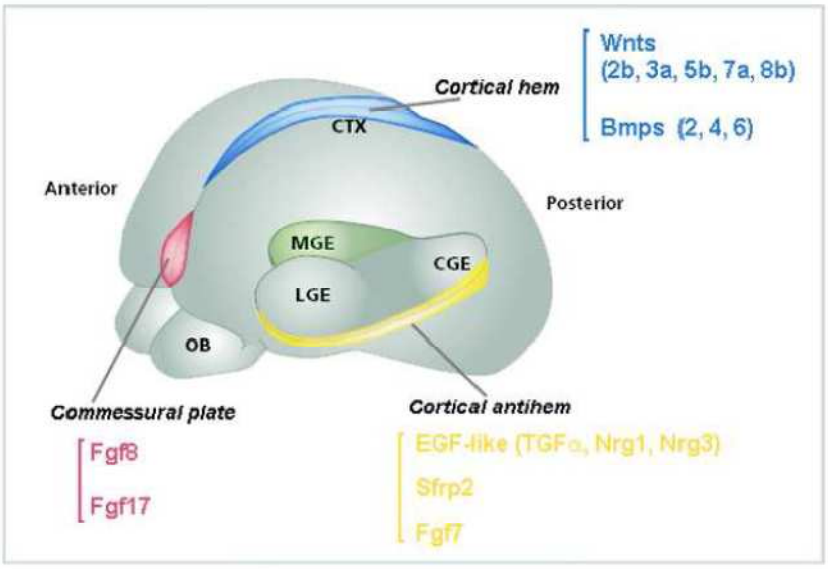

Figure16. Localization of the signaling centers involved in cortical arealization.
Abbreviations: Ctx, cortex; LGE, lateral ganglionic eminence; MGE, medial ganglionic eminence;CGE, caudal ganglionic eminence; OB, olfactory bulb. (Adapted from Corbin et al, *Nature Neuroscience* **4**, 1177 - 1182 ,2001).

1.4.1.Cortical specification: transcription factors.

At the onset of the primary neuronogenesis, a number of transcription factors involved in the specification of cortical areas are expressed in proliferative layers of the developing neocortex, according to distinct spatial gradients .

These TFs belong to different families and their gradient can be oriented in different ways.

Some of them are restricted to the pallial VZ (Emx2, Pax6), some are also detectable in subventricular and/or more MZs (Lhx2, Emx1, Foxg1, Couptf1, Sp8). The expression of these genes is regulated by patterning edges and the information flow from SLs to TFs takes place through a complex functional network**(Fig.17)**.

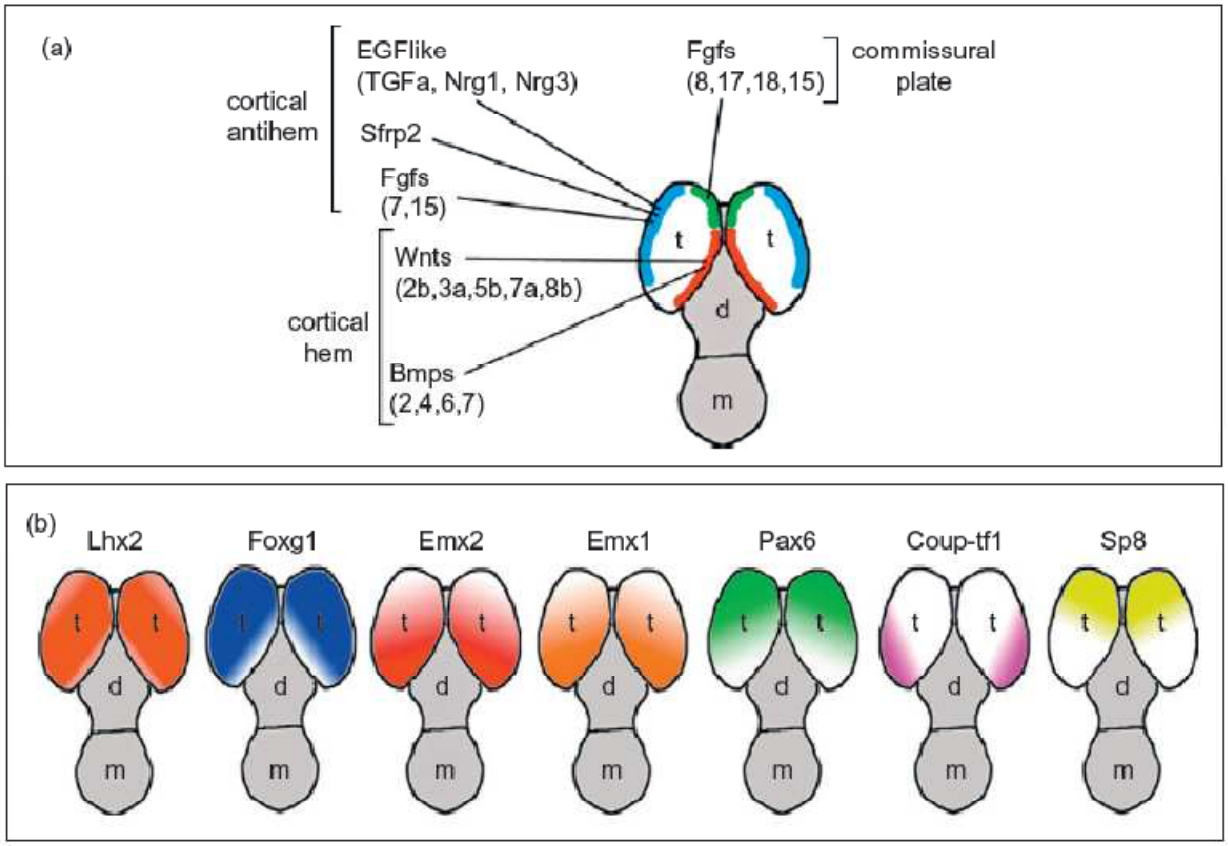

Figure 17. Expression patterns of SLs and TFs implicated in cortical arealization.
(a) Synopsis of SLs expressed by the three signaling edges of the cortical field. (b) Idealized representation of tangential expression gradients of patterned TFs. Dorsal views. Abbreviations: d, diencephalon; m, mesencephalon; t, telencephalon (Adapted from:Mallamaci A:Progress in Brain Research 189: 37-74, 2011).
.

1.4.2.Cortical Arealization "Master genes".

Genetic dissection of genes linked to arealisation showed that a large subset of TFs and secreted ligands involved in mastering this process not only impart specific areal identities to neuroblast located in distinctive parts of the cortical primordium but also control their kinetic behaviour (proliferation, differentiation, apoptosis), so finallyregulating:

(a) tangential expansion rates of distinct cortical regions

(b) radial neuronal output of distinct cortical regions

Among these genes, major roles are played by Foxg1,Pax6, Emx2 and Lhx2.

Lhx2 is stimulated by Bmps (2 and 4) at low concentrations and inhibited by the same ligands at high concentrations. This may account for the peculiar Lhx2 dorsomedial expression profile: absent in the hem, high in archicortex, lower in neo/paleocortex [56].

Foxg1 is inhibited by Bmps (2 and 4, but not 6 and 7) [43] and Wnt signaling [57], and strongly promoted by Fgf8[24].

Emx2 is promoted by Bmps and Wnts [73,74] as well as inhibited by Fgf8[24,58,59].

Pax6 is strongly inhibited by canonical Wnt signaling [60,61] and promoted by Fgf8, specifically in rostral pallium[24].

Lhx2 is a cortical selector gene. Lhx2 selector activity is specifically required by cortical stem cells, without which these cells eventually adopt hem or antihem fates rather than hippocampal or neocortical identities.

The absence of neocortex and hippocampus in Lhx2 null embryos contrasts with the preservation of one or both of these cortical structures in *Pax6, Foxg1*, and *Emx1/2* null mutants **(Fig. 18)** . These transcription factors are therefore likely to act after Lhx2, with Foxg1 being a mediator of Lhx2-dependent hem fate suppression . *Lhx2* is itself downstream of Six3 in zebrafish , which is required to form the entire rostral prosencephalon, suggesting that Six3 creates a rostral forebrain field within which Lhx2 specifies cortical identity.

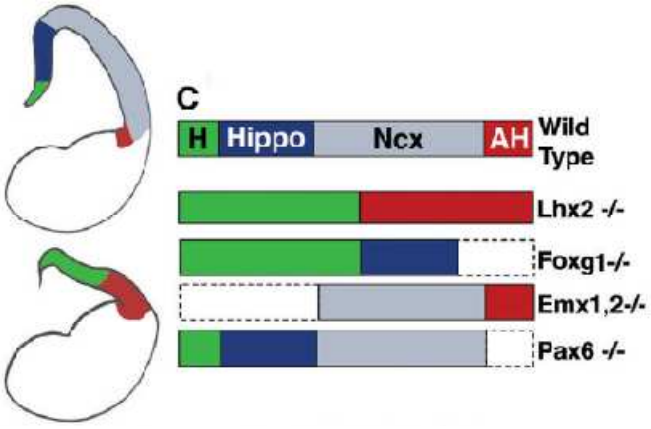

Figure 18. Schematics of mutant dorsal telencephalic phenotypes illustrating how the complete absence of hippocampus and neocortex is unique to the Lhx2 mutant (4,5,28-30). AH, antihem; H, hem; Hippo, hippocampus; Ncx, neocortex.(Adapted from Vishakha S. Mangale et al., *Science* **319**, 304 (2008); DOI: 10.1126/science.1151695).

At early ages, both *Foxg1* and *Lhx2* are expressed throughout the cortical neuroepithelium and eventually their expression delineates a sharp boundary between the cortical tissue and the hem. Further, in mice mutant in these genes, the cortical hem expands, suggesting their role in actively confining the lateral extent of the hem. An important difference between these two molecules is that in FoxG1 mutants both the hem and the medial part of the cortical neuroepithelium expand (Muzio and Mallamaci 2005); in Lhx2 mutants - however - only the cortical hem (as well as the lateral antihem) expands at the expense of the cortex[54,60]**(fig. 19).** This suggests a more specific role for the LIM homeodomain transcription factor Lhx2 in defining the hem--cortex boundary, whereas FoxG1 probably regulates the broad medial telencephalic domain**.**

In the pallium, Gli3 expression will be flanked by the combined expression of the transcription factors Pax6 and empty spiracles homeobox 2 (Emx2) **(Fig.20).**

They are expressed early in the dorsal forebrain (E8.5)[46,49] along opposite gradient (see below) and are both necessary for dorsal telencephalon specification: $Emx2^{-/-}$ $Pax6^{-/-}$ mice exhibit an expansion of the choroidal roof and the subpallium at the expense of the cortex **(Fig.20)**[63,64,65].

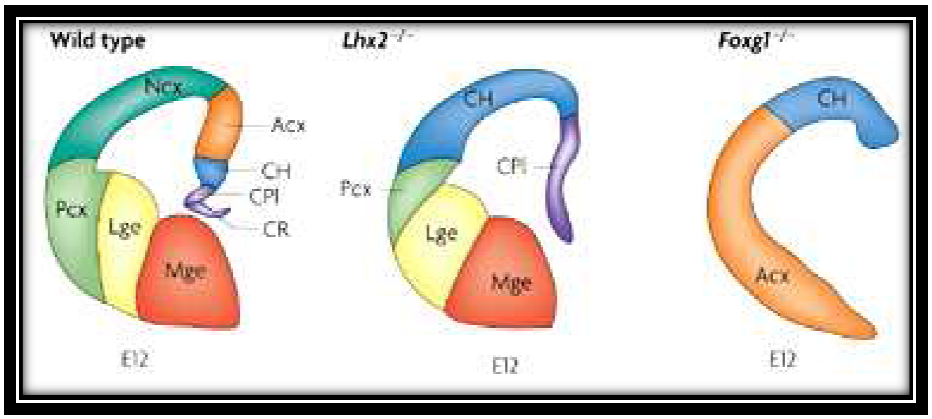

Figure 19 | Mutant phenotypes of mice knock-out for the Lxh2 and Foxg1, transcription factor involved in cortical specification. Abbreviations: CH, cortical hem; CR, choroidal roof; ChP, choroid plexus; Cx, cortex; Lge, lateral ganglionic eminence; Mge, medial ganglionic eminence; Pcx, paleocortex. Adapted from Molyneaux *et al.*, Nat Rev Neurosci. 2007. Jun;8(6):427-37.

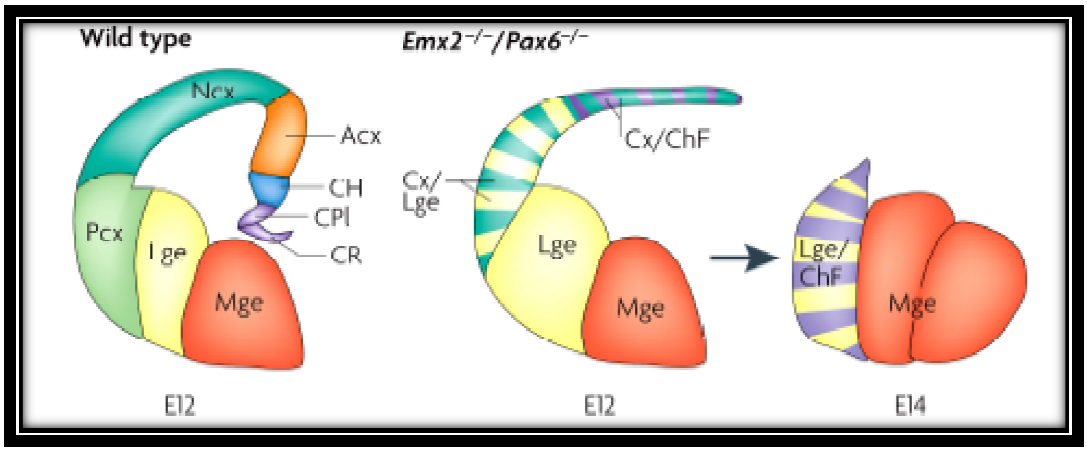

Figure20. Emx2 involvement in dorsal forebrain specification.
Loss of both Pax6 and Emx2 results in ventralization of cortical progenitors and the loss of the neocortical domain (Ncx), archicortex (Acx), cortical hem (CH) and choroid plexus (CPl), choroid field(choroid plexus and choroidal roof) (ChF) by embryonic day 14 (Adapted from Muzio & Mallamac Cereb Cortex. 2003 Jun;13(6):641-7 and Nat Rev Neurosci. 2007 Jun;8(6):427-37.).

Remarkably, in Gli3-/- mice Emx2 is downregulated[66] and $Gli3^{-/-}Pax6^{-/-}$ mice have a similar phenotype to $Emx2^{-/-}Pax6^{-/-}$[8], suggesting that Emx2 is downstream to Gli3.

The concerted activity of dorsal forebrain patterning centers and transcription factors expressed in the telencephalic field further subdivides the cerebral cortex in distinct anatomical and functional areas.

1.5. Development of the neocortex.

In mice, development of the neocortex begins at embryonic day 9.5 (E9.5) with the appearance of the cerebral vesicles from the dorsal surface of the rostral neural tube.

Initially, the neocortical primordium is comprised of an apparently homogenous pool of neural stem cells. The first postmitotic neurons of the neocortex, the Cajal-Retzius cells, appear at E10.5-E11.0 to form a transient structure known as the marginal zone that later becomes layer 1. The Cajal-Retzius cells (CR) secrete Reelin, anextracellular matrix protein that play a fundamental role for the formation of cortical layers during embryonic development and their maintenance in adulthood[64]. CR neurons arise from restricted locations at the borders of the developing pallium, the hem, the antihem and the septum[65,66], and spread into the cortex by tangential migration. The subsequent generation of the glutamatergic projection neurons of layers 2–6 by neocortical stem cells takes place from E11 until approximately E17, with neurons of deep layers (layer 6) produced before those of the outer layers (2/3) **(Fig. 21A).**

Postmitotic layer neurons born in the VZ migrate radially outwards to form the layers VI-II of the cortical plate. This migration takes place along the processes of radial glial cells that span the width of the developing neocortex **(Fig. 21B).**Neurons of layer 6 are first to leave the ventricular zone and migrate radially to form the nascent cortical plate. Neurons of layer V to II then migrate past those of layer VI and adopt successively superficial positions **(Fig. 21A).**

The glutamergic neuronal progeny of neocortical stem cells form radial columns that span the cortical plate[70,71]**(Fig. 21C**). By contrast, inwardly migrating inhibitory GABAergic interneurons arriving from the ganglionic eminences of the ventral forebrain migrate by tangential dispersion ([72,73,74]).

This model, known as ”radial unit hypothesis”, gave rise to the idea that a spatial pattern in neocortical stem cells is transferred to the neurons of the cortical plate.

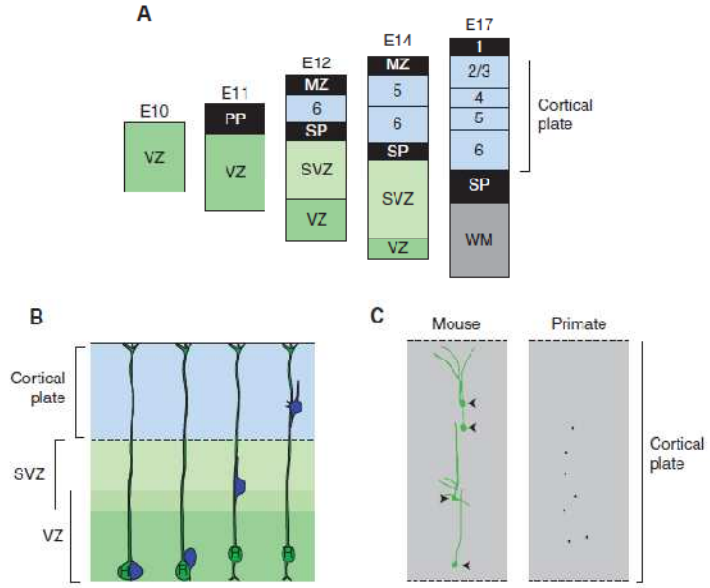

Figure21.Cortical stem cells are multipotent, generating neurons for each layer in a fixed temporal order.
(A) Layer-specific neurons are generated in a fixed temporal order in a classic inside-out pattern over 6 days in the mouse cortex. (B) Neurons (blue) and generated by radial glia stem cells (green) in the ventricular zone and subsequently migrate radially outwards into the cortical plate along the processes of the radial glia cells that span the width of the developing neocortex. (C) Cortical stem cells generate radially arranged clones of neurons in mice and primates. Examples of retrovirally labeled clones are redrawn from Kornack and Rakic Neuron 15:311–321.1995 and Yu et al. 2009.

1.5.1.Cortical progenitors.

Neural progenitors are initially generated in a proliferative layer adjacent to the lateral ventricles called ventricular zone (VZ). The first postmitotic cortical neurons form a transient structure called the preplate (PP). The PP persists until embryonic day (E) 13 in mice, when the earliest cortical plate cells reach the upper part of the neuroepithelium and divide the PP into two regions: the superficial marginal zone (MZ) (future layer 1) and the lower subplate (SP) [75,76]. The cortical plate (CP), which will become the mature six-layered neocortex, is formed between these two layers according to an “inside-out” neurogenetic gradient, with later generated neurons bypassing early gene rated cells to settle at the top of the cortical plate, forming the upper layers of the cerebral cortex. As cortical development proceeds, an additional

proliferative zone, called subventricular zone (SVZ), appears on top of the VZ. It will initially give rise to projection neurons and subsequently to glia[77]**(fig.22).**

Different types of progenitors, characterized by the expression of different genes, contribute to cortical neurogenesis. Two principal classes have been identified on the basis of their nucleus position during the M-phase of the mitotic cycle:

(1) apical progenitors, so called because dividing at the ventricular (apical) surface of the VZ and expressing Pax6 gene [78]. They include neuroepithelial cells (NE)and radial glia cells (RGCs), which contact both the ventricular cavity and the meninges, as well as short neuronal precursors (SNPs) **(Fig.23a)** [79,80].Short Neural Precursors (SNP) are similar to RGCs, however, they have a basal process which does not reach the MZ, so showing a "pin-like" morphology **(fig.23).** They undergo IKNM similarly to NE and RGC cells, but can be distinguished from other apical progenitors by the activity of the alpha 1 tubulin promoter (pTα1)[80,83].

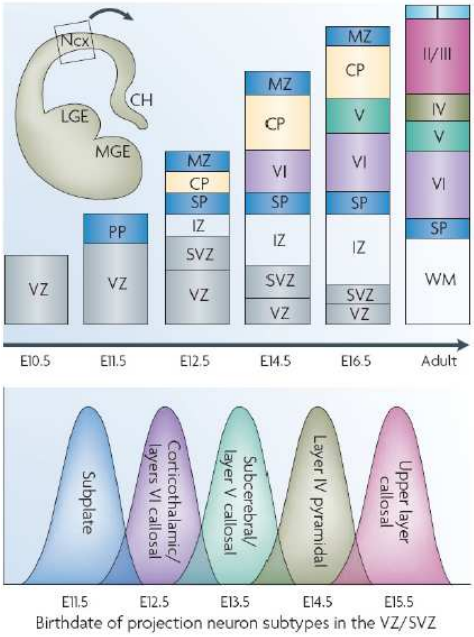

Figure 22. Mouse cortical neurogenesis. Abbreviations: CP, cortical plate; IZ, intermediate zone, PP, preplate; MZ, marginal zone; SP, subplate; SVZ, subventricular zone; VZ, ventricular zone.

(2) basal or *intermediate progenitors* (IPC), that undergo division away from the ventricular surface, often at the VZ/SVZ border **(Fig.23b)** [81,82] and express the transcription factor Tbr2[78].

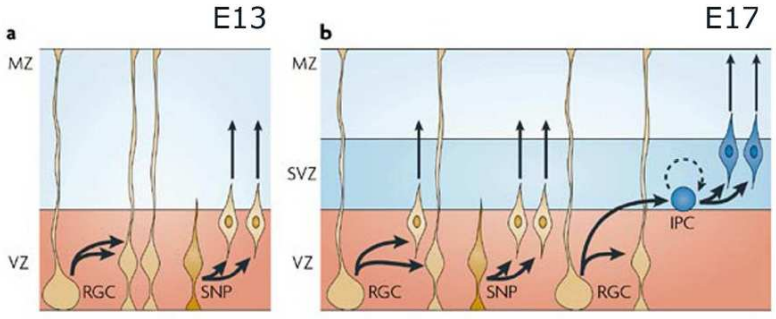

Figure 23.Schematic overview on different types of mouse cortical precursors.
Abbreviations: IPCs, intermediate progenitor cells; RGCs, radial glia cells; SNP, short neural precursors. Image modified from Dehay and Kennedy, Nat Rev Neurosci 8:438-50,2007.

At early stages, NE cells undergo a symmetrical self-renewing pattern of cellular divisions, so leading to an increase of the surface area of the VZ. Around E10 in mouse, the NE division pattern progressively switches to a more asymmetric one, giving rise to the first neurons and to Radial Glial Cells (RGCs). RGCs share with NE cells many histological, morphological and molecular properties, including full histogenetic potentials, radial morphology and IKNM. At a molecular level, both populations express the transcription factor Pax6 and the intermediate filament protein Nestin [84].

Remarkably, the basic-helix– loop–helix (bHLH) Hes transcription factors seem to be important for the NE-to-RGC transition: mice deficient in Hes1 and Hes5 show normal NE cells at E8 but impaired RGC differentiation at E9.5 [85]. Thus, Notch signalling mediated by Hes transcription factors seems not to be required by NE cells.

Basal progenitors, also called Intermediate Progenitor Cells (IPC), originate from apical progenitors and (1-3 mitoses). They show a multipolar morphology and do not undertake INKM. Their post-mitotic output forms the vast majority of the glutamatergic neuronal complement of the cortex.

1.5.2.Gene expression profiles of cortical progenitor subtypes.

A large number of transcription factors regulate the choice between proliferationand differentiation, inhibiting or promoting the exit from the cell cycle. In particular, *Emx2*and *Tlx* genes favor progenitors proliferation [86–88], *Pax6* promotes the maintenance of the size of the

cortical progenitor pool[89]. Proneural genes (*Ngn1* and *Ngn2*) promote neuronal fatecommitment, whereas members of the *Hes* and *Id* families are important inhibitors ofneuronogenesis. RGCs cells are maintained in the proliferative state by the simultaneously action of different genes (such as *Emx2*, *Hes1*, *Hes5*, *Id3*, *Id4*) **(Fig. 24**). The direct transition from radial glia to newborn neurons is regulated by *Ngn1* and *Hes5* genes and correlate with downregulation of radial glia marker *Pax6* and upregulation of postmitotic neuronal markers *Tbr1*, *Math2*, and *neuroD2* [78,90,91].

In the case of indirect neurogenesis, the transition from radial glia to basal progenitors involves upregulation of *Tbr2* and downregulation of *Pax6*[78] (**Fig.25**). The subsequent transition from IPCs to neurons correlated withdownregulation of *Tbr2* and upregulation of *Tbr1*, *Math2*, and *NeuroD2, NeuroD* (whichare all expressed by newborn cortical

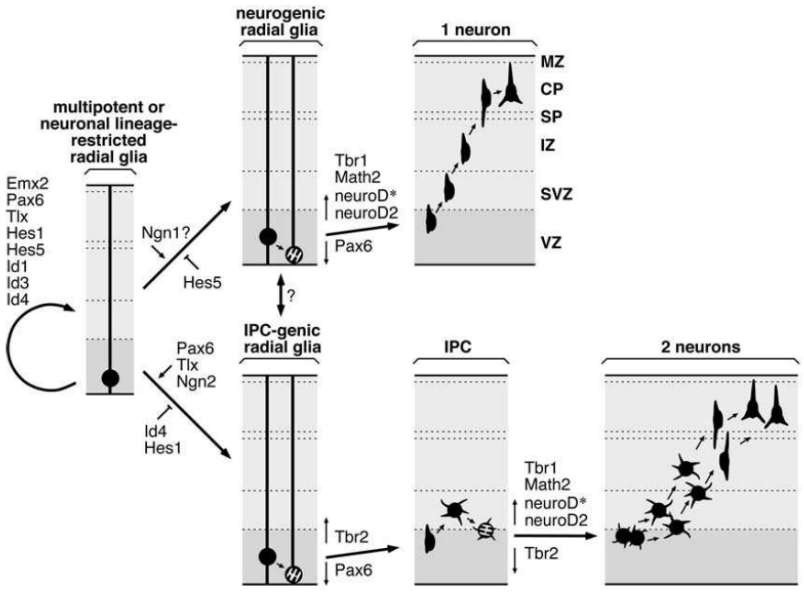

Figure 24. Model for TF regulation of direct and indirect pathways of cortical neurogenesis.*(Adapted* from HevnerMol Neurobiol 2006;33:33-50).

projection neurons, at least transiently). So, the TF sequence *Pax6→Tbr2→Tbr1* characterizes the transition RGC→IPC→postmitotic neuron [78].

In Pax6 -/-, radial glial progenitors present defects in their mitotic cycle, molecular phenotype and morphology[92]. Moreover, a loss of Tbr2+ cells corresponding to basal progenitors can be identified, indicating that Pax6 is necessary for the activation of Tbr2 expression [89]. The expression of Pax6 protein in cortical progenitors determines also the expression of the proneural gene Ngn2, providing evidence of a direct regulatory link between neural patterning and neurogenesis [93].

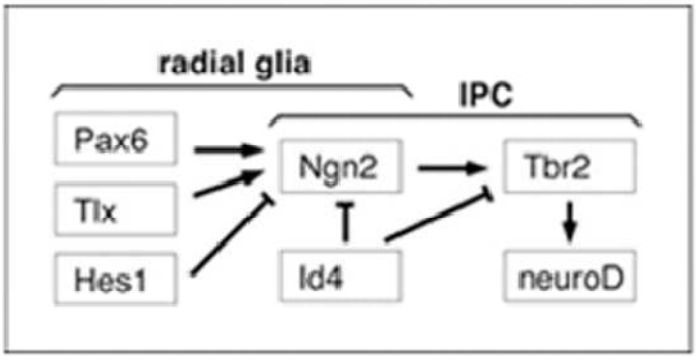

Figure 25. Transcription factors implicated in regulating IPC production from radial glia. A balance of TFs promotes (Ngn2, Pax6 and Tlx) or inhibits (Hes1, Id4) IPCs production from radial glia. (Image taken from Hevener, Mol Neurobiol 2006;33:33-50).

CHAPTER 2. INTRODUCTION: REPROGRAMMING AND TRANSDIFFERENTIANTION IN REGENERATIVE MEDICINE.

A major health challenge is posed by diseases involving postmitotic tissues, whose cells have very low or no proliferative capacity.

The aim of regenerative medicine is to regenerate tissues with no initial capacity for regeneration, and there has been increasing scientific interest in the use of cellular therapy for this purpose**(Fig.26).**

Cell-differentiation and specialization were originally thought to be unidirectional and spontaneous reprogramming was rarely observed.

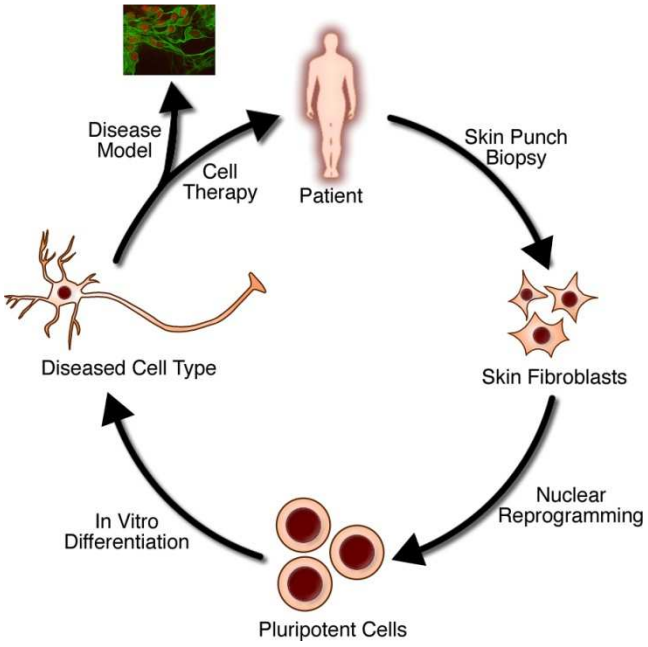

Figure 26. The steps of regenerative medicine. Setting up cellular therapies requires the optimization of four steps: first, isolating and culturing cells that can be easily get from a patient. Second, the reprogramming of these cells into a pluripotent state. Third, the differentiation of those patient-specific pluripotent cells into the cell type relevant to their disease. Fourth, transplantation of the repaired, differentiated cells into the patient. Remarcably, disease-relevant patient cells can also be used for *in vitro* disease modeling which may be a powerful tool for disease mechanisms understanding and drug discovery.

Nuclear-transfer studies have shown that adult cells can be reprogrammed into embryonic state through transfer of nuclear content from somatic cells into viable oocytes or via fusion of somatic cells with ES cells. However, these techniques still require the use of embryos,implying major ethical and immune rejection problems.

Two main approaches has been developed to overcome these issues**(fig 27):**

1) the generation of induced pluripotent stem cells (IPs), derived directly from the patient's own somatic cells, having the capacity to replace tissue and, thus, avoiding allotransplantation problems. This approach has a great clinical potential, however employment of iPS cells in therapy is presently limited by the not negligible risk of tumor formation.

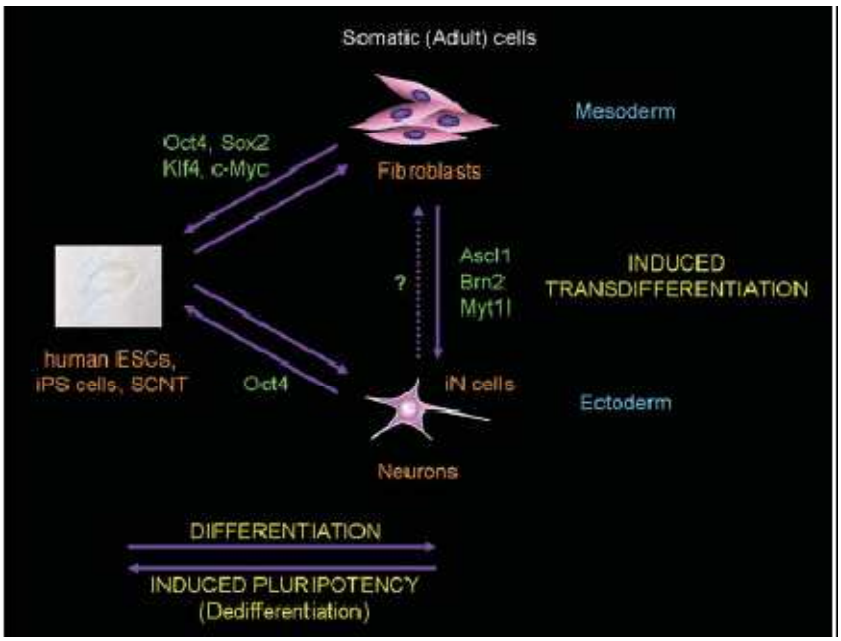

Figure 27. Main strategies cell fate change. It is possible to achieve de-differentiation or induced pluripotency by the ectopic expression of four transcription factors (Oct4,Sox2,klf4,c-Myc; Takahashi and Yamanaka,2006) in fibroblasts or just one(Oct4) in neurons. The direct transdifferentiation from fibroblasts (mesoderm) to functionalinduced neurons (iN) cells (ectoderm) require the ectopic expression of three transcription factors :Ascl1,Brn2,Mytl1 (Vierbuchen et al.,2010). The reversal conversion has not been described yet (Adapted from Masip et al., Molecular Human Reproduction, Vol.16, No.11 pp. 856–868, 2010).

2) the so-called transdifferentiation process , by which differentiated cells can change fate and become another differentiated cell type. This approach should provide the large numbers of cells required for transplantation.

3) However, considerable work is still needed to develop a definitive method for the long-lasting differentiation of cell types with therapeutic value.

2.1. Generation of pluripotent stem cells.

Research on embryonic stem (ES) cells has started since 1980s. ESC are derived from the inner cell mass of mammalian blastocysts and are characterized by peculiar features, such as the ability to grow indefinitely while maintaining pluripotency and the ability to differentiate into cells of all three germ layers [94,95]. Human ES cells might be used to treat a huge number of diseases, such as Parkinson's disease, spinal cord injury, and diabetes [96]. However, ethical difficulties regarding the use of human embryos, as well as the problem of tissue rejection following transplantation in patients have been hampering the research progress.

There are several ways to circumvent these issues. One is the employment of somatic (adult) stem cells (ASCs) as a source of pluripotent cells. Unfortunately, this strategy has many limitations, in particular:

(i) ASCs are relatively rare undifferentiated cells found in many organs and differentiated tissues,

(ii) their isolation into pure populations is not always possible

(iii) they have a limited capacity for both self-renewal (*in vitro*) and differentiation since these cells are notpluripotent but multipotent (their differentiative potencial is strongly linked to the tissue from which they originated)

(iv) moreover, anisogenic ASCs can cause rejection after allotransplantation.

For these reasons, in the last years researchers focused on the generation of induced pluripotent cells derived directly from the patients' own cells.

Somatic cells can be reprogrammed by three main strategies**(fig.28):**

a) exposure to oocyte-specific factors through somatic cell nuclear transfer (SCNT)

b) exposure to factors expressed in pluripotent cells (i.e. embryonic stem cells) through cell fusion

c) overexpression of defined transcription factors involved in manteining pluripotency in ES cells(direct reprogramming)[97].

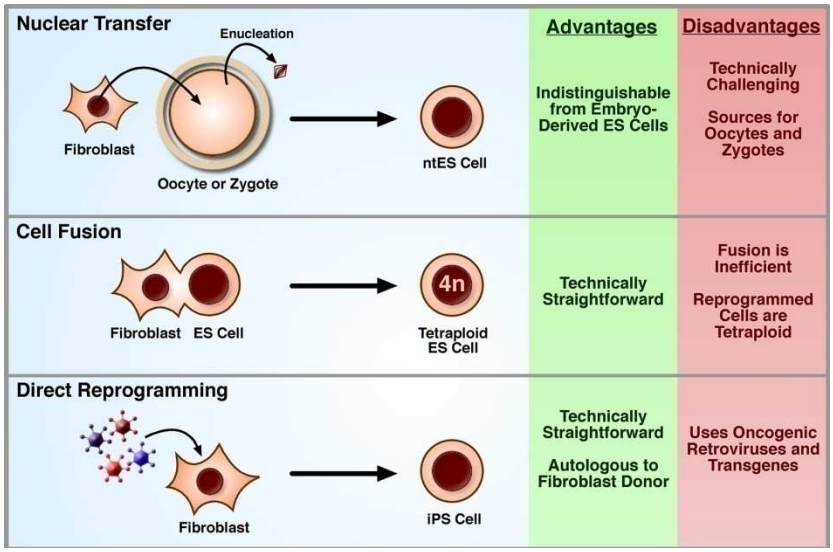

Figure 28. Strategies of nuclear reprogramming: advantages and limitations.
There are three main techniques for restoring developmental potential to a somatic nucleus. The nuclear transfer, by which the genetic material of an oocyte or zygote is replaced with that of a differentiated cell. The cellular fusion is an hybridization between ES cells and somatic cells, generating tetraploid ES cell lines. The direct reprogramming bases on the retroviral mediated introduction of a small group of transcription factors able to induce a pluripotent state (Adapted from stem book).

a) Somatic cell nuclear transfer (SCNT).

It has been described in 1997 by*Wilmut et al.*[98], who showed that adult somatic cells could be reprogrammed back into an undifferentiated embryonic state by transferring diploid donor nuclei into enucleated MII oocytes that are activated on, or after transfer. The reconstructed embryos are then cultured and selectedembryos transferred to surrogate recipients for development to term.Unfortunately, since then, attempts to generate patient-specific cells using SCNT have proven unsuccessful [99–101].

b) Cell fusion.

There are many examples in literature showing that a pluripotent phenotype arise following the fusion of murine somatic cells to EC [102], embryonic germ [103], and ES[104,105] cells. These studies seemed to promise that somatic-stem cell fusion might be an appealing alternative to inefficient and challenging NT.

It was hoped that this system could be used for either the study of the mechanisms of nuclear reprogramming or ,possibly, the direct production of patient-specific pluripotent stem cells. In *2005 Cowan et al*[106]*.* demonstrated that this capacity to reprogram somatic cells is conserved in human, as well as in mouse.

Cowan et al. fused hES cells with human BJ fibroblasts **(Fig. 29)** and assayed the ability of hybrid cells to differentiate in vitro and in vivo. They found that :

- when cultured in suspension, hybrid cell lines formed embryoid bodies (EBs),
- after injection into nude mice , they formed teratomas,
- both a teratoma (**Fig. 30**, C to E) and EBs (not shown) contained cells expressing βIII-tubulin (neurectoderm) muscle-specific myosin (mesoderm) and alpha-fetoprotein (endoderm).

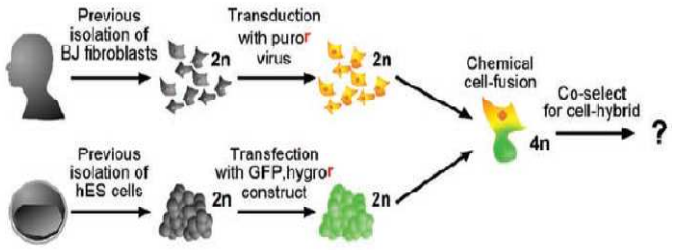

Figure 29.Fusion of hES cells and human somatic cells. Somatic and hES cell lines were stably transduced or transfected with independent drug-resistant markers . In a second step, they were treated with PEG to induce cellfusion. The selection of cell hybrids was achieved by growing fused cells in standard culture medium of hES cells inthe presence of antibiotics (Adapted from Chad A. Cowan,*Science* **309**, 1369 ,2005).

Hybrid cells also expressed the embryonic gene Rex-1, encoding for a retinoic acid–regulated zinc-finger protein expressed in ES cells (not shown).

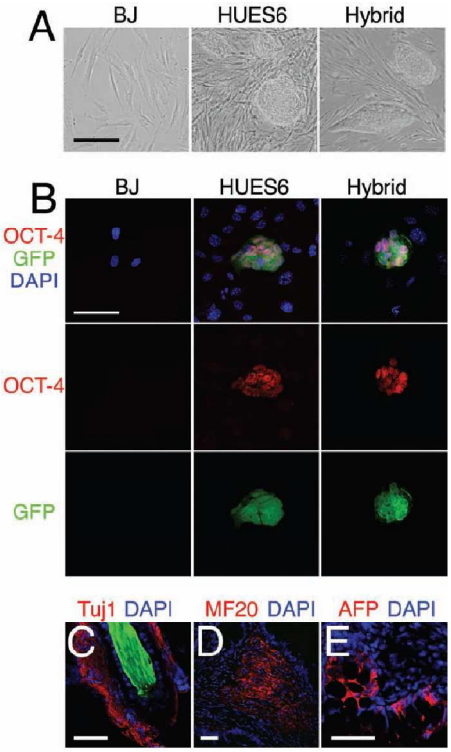

Figure30. Hybrid cells phenotype.
(A) Drug-resistent hybrid cells shown a HES cells –like morphology **(B)** Both HES cells and hybrid cells expressed the GFP (green) and the transcription factor OCT4 (red), whereas the GFP-negative BJ fibroblasts cells were negative for Oct4. **(C)** Hybrid cells-derived teratomas showed various cell types, including neurons expressing a neural-specific tubulin (Tuj1, red) **(D)**, skeletal muscle expressing myosin heavy chain (MF20, red)and **(E)**alpha-fetoprotein(AFP,red) (Adapted from Chad A. Cowan,*Science* **309**, 1369 ,2005).

c) *Direct reprogramming.*

Despite the initial xcitement, the fusion of ES and somatic cells, as well as the subsequent reprogramming, resulted to be quite inefficient [105–107], limiting usefulness of this approach to the study of the genetics and epigenetics of reprogramming. Moreover, the presence of two complete genomes put severe limits to the utility of this methodology for the study of reprogramming and represented an enormous technical barrier to the production of autologous stem cells.

However, these works strongly suggested that unfertilized eggs and ES cells contain factors that are sufficient to confer totipotency or pluripotency to somatic cells.

This awareness has inspired the subsequent development of the third strategy, the direct reprogramming.

This brilliant approach was described for the first time in 2006, by*Yamanaka and Takahashi*[97].They reported that mouse embryonic fibroblasts (MEFs) and adult tail tip fibroblasts could be reprogrammed back to a pluripotent state by introducing four transcription factors (Oct3/4, Klf4, Sox2, and c-Myc) *via* retroviral delivery, coupled to reactivation of endogenous loci of genes that are essential to pluripotency: Oct4 and Nanog.

They termed these cells "induced pluripotent stem" (iPS) cells[97].Detailed characterization revealed that iPS cells share many features with ESCs (**fig.33-34-35**), such as morphology, marker genes expression, immortal proliferation and pluripotency, as defined by their ability to generate teratomas and differentiate into all the lineages of the three germ layers, including germ cells that can ultimately give rise to offspring [97,108–110].

In a first step of their study, *Yamanaka et al*.selected and introduced 24 candidate genes intomouse embryonic fibroblasts (MEFs)(**Box1**) and generated, in this way, 22 Fbx15 expressing colonies **(Fig.31B),** where Fbx15 is a marker specifically expressed in mouse ES cells and early embryos. About an half of these clones exhibited morphology similar to ES cells, including a round shape, large nucleoli, and scant cytoplasm **(Fig.31C).**

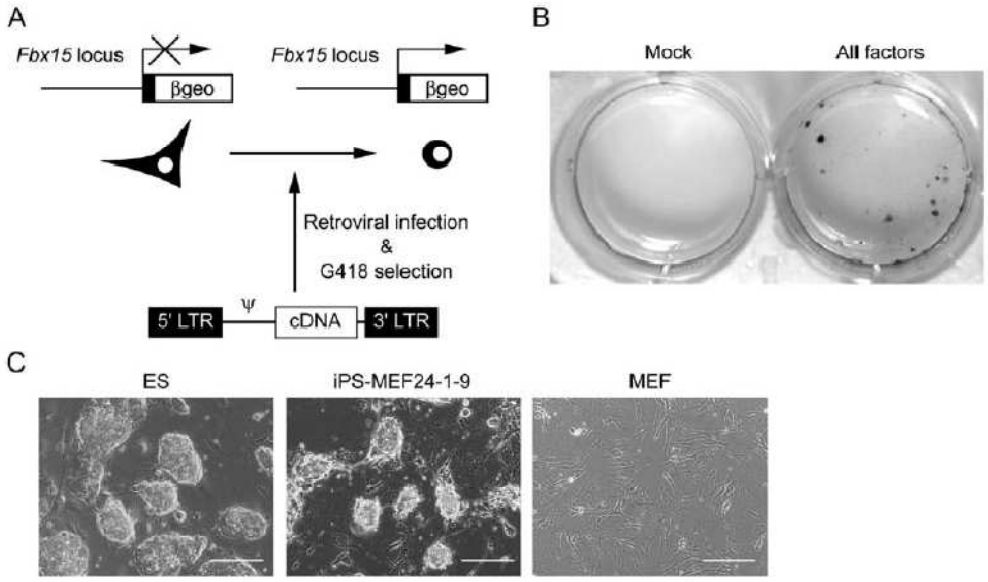

Fig.31. Generation of iPS Cells from MEF Cultures via 24 Factors(A) Experimental Strategy **(B)** G418-resistant colonies resulting from the transduction with a combination of 24 factors. Cells were stained with crystal violet 16 days after infection. **(C)** Morphology of ES cells, iPS cells and MEFs. Scale bars = 200 mm. (Adapted from Takahashi and Yamanaka, volume 126, Issue 4, 25 August 2006, Pages 663–676).

Next, by removing individual factors from the 24 genes pool , they could identify 10 factors (3, 4, 5, 11, 14, 15, 18, 20, 21, and 22) whose individual withdrawal from the bulk transduction pool resulted in no colony formation, 10 days after transduction, and fewer colonies 16 days after transduction.Interestingly, transduction of MEFs with the pool of these 10 factors resulted in increased frequency of colony formation, compared to the original 24 genes pool.

Yamanaka et al. also evaluated the formation of colonies after withdrawal of individual factors from the 10-factor pool transduced into MEFs **(Fig.32B).**Remarkably, Fbx 15 expressing colonies did not form when either Oct3/4 (factor 14) or Klf4 (factor 20) were removed. Removal of Sox2 (factor 15) resulted in only a few Fbx 15 expressing colonies. After c-Myc withdrawal (factor 22), Fbx 15 expressing colonies were more numerous, but they had a flatter, non-ES-cell-like morphology.

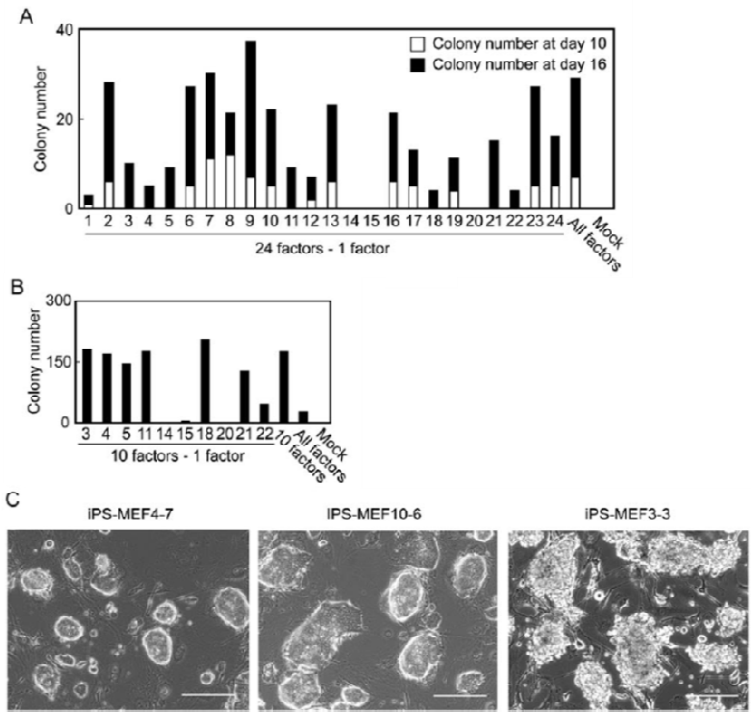

Figure32. Identification of the 4-factors-pool(Adapted from Takahashi and Yamanaka, volume 126, Issue 4, 25 August 2006, Pages 663–676).

These results allowed to identifyOct3/4, Klf4, Sox2, and c-Myc as "main players" in the generation of iPS cells from MEFs. In particular, they found that :

- Oct3/4 and Sox2 were essential for the generation of iPS cells

- Nanog was dispensable
- the two tumor-related factors c-Myc and Klf4 were essential factors and could not be replaced by other oncogenes including E-Ras, Tcl1, b-catenin, and Stat3 (**Fig.32A and 32B)**.

RT-PCR analysis revealed that, iPSMEF10 and iPS-MEF4 clones expressed the majority of ES marker genes, with the exception of Ecat1**(fig.33).**

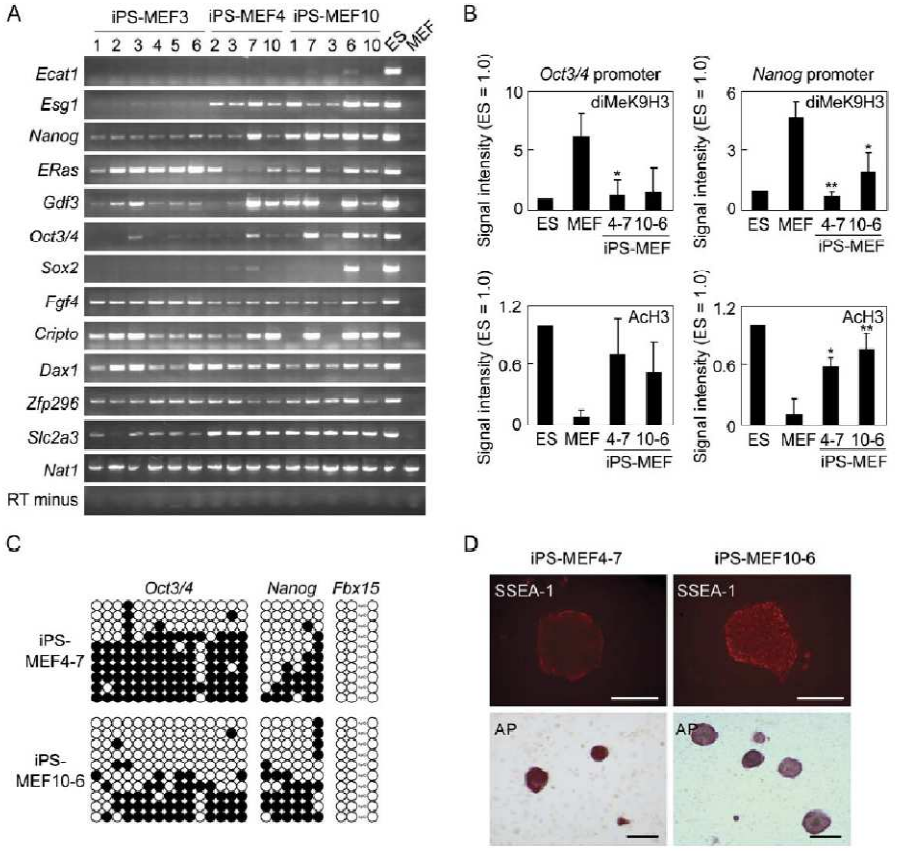

Figure 33. Gene-Expression Profiles of iPS Cells.
(A) RT-PCR profiling of IPS-MEFs3-4-10. **(B)** Chromatin immunoprecipitation analyses.
(C) CpG dinucleotides in these promoters remained partially methylated in iPS cells. **(D)** Immunostaining for alkaline phosphatase and SSEA-1 (Adapted from Takahashi and Yamanaka, volume 126, Issue 4, 25 August 2006, Pages 663–676).

Moreover, the promoters of Oct3/4 and Nanog showed an increased acetylation of histone H3 and decreaseddimethylation of lysine 9 of histone H3 **(Fig.33B).**

From the global gene expression point of view, iPS cells were clustered closely with ES cells but separately from fibroblasts and their derivatives **(Fig.34A).** In particular, iPS-MEF4 and iPSMEF10 cells expressed alkaline phosphatase and SSEA-1 **(Fig. 33D).**

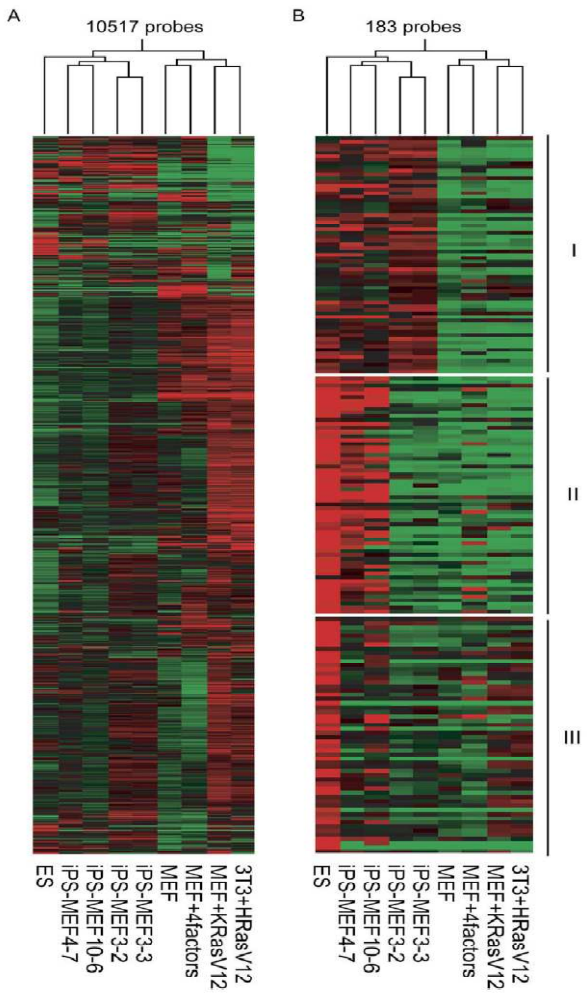

Figure 34. Pearson correlation analysis of the global gene-expression profiles in ES cells, iPS cells, and Fbx15bgeo/bgeo MEFs by DNA microarrays(Adapted from Takahashi and Yamanaka, volume 126, Issue 4, 25 August 2006, Pages 663–676).

The iPS cells pluripotency was also analysed by teratoma formation **(Fig.35).** Histological examination revealed that the majority ofiPS-MEF10 and iPS-MEF4 clones exhibited pluripotency (meant as the capability to differentiate into all three germ layers, **fig. 35D**).

Hence, iPS-MEF4 and iPS-MEF10 cells were similar, but not identical, to ES cells.

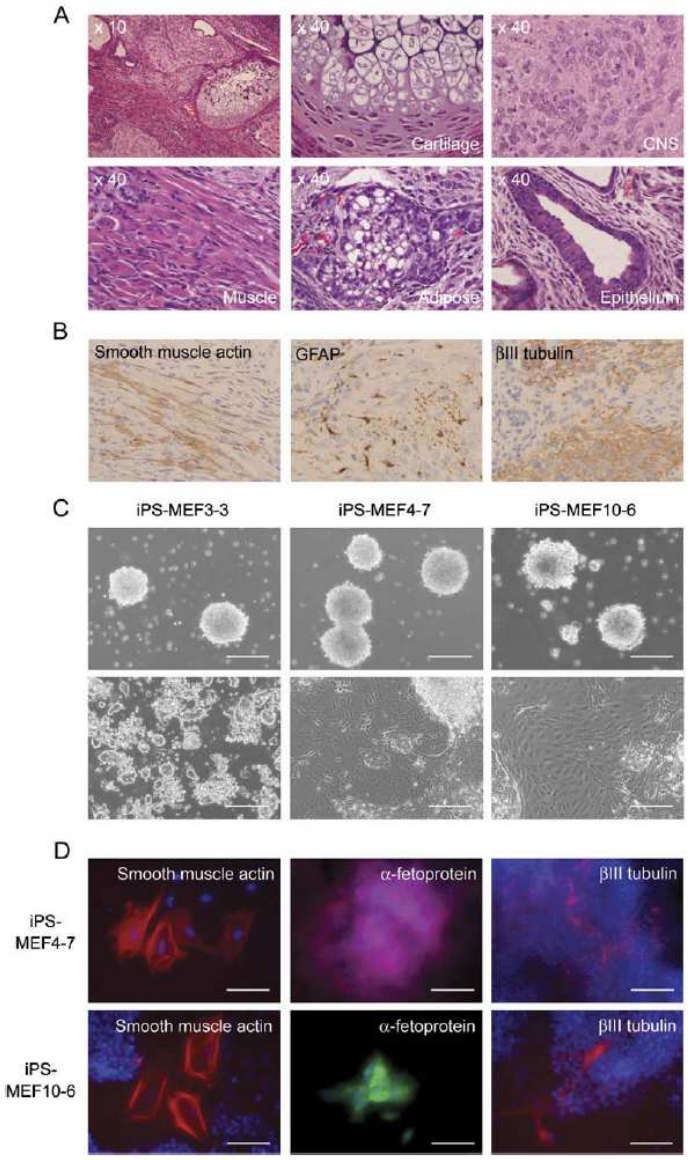

Figure 35. Pluripotency evaluation of iPS-MEF10 and iPS-MEF4 clones.

(A) Tissues present in teratomas derived from iPS-MEF4-7 cells. When grown in tissue culture dishes, the embryoid bodies from iPS-MEF10 and iPS-MEF4 cells attach to the dish bottom and initiate differentiation**(B)**Ddifferentiation into neural tissues and muscles in teratomas derived from iPS-MEF4-7.**(C)** Embryoid bodies from iPS-MEF3 cells remained undifferentiated even when cultured in gelatin-coated dishes These data confirmed pluripotency of iPS-MEF10 and iPS-MEF4 and nullipotency of iPS-MEF3 in vitro.

(D) Immunostaining for germ layers markers. fter 3 days, immunostaining detected cells positive for a-smooth muscle actin (mesoderm marker), a-fetoprotein (endoderm marker), and bIII tubulin (ectoderm marker)*(Adapted from* Takahashi and Yamanaka, volume 126, Issue 4, 25 August 2006, Pages 663–676*).*

Box1. Fibroblast employnment in reprogramming experiments. So far, fibroblasts have been the main substrate for cell fate reprogramming to generate neurons, but other cell types, including somatic cells such as hepatocytes as well as germ cells, have been successfully reprogrammed into functional iNs, demonstrating that interlineage transdifferentiation is possible (Marro S et al., 2011; Tursun B et al., 2011). Nevertheless, fibroblasts remain the preferred cell type due to their relative availability. Infact, since fibroblasts can be easily obtained from patients through minimally invasive methods, the generation of patient-specific cells is relatively simple.

Another important factor that must be considered in cell fate reprogramming is the origin of the cell lineages. Fibroblasts differentiate from mesenchymal progenitor cells, some of which are derived from neural crest lineages. Neural crest cells originate in the ectoderm on the dorsal tip of the early embryonic neural tube. From there, they progress through an epithelial–mesenchymal transition and pervasive migration, ultimately differentiating into an array of tissues throughout the body. Consequently, fibroblasts share a neuro-ectodermal lineage with neuronal cells, unlike, for example, hepatocytes, which are derived from the endoderm. Moreover, fibroblast cultures are likely heterogeneous in cell types and often contain neural crest-derived stem cells (Bayreuther K et al., 1988). These cultures may contain multipotent stem cells with the capacity to differentiate into neurons, due in part to their shared lineage. Therefore, easy access and lineage features make fibroblasts the favorite cell type for reprogramming to neurons.

2.2. Induced pluripotency by defined factors in human somatic cells.

iPS cells can be generated also from adult Human Dermal Fibroblasts (HDFs) and other somatic cells(i.e. IMR90 fetal fibroblast line[111], as well as post-natal fibroblasts[112]) by retroviral transductionof two different cocktails of factors:

-the so-called “Yamanaka factors”, Oct3/4, Sox2, Klf4, and c-Myc[112]

- OCT4, SOX2,NANOG, and LIN28[111]**.**

So-generated human iPSCsfrom adult HDFs and other somatic cells are similar to hES cells for what concerns morphology, proliferation, feederdependence, surface markers, gene expression, promoteractivities, telomerase activities, in vitro differentiation,and teratoma formation**(fig.36-37)**[112].

Remarkably, Oct3/4, Sox2, Klf4, and c-Myc expressing retroviruses arestrongly silenced in human iPS cells, indicating that the new pluripotent state acquired by theseelements do not depend oncontinuous expression of the transgenes for self renewal[112].

Remarkably, fibroblasts are not the only kind of somatic cell which may be reprogrammed. In humans, many different cell types have been reprogrammed, including keratinocytes [113,114], CD34+ hematopoietic stem cells [115], cord blood-derived CD133+ stem cells [116], cord blood-derived endothelial cells [117], melanocytes [118], neural stem cells

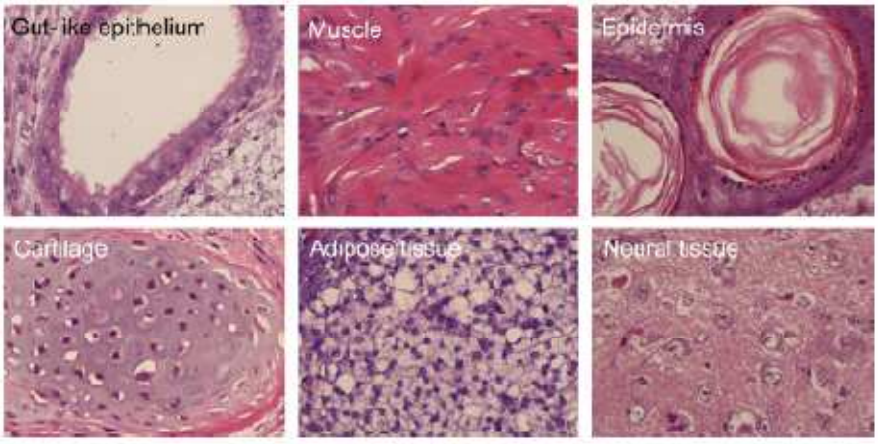

Figure 36. Teratoma Derived from Human iPS Cells.
hIPs were transplanted subcutaneously into four parts of a SCID mouse. The teratoma derived from iPS cells was stained for hematoxylin and eosin (adapted from Takahashi, K. *et al.,* 2007; Volume 131, Issue 5, 30 November 2007, Pages 861–872.

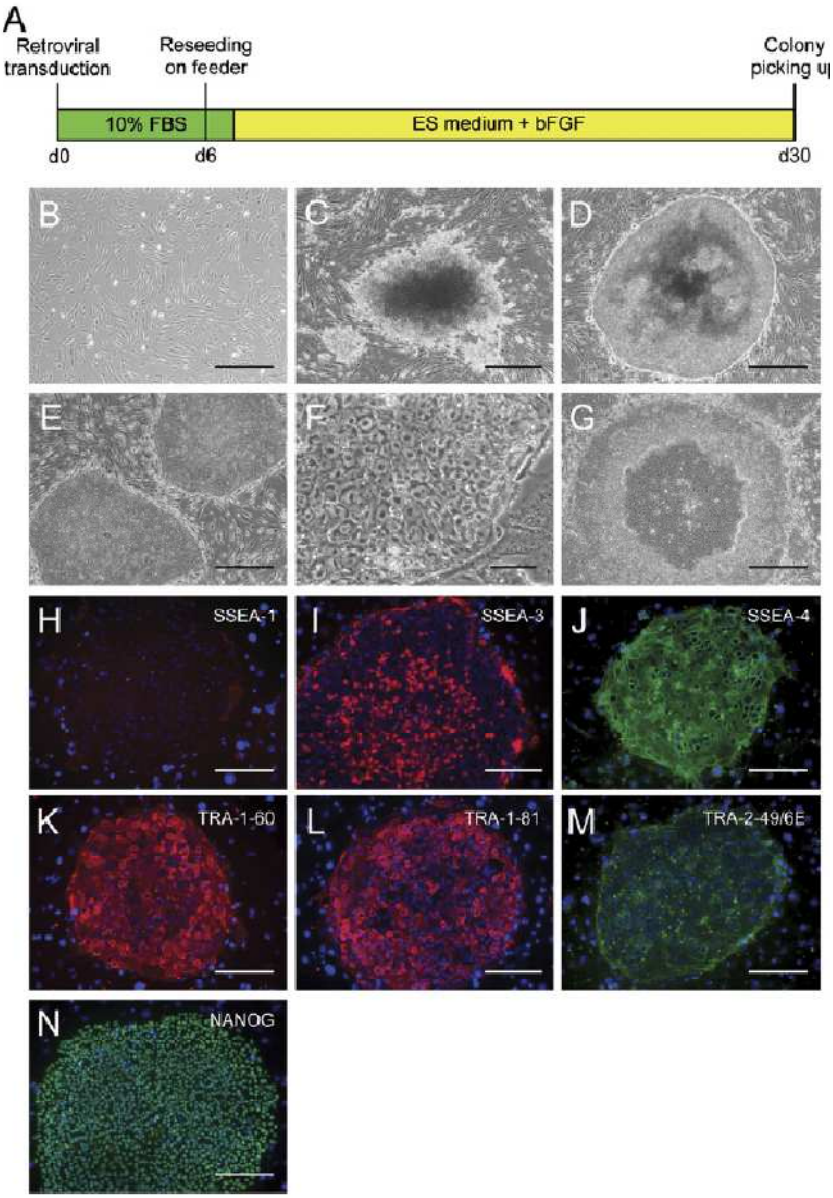

Figure 37. iPS Cells from Adult HDF.

(A) iPS cell generation protocol.
(B) Morphology of HDF.
(C) Example of non-ES cell-like colony.
(D) hES cell-like colony.
(E) Typical morphology of iPS cell line at
passage number 6.
(F) Image of iPS cells with high magnification.
(G) Spontaneously differentiated cells in the center part of human iPS cell colonies.
(H–N) Immunoprofiling for SSEA-1 (H), SSEA-3 (I), SSEA-4 (J), TRA-1-60 (K), TRA-1- 81 (L), TRA-2-49/6E (M), and Nanog (N). Nuclei were stained with Hoechst 33342 (blue). Bars = 200 mm (B–E, G), 20 mm (F), and 100 mm (H–N).
(adapted from Takahashi, K. *et al.,* 2007, Volume 131, Issue 5, 30 November 2007, Pages 861–872)

(NSCs)[119], amniotic fluid-derived cells [120], CD34+ peripheral blood cells from patients with myeloproliferative disorders [121], adult human adipose stem cells from lipoaspirate [122], human mesenchymal-like stem/progenitor cells of dental tissue origin[123] and mesenchymal stem cells from umbilical cord matrix and amniotic membrane[124].

The original work of Takahashi and Yamanaka in 2006 demonstrated the possibility of generating iPS cell colonies by the co-transduction of Oct3/4, Sox2, Klf4 and c-Myc. Apparently,

the most important factor is Oct3/4, since its expression is highly specific for pluripotent stem cells and cannot be replaced by other members of the Oct family[125].

Moreover,the ectopic expression of Oct3/4 alone is sufficient to generate iPS cells from human NSCs derived from human fetal brain tissue **(Fig. 38)**[126].

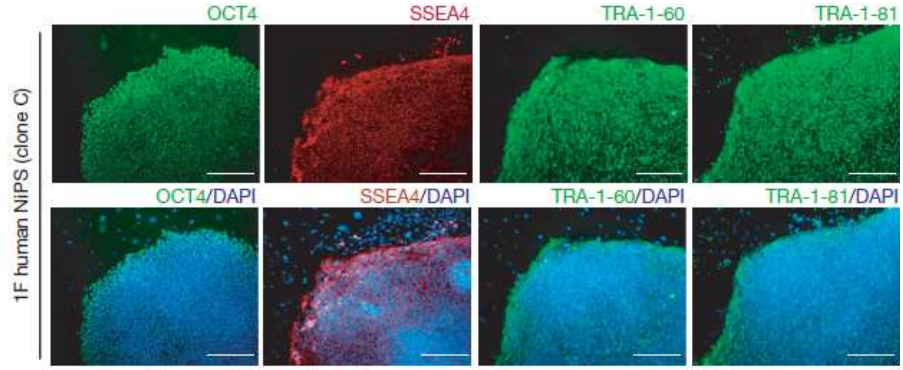

Figure 38. 1F human NSC-derived iPS cell colony. Analysis of pluripotency and surface markers (OCT4, SSEA4, TRA-1-60 and TRA-1-81) in 1F human NiPS cells. Nuclei are stained with DAPI (blue). Scalebars, 250 mm. (Adapted from Kim et al.,2009; *Vol 461| 1 October 2009|*

Clones from one-factor iPS cell colonies are able to generate teratomas and adult chimeric mice.

These studies revealed the importance of Oct4 in inducing pluripotency in NSCs, although it must be emphasized that these cells endogenously express the rest of the Yamanaka factors, as well as several intermediate reprogramming markers, which possibly facilitates reprogramming in the absence of exogenous addition of these factors.

- ***Generation of iPS by alternative combination of factors***

  It has been subsequently shown that, in addition to the original "Yamanaka cocktail ", it is possible to generate iPS cells by retroviral transduction of several other factors combinations. Among them :

- Oct4 and Sox2 with Lin28 and Nanog [117,127],
- Oct4 together with either Klf4 or c-Myc [128],
- Oct4, Sox2, Nanog [129]
- Oct4 and Sox2 [116,130,131],

- Oct4 and Klf4[132],
- Sox2, c-Myc and Tcl-1A [133].

Moreover, it has been studied if and how each of the four "Yamanaka genes" may be eliminated or replaced. **Sox2**has been reported to be dispensable for reprogramming neural progenitor cells (Eminli et al., 2008), and also melanocytes and melanoma cells [118].

Klf4 can be replaced with Esrrb, an orphan nuclear receptor, in reprogramming mouse embryonic fibroblasts (MEFs) [134]. Interestingly, it has been shown impossible to replace **Oct4** with its closely related family members Oct1 and Oct6 [125] to date. However a recent report describes how the nuclear receptor Nr5a2 can replace exogenous Oct4 in the reprogramming of murine somatic cells to iPS cells[135].

In summary, these studies reveal that the differences needed in the cocktail of factors for reprogramming specific cell types are directly related to the endogenous levels of these factors in the target cell(s).

2.3. Clinical employment of iPS cells: limitations and possible solutions.

The progress from mouse to human iPSCs has opened the possibility of autologous regenerative medicine whereby patient-specific pluripotent cells could be derived from adult somatic cells. However, several **limitations** of most existing iPSCs prohibittheir usage in the clinical setting [136]:

- virus-mediated delivery of reprogramming factors introduces unacceptable risks of permanent transgene integration into the genome. The resulting genomic alteration (insertional mutagenesis) and possible reactivation of viral transgenes pose serious clinical concerns.
- reprogramming factors Klf4 and c-Myc are oncogenic.
- iPSC reprogramming is an inefficient and slow process.

For these reasons, several alternative strategies have been developed, as reported in the next paragraph.

2.3.1. Generation of Induced Pluripotent Stem Cells Without Viral Integration.

Mouse and human iPS cells possess morphological, molecular and developmental features that closely resemble those of blastocyst-derived ES cells.

A major limitation of this technology is the use of potentially harmful genome-integrating viruses. A common strategy for avoiding genomic insertion has been to use a different vector for input: plasmids, adenoviruses, and transposon vectors have all been explored.

In 2008, it was demonstrated that it is possible to derive mouse induced pluripotent stem (iPS) cells from fibroblasts and liver cells by using non integrating adenoviruses transiently expressing Oct4, Sox2, Klf4, and c-Myc or by repeated transfection of two expression plasmids**(Fig. 39),** one containing the complementary DNAs (cDNAs) of Oct3/4, Sox2, and Klf4 and the other containing the c-Myc cDNA, into mouse embryonic fibroblasts[137].

However, the frequency of reprogramming achieved by this approach is extremely low and a high percentage of clones are tetraploid.

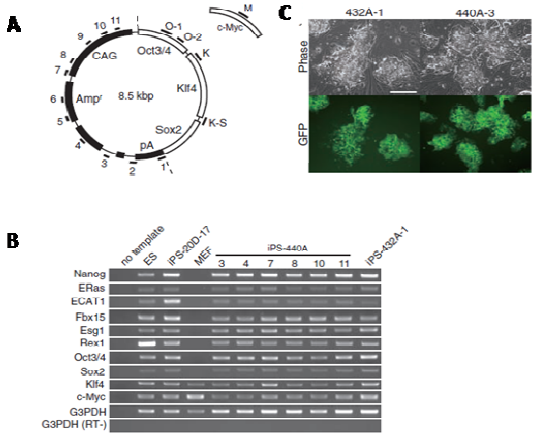

Figure 39. Generation of virus-free iPS cells.
(A) Expression plasmids for iPS cell generation. The three cDNAs encoding Oct3/4, Klf4, and Sox2 were connected in this order with the 2A peptide and inserted into the pCX plasmid (pCX-OKS-2A). In addition, the c-Myc cDNA was inserted into pCX (pCX-cMyc).(B)Gene expression. Total RNAs isolated from ES cells, retrovirus-induced iPS cells (clone 20D-17), plasmidinduced iPS cells (clones 440A-3, -4, -7, -8, -10, and -11 and clone 432A-1), and MEFs were analyzed with RT-PCR (C) Colonies of virus-free iPS cells. Scale bar, 200 mm.(Adapted from *Okita et al., 2008,322 (5903): 949-953*).

2.3.2. Enhancing Reprogramming of Somatic Cells to Induced Pluripotent Stem Cells.

In general, the efficiency of the iPS cells generationprocess is poor when any of the approaches described above are used [125,138–140].

In order to improve the efficiency of inducing pluripotency and to avoid safety issues related to viral transduction and genomic integration, it would be ideal to reprogram somatic cells by a radically different approach, i.e. by treating them with small molecules, able to trigger the activation of gene circuitries which sustain the ES/iPS cell state.

Several chemicals have recently been reported to either enhance reprogramming efficiencies or substitute for specific reprogramming factors **(fig.40)**. In particular, it is possible distinguish two main classes of reprogramming drugs:

- molecules affecting chromatin modifications
- molecules influencing signal transduction pathways**(table 1)**.

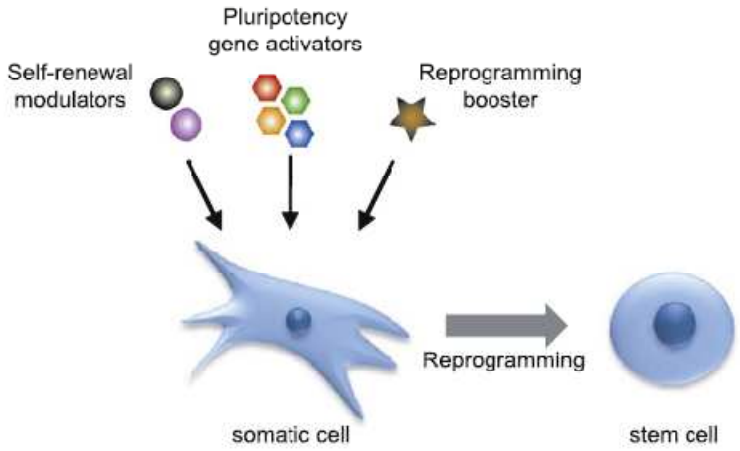

Figure 40. Reprograming somatic cells by treatment with small molecules. Molecules such as self-renewal modulators (e.g., LIF, MEK inhibitor, and GSK3 inhibitor), pluripotency gene activators and reprogramming boosters may be combinatorially used to induce efficient reprogramming. Reprogramming boosters : epigenetic modulators such as VPA or AZA that exert global activation or remove repressive chromatin mark, respectively (Adapted from Feng et al.,Nature Cell Biology 11, 197 – 203,2009).

- ***Chromatine remodelling drugs***

The covalent modification of nucleosomal DNA and core histones, and ATP-dependent chromatin remodelling, are important in the regulation of gene expression, DNA replication and many other biological processes. A huge number of proteins that carry out these modifications and chromatin remodelling has been identified.

In ESCs, the Yamanaka transcription factors were found to coregulate the expression of epigenetic factors that participate in the maintenance of self-renewal and pluripotency.

Oct4 and Sox2 co-bind to a group of genes that encode epigenetic factors impacting the covalent state of chromatin, such as Smarcad1, Myst3, Jmjd1a, and Jmjd2c[141,142]. Moreover, several findings imply that chromatine remodelling represents a major barrier preventing the complete reprogramming to iPS cells[97,143].

These general chromatin-modification and chromatin-remodelling proteins do not act alone, but interact with one another, often by forming large protein complexes that regulate higher-order chromatin structures and the accessibility of chromatin to various factors.

The stable inheritance of chromatin structure and changes to its accessibility are likely to be essential for all chromatin-associated biological processes.

DNA methylation and histone modification serve as epigenetic marks for active or inactive chromatin, and such epigenetic marks are heritable. In mammaliancells,DNA methylation occurs predominantly at CpG dinucleotides and is catalysed by two important classes of DNA methyltransferases.DNA methyltransferase 1 (Dnmt1) is amaintenance enzyme that methylates hemi-methylated CpG dinucleotides in the nascent strand of DNA after DNA replication[144], and its function is essential for maintaining DNA-methylation patterns in proliferating cells[145]. Dnmt3a and Dnmt3b are required for the initiation of de novo methylation in vivo and for establishing new DNA-methylation patterns during development[146–148]. Both Dnmt1 and Dnmt3a have been shown to interact with histone deacetylases (HDACs) and can repress transcription[149].

There are evidences showing that DNA methylation is an important epigenetic barrier that partially reprogrammed cells may encounter and fail to overcome[150].

The isolation of partially reprogrammed stable cell lines, which morphologically resembled mouse ESCs but displayed certain transcriptional and epigenetic differences from ESCs, supports this notion [97,143]. Despite the expression of several ESC-related genes such as Fbx15, Fgf4, and Zic3, chimeras could not be derived from such cell lines. Endogenous pluripotency genes such as Oct4 and Nanog were not fully reactivated as their respective promoters retained DNA methylation.

Recently, several reprogramming studies described how small molecules involved in epigenetic processes, such as AZA, VPA, and BIX can improve reprogramming efficiencyif combined with conventional reprogramming factors. [151,152]

Treatment with theDNMT inhibitor 5-aza-cytidine (**AZA**) induces partially reprogrammed cells to transit the reprogramming path and form iPSCs[153]. The iPSCs derived with AZA treatment reactivated endogenous Oct4, exhibited demethylation at the promoters of pluripotency genes, achieved viralsilencing, and formed teratomas when injected into severe combined immunodeficiency (SCID) mice.AZA also improved the number of ESC-like colonies by 4-fold [150].

Chemicals	Function	Yamanaka Factors Used	Species and Cel Type	Comments	References
BIX-01294	G9a histone methyltransferase inhibitor	CK	mouse fibroblast	CK + BIX-01294 enhances efficiency approximately five times more than CK and is able to replace S	(Shi et al., 2008a)
		CK	mouse NPC	CK + BIX-01294 enhances efficiency approximately 1.5 times more than OSKM and approximately eight times more than CK, and BIX-01294 is able to replace S	(Shi et al., 2008b)
		SKM		able to replace O in NPC reprogramming, but with extremely low efficiency	
RayK8644	L-type calcium channel agonist	CK	mouse fibroblast	CK + BIX-01294 + RayK8644 enhances efficiency ~15 times more than CK	(Shi et al., 2008a)
RG108	DNA methyltransferase inhibitor	CK	mouse fibroblast	CK + BIX-01294 + RG108 enhances reprogramming efficiency ~30 times more than CK	(Shi et al., 2008a)
AZA	DNA methyltransferase inhibitor	CSKM	mouse fibroblast	~4-fold increase in efficiency with OSKM and promotes full reprogramming	(Mikkelsen et al., 2008)
				~10-fold increase in efficiency with OSKM	(Huangfu et al., 2008a)
				~3-fold increase in efficiency with OSK	
dexamethasone	steroid glucocorticoid	CSKM	mouse fibroblast	increases the effect of 5' azacytidine by 2.6-fold	(Huangfu et al., 2008a)
VPA	histone deacetylase inhibitor	CSKM	mouse fibroblast	more than 100-fold increase efficiency with OSKM	(Huangfu et al., 2008a)
		CSK		~50-fold increase in efficiency with OSK	
		CSK	human fibroblast	10- to 20-fold increase compared to OSK	(Huangfu et al., 2008b)
		CS		VPA is able to replace K and M	
TSA	histone deacetylase inhibitor	CSKM	mouse fibroblast	~15-fold increase in efficiency with OSKM	(Huangfu et al., 2008a)
SAHA	histone deacetylase inhibitor	CSKM	mouse fibroblast	~2-fold increase in efficiency with OSKM	(Huangfu et al., 2008a)
PD0325901 + CHIR99021 (2i)	inhibitor of MEK and GSK3 respectively	CK	mouse NSC	together with LIF, promote ground state plurpotency in CK pre-iPSCs.	(Silva et al., 2008)
			mouse NPC	PD0325901 promotes growth of true iPSCs and inhibits growth of non-iPSCs	(Shi et al., 2008b)
A-83-01	TGF-β inhibitor	CSK	rat liver progenitor	together with LIF and 2i to maintain mESC-like rat iPSCs	(Li et al., 2009)
			human fibroblast	Together with LIF and 2i to maintain mESC-like human iPSCs	

Table 1. Examples of small molecules able to enhance the reprogramming process or to replace core reprogramming factors.O, Oct4; S, Sox2; K, Klf4; M, c-Myc. (Adapted from Feng et al.,Nature Cell Biology 11, 197 – 203,2009).

Besides AZA, many other chemical inhibitors have been tested for their capability of promote the reprogramming. Among them, several histone deacetylase (HDAC) inhibitors such as valproic acid (VPA), trichostatin A (TSA), and suberoylanilide hydroxamic acid (SAHA) significantly enhanced reprogramming efficiencies [130].

Remarcably, Huangfu et al. demonstrated that by treating cells with valproic acidfor a week it is possible to improve the percentage of Oct4-GFP-positive cells by more than 100-fold and 50-fold in case of for three-factor (OSK) and four-factor (OSKM) reprogramming, respectively[154].

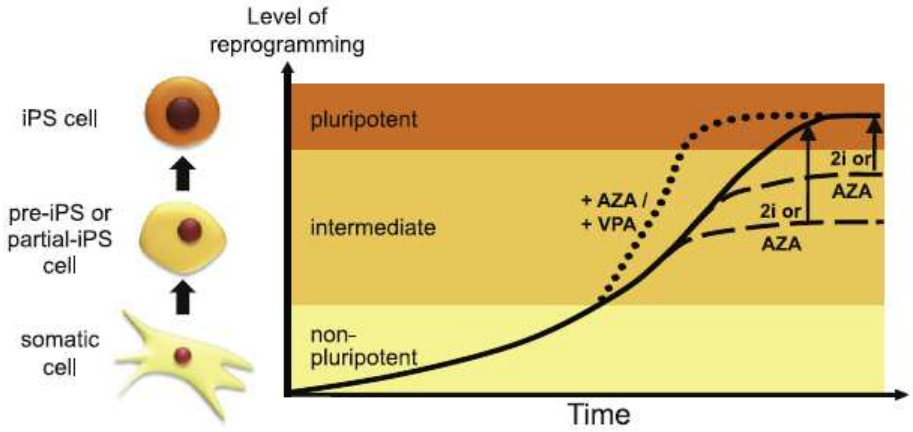

Figure 41.AZA and VPA promotefully induced pluripotency and accelerate thereprogramming kinetics (Adapted from Feng et al.,Nature Cell Biology 11, 197 – 203,2009).
).

In addition, combined AZA and VPA treatment induced Oct4-GFP-positive colonies 2 daysearlier than nontreated controls [130]. Hence,HDAC-inhibitors treatment could be useful to improve both the kinetics and efficiency of reprogramming.

Another important molecule is a well established inhibitor of G9a histone methyltransferase, named BIX-01294 (**BIX**). This drug was found to improve reprogramming efficiencies of OK-infected NPCs by approximately 8 fold [152](see **fig. 42).**

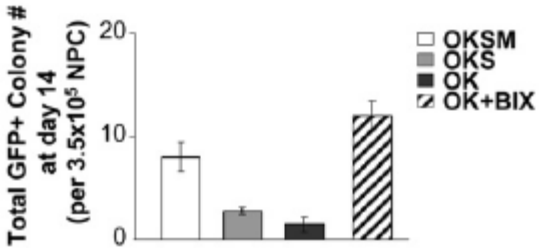

Figure 42. (Image taken from *Shi et al. Cell Stem Cell***3**, 568–574,2008).

G9a inhibition by BIX could facilitate the reactivation of Oct4 [155]and promote reprogramming, bypassing the need forexogenous Oct4 in SKM-infected NPCs.[152].Besides Oct4, recently several early embryonic genes that are inactivated by G9a have been identified (i.e. Nanog and Dnmt3l)[156]. This suggests that BIX, by inhibiting these repressive activities of G9a, could derepress pluripotency genes and induce passive demethylation and relaxation of chromatin.

- ***Signalling pathway modulation***

Reprogramming induce drastic molecular changes that involve both the upregulation of pluripotency genes and repression of differentiation genes. By blocking routes to differentiation, one may be able to more effectively direct transduced cells back along the desired path toward pluripotency.

TGFβpathway inhibition.The transforming growth factor beta (TGFβ) signaling pathway is involved in many cellular processes in both the adult organism and the developing embryo including cell growth, cell differentiation, apoptosis, cellular homeostasis and other cellular functions**(fig. 43).** TGFβ is a prototypical cytokine for induction of epithelial to mesenchymal transition and maintenance of the mesenchymal state[157].

A major end point of this signaling, in this context, seems to be downregulation of E-cadherin [158], an important factor for the maintenance of pluripotency of embryonic stem cells, recently suggested to be a regulator of *NANOG* expression [159].

In a recent study, it was shown that administration of the Alk5 inhibitor during expression of four reprogramming factors Oct4, Sox2, c-Myc, and Klf4, elicited a striking increase in the

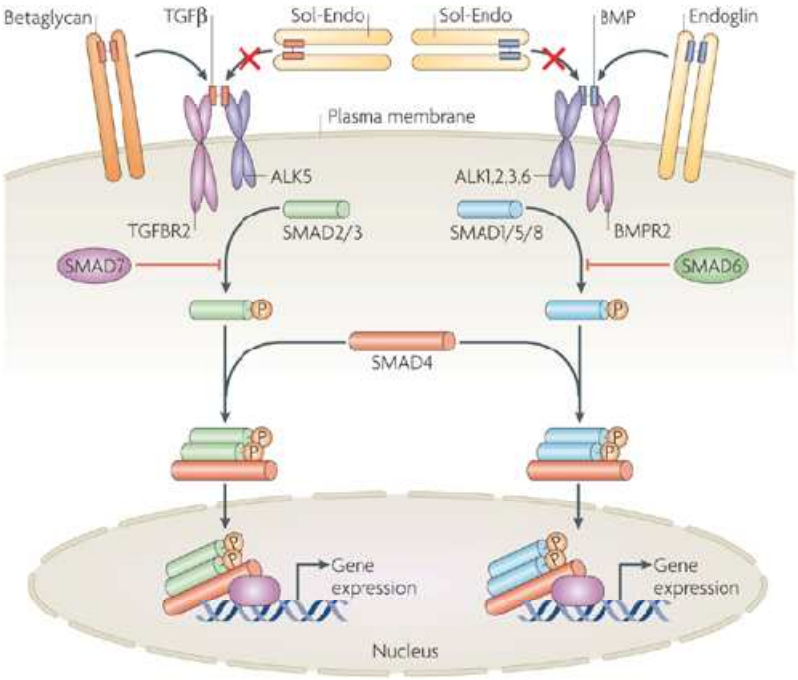

Figure 43.Tgfβ pathway. (Adapted from Nature Reviews/Molecular biology).

number of iPSC colonies [160]**(Fig.44A)**. Moreover Tgfβ signaling inhibition enabled faster iPSC induction**(fig.44B)** and allowed to bypass the requirement for exogenous cMyc or Sox2**(fig.44 C-D).**

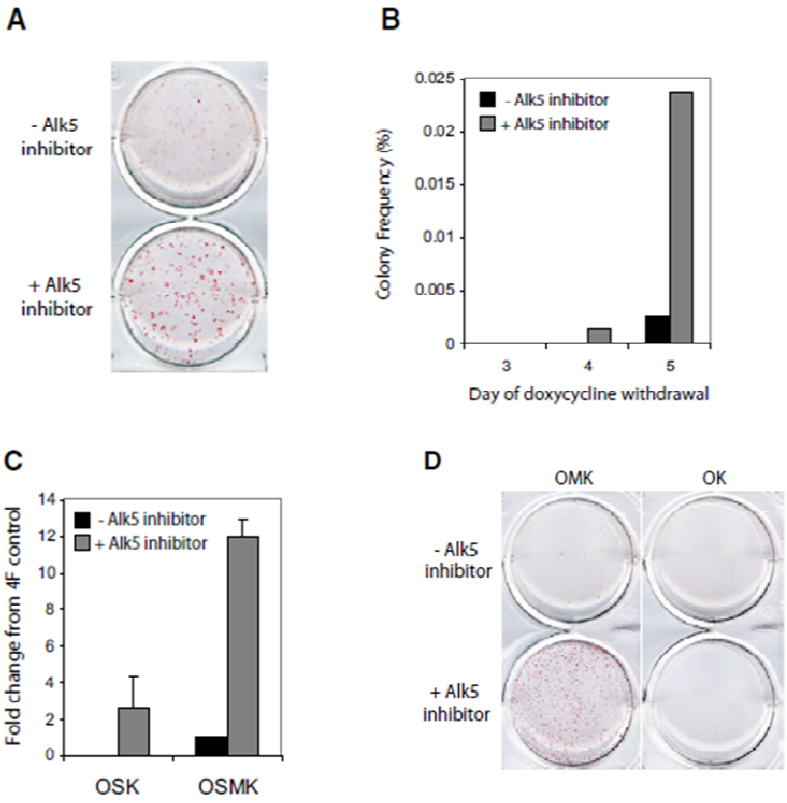

Figure44.Tgfβ Signal Inhibition Cooperates in the Induction of iPSCs and Replaces Sox2 and cMyc (Adapted from*N. Maherali and K. Hochedlinger, Curr. Biol.***19**, 1718–1723, 2009).

Wnt signaling activation.The Wnt/β-Catenin pathway (Wnt canonical pathway) regulates cell fate decisions during development of vertebrates and invertebrates**(fig.45).**

The stimulation of the Wnt canonical pathway can be used in combination with nuclear factors Oct4, Sox2 and Klf4 in order to increase somatic cells reprogrammingto an induced pluripotent state [161](see **fig. 46**). This is probably due to the fact that Tcf3, one of the key transcriptional regulators downstream of the Wnt pathway in embryonic stem cells, co-occupies almost all promoter regions occupied by ESC-specific transcription factors, including Oct4 and Nanog, and can regulate the expression of key ESC transcription factors [162–164].

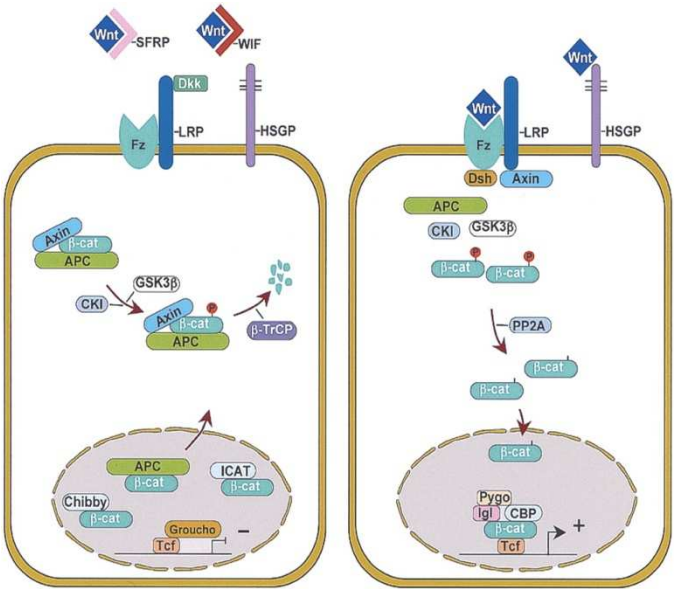

Figure 45. Wnt canonical pathway. The Wnt-ligand is a secreted glycoprotein that binds to Frizzled receptors, which triggers a cascade resulting in displacement of the multifunctional kinase GSK-3β from the APC/Axin/GSK-3β-complex. In the absence of Wnt-signal (Off-state), β-catenin, an integral cell-cell adhesion adaptor protein as well as transcriptional co-regulator, is targeted for degradation by the APC/Axin/GSK-3β-complex. Appropriate phosphorylation of β-catenin by coordinated action of CK1 and GSK-3β leads to its ubiquitination and proteasomal degradation through the β-TrCP/SKP complex. In the presence of Wnt binding (On-state), Dishevelled (Dvl) is activated by phosphorylation and poly-ubiquitination, which in turn recruits GSK-3β away from the degradation complex. This allows for stabilization of β-catenin levels, Rac1-dependent nuclear translocation and recruitment to the LEF/ TCF DNA-binding factors where it acts as an activator for transcription by displacement of Groucho-HDAC co-repressors. (Adapted fromGregorieff and Clevers, Genes Dev. 2005 Apr 15;19(8):877-90.).

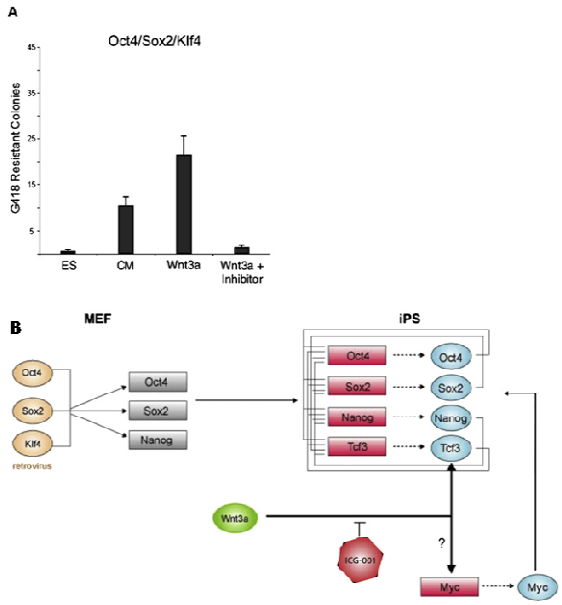

Figure46. Wnt Signaling Promotes Reprogramming of Somatic Cells to Pluripotency. (A) Soluble Wnt3a promotes the generation of iPS cells in the absence of c-Myc retrovirus (substrate:MEFs carrying a G418 resistance cassette downstream of the Oct4 promoter). ICG-001: inhibitor of the Wnt/b-catenin pathway strongly inhibite the effect of Wnt3a-CM on Myc- iPS formation. (B)The Wnt signaling pathway has been shown to connect directly to the core transcriptional regulatory circuitry of ESCs, suggesting a mechanism by which this pathway could directly promote the induction of pluripotency in the absence of c-Myc transduction (Adapted from *Marson et al., Cell Stem Cell**3**, 132–135 ,2008*).

p53 pathway inhibition.p53 is an estabished tumor suppressor-protein whose malfunction is involved in most human cancers[165]. However, the role of p53 is not restricted to tumor prevention. In fact, several studies have shown that p53 plays an active role during development thanks to its capability to inhibite or promote differentiation, depending on the cell type and lineage. For example, p53 knock-out mice are characterized by birth defects in neural tube closure, bone development and polydactyly[166].

p53 levels act as a fate switch between the mesodermal and ectodermal differentiation programs in vitro, redirecting differentiation from neuronal lineage to muscle when downregulated [167]. Moreover, p53 levels control the pluripotency and differentiation of ES cells through the regulation of Wnt signalling[168]. Importantly, under stress conditions, p53 inhibits the Nanog promoter toinduce differentiation in ES cells, sopreventing the proliferation of damaged cells with unlimited self-renewing capacities[169].

A wide range of of stress signals (i.e. overexpression of oncogenes such as c-Myc[170,171]) activate p53, leading to cell cycle arrest, a program that induces cell senescence/cellular apoptosis[172]. Klf4 can either activate or antagonize p53 depending on the cell cycle target and the level of expression[173]**(Fig.47).** Therefore, overexpression of c-Myc and Klf4 oncogenes seems to activate the p53 pathway, leading to cell cycle arrest and/or to apoptosis, and ultimately to reduced reprogramming efficiency.

These functional interactions among p53, cMyc, Klf4, Nanog may account for the well described capability of p53 to affect iPSCs generation. Recently, p53 has been demonstrated to play a crucial role in inducing pluripotency . In 2008, a a short-interfering RNA (siRNA) directed against the gene encoding for p53 (also known as TP53 in humans and Trp53 in mice) was described to enhance the efficiency of iPS cell generation by up to 100-fold, even when the oncogene c-Myc had been removed from the reprogramming gene combinations [174].

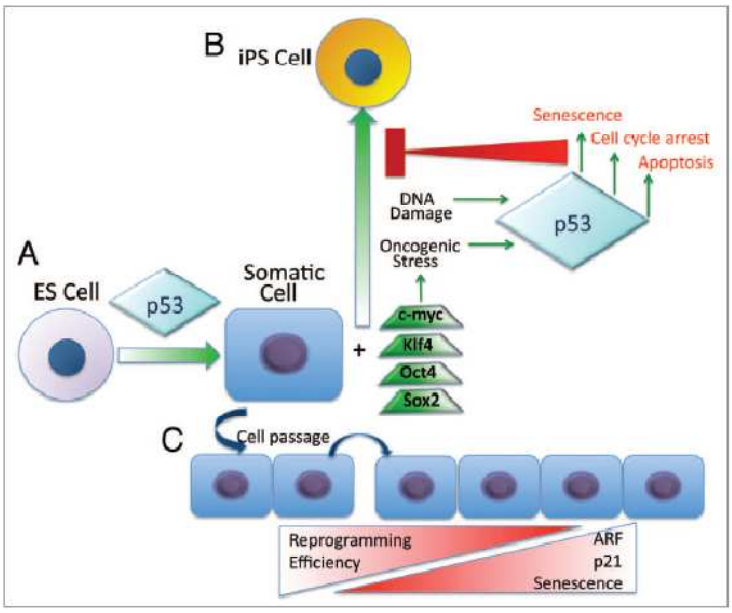

Figure 47. (A) During development the p53 pathway affect differentiation of ES cells to certain cell types. (B) The reprogramming of somatic cells to iPS cells is inhibited by p53. The induction of the pluripotant state through introduction of the Yamanaka factors C-myc, Klf4, Oct4 and Sox2 leads to an activation of p53. The various outcomes of p53 activation (senescence, cell cycle arrest and apoptosis) decrease the reprogramming efficiency, thereby forming a negative feedback loop. Hence, the disruption of the p53 pathway increases the efficiency of reprogramming but, simultaneously, removes the "guardian" of genomic integrity, resulting in an increased mutational burden (not shown).(C) The reprogramming efficiency is reduced when passaging of somatic cells prior to reprogramming is increased. In fact, it leads to senescence and cause an increasein p21 and p19ARFlevels, which in turn promote cell cycle arrest and p53 activation, respectively(Adapted from Menendez et al.,Cell Cycle 9:19, 3887-3891; October 1, 2010).

In 2009, five different worksshowed that the suppression or alteration of the p53 pathwayenhances the efficiency of human iPS cell generation [175–178](see **fig.48).**These works are extremely interesting as they provide suggestions about a molecular tool, p53 downregulation, available to facilitate changes of tissue identity.

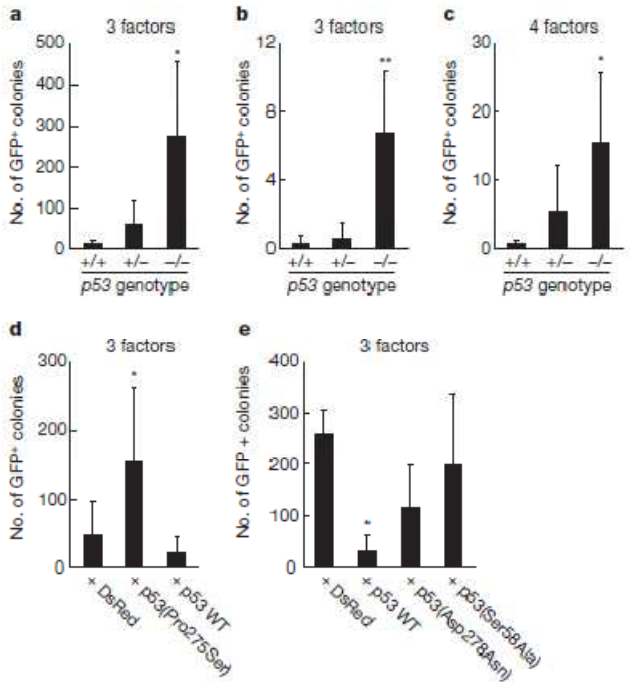

Figure 48. p53 and p21 suppress iPS cell generation. The suppressive effects of these tumour suppressor gene products on cell proliferation, survival or plating efficiency should contribute to the observed effect In addition, they may have direct effects on reprogramming(Yamanaka,2009).**(***Adapted from H. Hong et al., Nature***460**, 1132–1135 ,2009).

However, inactivation or suppression of the p53 pathway to enhance reprogramming efficiency may pose serious problems, since p53 inactivation can contribute to tumorigenesis by propagation of genomic instability. Thus, inhibition or alteration of p53 pathway couldincrease the reprogramming efficiency in global terms, regarding number of cells reprogrammed, but not in terms of safety, as an altered p53 pathway could render iPS cells with genomic instability and tumorigenesis. For these reasons, p53 downregulation, albeit potentially useful, has to be considered with extreme caution for clinical use and exploitation.

2.4. Direct transdifferentiation.

Transdifferentiation is a naturally occurring mechanism that was first observed in the regenerating lens of the newt, over 100 years ago (Wolff, G.,1895)[252]. This process implies a dedifferentiation step by which cells regress to a point where they can switch lineages and differentiate into another cell type **(Fig.49).**The " artificial transdifferentiation", also known as lineage reprogramming[180]has been more recently described and is the process by which one mature somatic cell gets converted into another mature somatic cell by avoiding the intermediate pluripotent state.

The first instance of transdifferentiation was reported in 1987 by Davis R.L. et al.,who showed

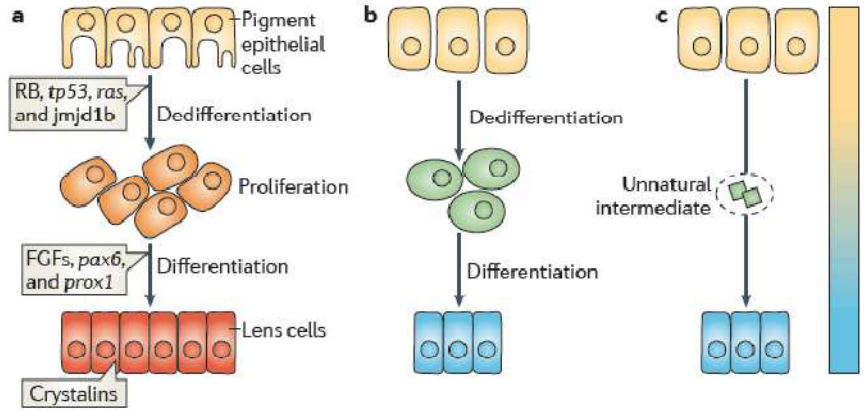

Figure 49. Transidifferentiation : Natural and artificial. (Adapted from Jopling et al.,Nat Rev Mol Cell Biol. 2011;12:79–89).

that expression of a myoblast-specific, subtracted cDNA transfected into mouse C3H10T1/2 fibroblasts (where it is not normally expressed) is sufficient to convert them to stable myoblasts**(fig. 50A).**

Subsequent studies showed that the erythroid megakaryocyte- affiliated transcription factor GATA1, when ectopically expressed in cell lines of monocytes (macrophage precursors) at high levels, induce the expression of erythroid-megakaryocyte lineage markers and also downregulate monocytic marker (**fig. 50B**).

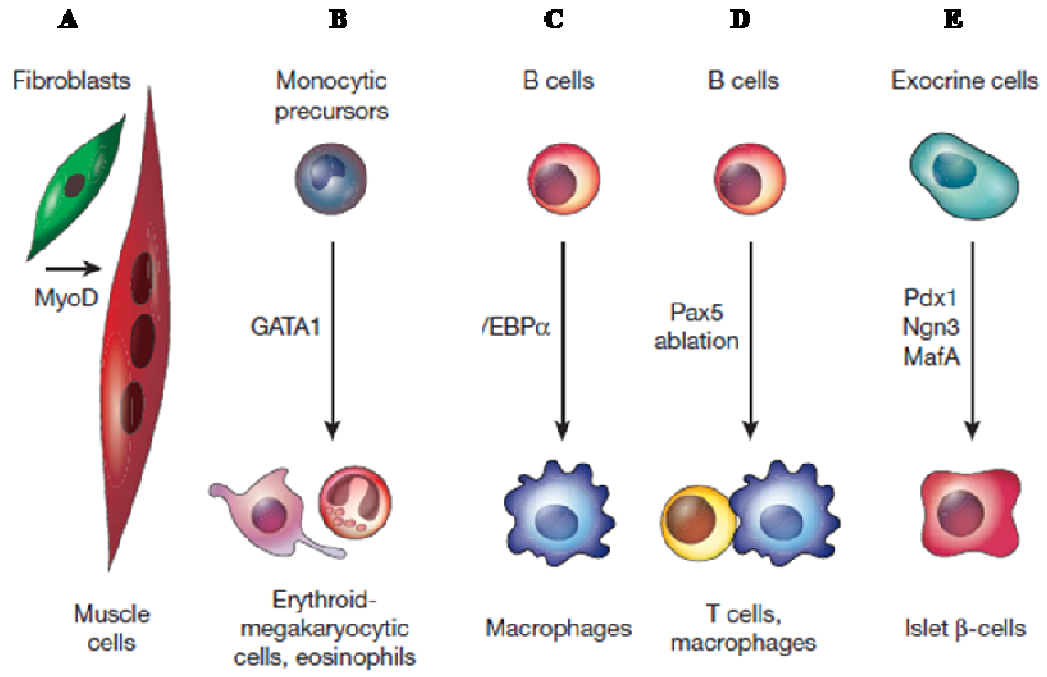

Figure50. Examples of cell fate switches achieved by transcription factor overexpression or ablation experiments(Adapted from Thomas Graf & Tariq Enver, *Nature* **462**, 587-594,2009| doi:10.1038/nature08533).

More recently it was shown that also fully differentiated cells can be switched: the transcription factor C/EBPa, involved in the formation of granulocyte-macrophage precursors,is able to convert committed B- and T-cell progenitors into functional macrophages at frequencies of about 100%. Also mature immunoglobulin-producing B cells can be switched, even if at lower frequencies [181] (**Fig. 50C**). Moreover, in 2007 it was demonstrated that transplantation of Bcl2-stabilized Pax5-deficient B cells into immunodeficient mice generates T cells, containing immunoglobulin rearrangements [182] (**Fig. 50D**).

As easily predictable, the efficiency by which transcription factors induce lineage conversions depends on the proximity of the cell type in question : greater distances may require additional factors acting at earlier common branch points. An explanatory example is the observation that switching of hepatic progenitors into endocrine pancreas β-cells only requires Ngn3[183], whereas to switch exocrine pancreas cells, alsoPdx1 and MafA [184]**(fig. 50E)** are require.

2.4.1. Direct reprogramming of mouse and human fibroblasts into functional neurons by defined factors.

In 2010,there was a great breakthrough in the emerging field of transdifferentiation, when Marius Wernig and co-workers described for the first time the direct conversion of mouse fibroblasts into functional neurons, by defined factors [185]. They screened 19 genes, specifically expressed in neural tissues or implicated in neural development, for their capability to induce this conversion. They found that just three factors (Brn2, Ascl1 and Myt1l, shortly "BAM"**)(see fig.51a)**can rapidly and efficiently convert mouse fibroblasts (derived from Tau-EGFP transgenic mice) into functional "induced neurons" (BAM-iN cells), expressing MAP2,Synapsin and Tubb3 **(fig.51d-e-f).** Moreover, individual analysis revealed that only ASCl1 can induce a neuronal phenotype in fibroblasts, albeit an immature one **(fig. 51i).** On the other hand, they also found that, although the single factor Ascl1 is sufficient to induce immature neuronal features, the additional expression of Brn2 and Myt1l gives rise to iN cells with efficiencies up to19.5%. Moreover, three-factor iN cells display functional properties of mature neurons, such as the generation of trains of action potentials, integration into a preexisting neuronal network and iN-iN synapse formation(**fig.51i**). Finally, the most part of iN cells described by Vierbuchen et al. showed an excitatory phenotype and expressed the vesicular glutamate transporter 1 vGLUT1. Conversely, a lower proportion of them expressed markers of GABAergic neurons.

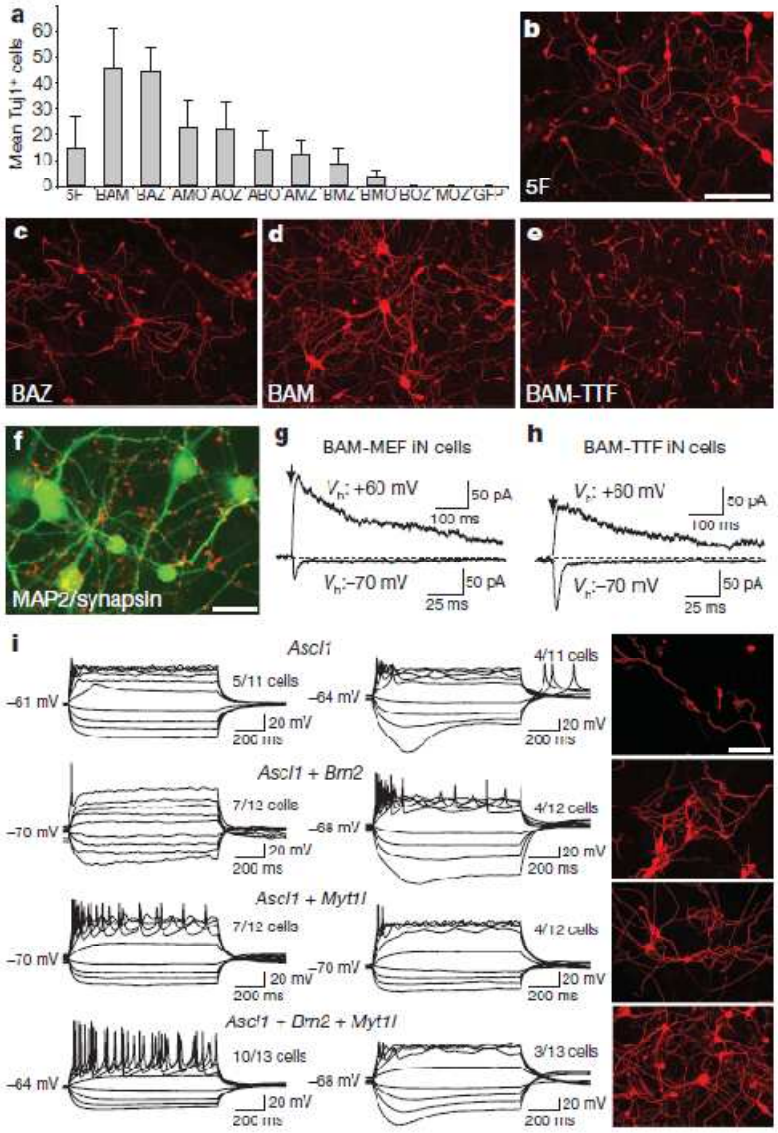

Figure 51. Induction of functional iN cells by 3 factors.(a)Breakdown experiments identificating the 3F pool that is sufficient to efficiently generate iN cells (Adapted from Vierbuchen et al.,Nature. 2010 February 25; 463(7284): 1035–1041).

From this point on, several groups independently used the so-called BAM cocktail in addition to other neurogenic factors to directly convert fibroblasts into iNs[186–190].

2.4.2.Generation of iN cells from human fibroblasts.

Taking advantage of ectopic expression of the BAM cocktail, Pfisterer et al. [188]could achieve the reprogramming of embryonic and adult human fibroblasts to human iNs (hiNs) with efficiencies of 16 and 4 %, respectively. They observed that the successful conversion of human fetal fibroblasts to immaturehiNs required 20 days of transgene expression.

In the same year, Pang et al. showed that the BAM cocktail, when combined with the basic helix-loop-helix transcription factor *NeuroD1*, is also able to convert fetal and postnatal human fibroblasts into iN cells displaying typical neuronal morphologies and expressing multiple neuronal markers, even after downregulation of the exogenous transcription factors. Remarkably, the most part of these human iN cells were able to generate action potentials and to receive synaptic contacts when co-cultured with primary mouse cortical neurons[187]**(fig. 52**).

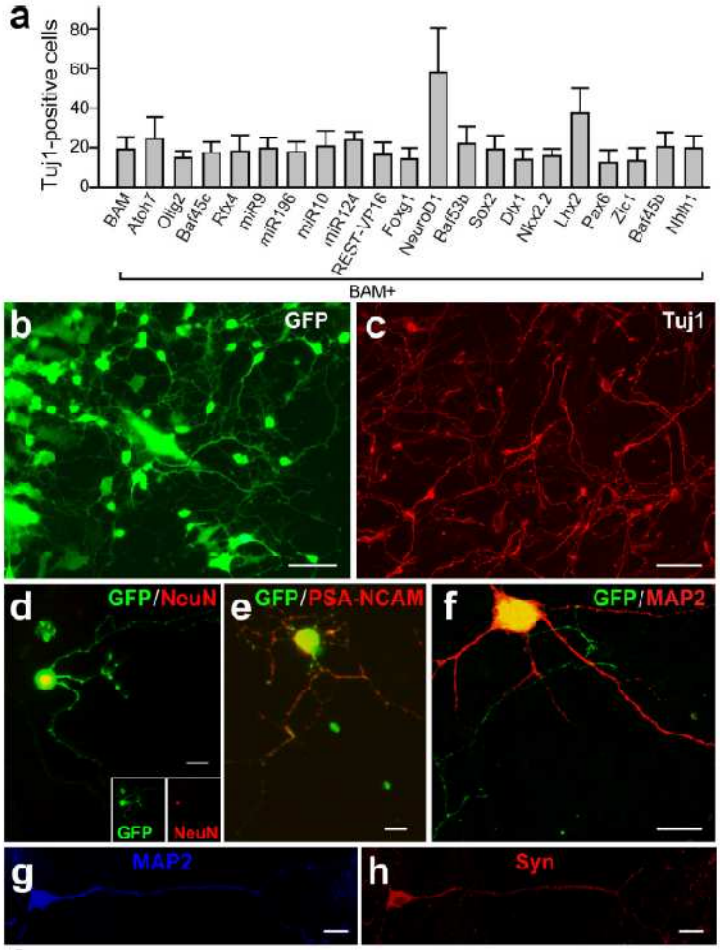

Figure 52. Characterization of BAM+NeuroD1 iNs derived primary human fetal fibroblasts. (a) Tuj1-positive BAM-iN cells + additional factors, quantified 3 weeks after transgenes activation. **(b)**Neuronal morphologies arising three weeks after doxy addition in BAM+NeuroD1 iN cells. **(c)** Tuj1 expression, 3 weeks after doxy . **(d–f)** Expression of pan-neuronal markers in iN cells 2 weeks after dox. **(g–h)** Example of iN cell expressing MAP2 (g) and synapsin (h) 4 weeks after dox and co-cultured with primary astrocytes (Adapted from *Pang et al., Nature***476**, 220–223 (2011)).

2.4.3. Generating distinct functional subtypes of iN cells.

Undoubtely, subtype-specific induced neurons, expecially if derived from human somatic cells, could be an extremely valuable tool for disease modeling and cell replacement therapy. For this reason, several Teams dedicated special efforts to address this issue.

Induced Dopaminergic neurons (iDA).

Transplantation of dopaminergic neurons can potentially improve the clinical outcome of Parkinson's disease, a neurological disorder resulting from degeneration of mesencephalic dopaminergic neurons.Several groups have directly reprogrammed fibroblasts to induced dopaminergic neurons (iDA) by overexpressing dopamine neuron lineage-specific factors that act during brain development, including genes involved in midbrain dopamine neuron development. Among them, Pfisterer et al.[188]found that iNs can be directed towarddistinct functional neurotransmitter phenotypes by overexpressing the BAM cocktail with two genes involved in dopamine neurongeneration, Lmx1a and FoxA2**(fig.53)**. In this way, they could direct the phenotype ofthe converted cells toward dopaminergic neurons.

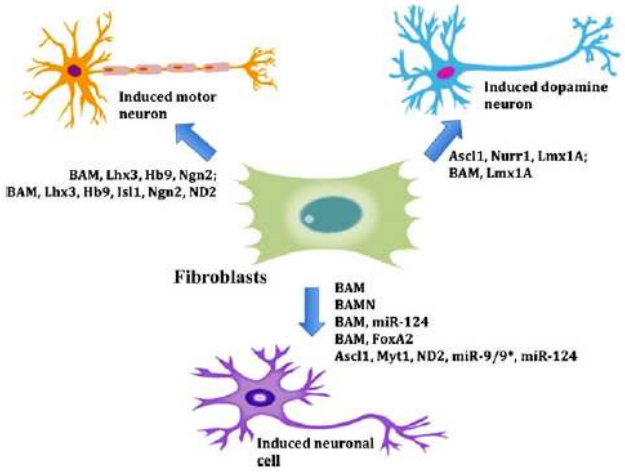

Figure 53. Direct conversion of fibroblasts into specific neuronal subtypes.
Two genes involved in midbrain dopamine neuron development , Lmx1a and FoxA2, optimize generation of
human iDAs when added to the BAM cocktail. Mouse embryonic fibroblasts are converted into functional iMN with an efficiency of 5–10 %. The application of the BAM cocktail with the addition of NeuroD1, to HEFs, is able to induce the generation of functional cholinergic iMNs in 2 weeks (Adapted from Abdullah A. I. et a.,Molecular Neurobiology June 2012, Volume 45, Issue 3, pp 586-595).

Caiazzo et al. identified a minimal set of three transcription factors—*Mash1* (or *Ascl1*), *Nurr1* (or *Nr4a2*) and *Lmx1a*—that are able to directly convert mouse and

human fibroblasts into functional dopaminergic neurons[191].So-induced dopaminergic (iDA) cells release dopamine and show the tipical pacemaker activity of brain dopaminergic neurons. TheMash1-Nurr1-Lmx1a cocktail induces dopaminergic neuronal conversion in prenatal and adult fibroblasts, from healthy donors and Parkinson's disease patients. Direct generation of iDA cells from somatic cells might have significant implications for understanding critical processes for neuronal development, *in vitro* disease modelling and cell replacement therapies.

Induced Motorneurons(iMNs)

This neuron subtype can be efficiently derived from embryonic fibroblasts by adding to the BAM cocktail several combinations of seven known motor neuron-specific factors[189]:Lhx3, Hb9, Isl1, Ngn2 and Lhx3, Hb9, Isl1, Ngn2, NeuroD1 (**fig.53)**.

2.4.4. Direct generation of induced neural stem cells from fibroblasts.

Although iN cells are functional neurons, they may not be very suitable to the study of certain neurological diseases, due not only to their non proliferative state (which severely limits their numbers), but also to their inability to recapitulate disease phenotypes occurring at the neural progenitor stage [192]. For this reason, many authors started focusing on an alternative way to generate neurons based on the preliminary convertion of fibroblasts into iNSCs that, in a second step, can be differentiated in all neural cell type: astrocytes, oligodendrocytes and neurons**(fig.54).**

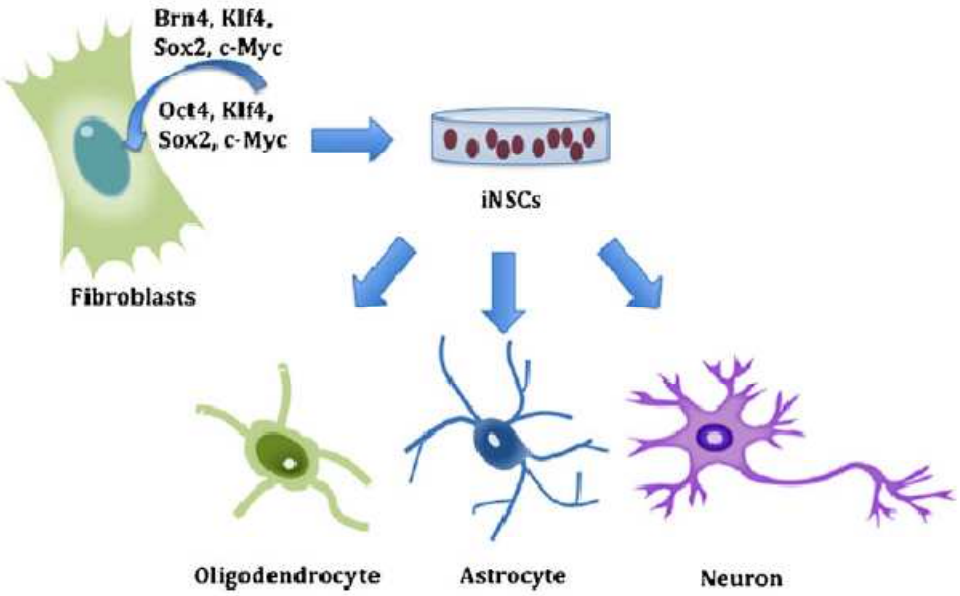

Figure 54. Convertion of fibroblasts into iNSCs(Adapted from Abdullah A. I. et a.,Molecular Neurobiology June 2012, Volume 45, Issue 3, pp 586-595).

Recently, several authors could achieve the direct convertion of fibroblasts into induced NSCs (iNSCs), bypassing the pluripotent stage [193–196].

The first evidence of this process was described in 2011 by Kim and collaborators. They reported that transient induction of the four Yamanaka reprogramming factors (Oct4, Sox2, Klf4, and c-Myc) followed by cells exposition to neural reprogramming medium can efficiently transdifferentiate fibroblasts into functional neural stem/progenitor cells (NPCs)[126]. This transdifferentiation process is highly specific and efficient, reaching completion within 9–13 days. If compared with the direct generation of iN cells, this method provides one critical advantage: the resulting cells are expandable progenitor cells. These reprogrammed NPCs were generated from both embryonic and adult TTFs. They expressed neural rosette markers (PLZF and ZO-1, **fig. 55a**), Pax6 (not shown) and were able to differentiate into Dcx-, TH-, GABA-, Map2-, NeuN-, and synapsin I-expressing neurons**(Fig. 55 b-f)**.

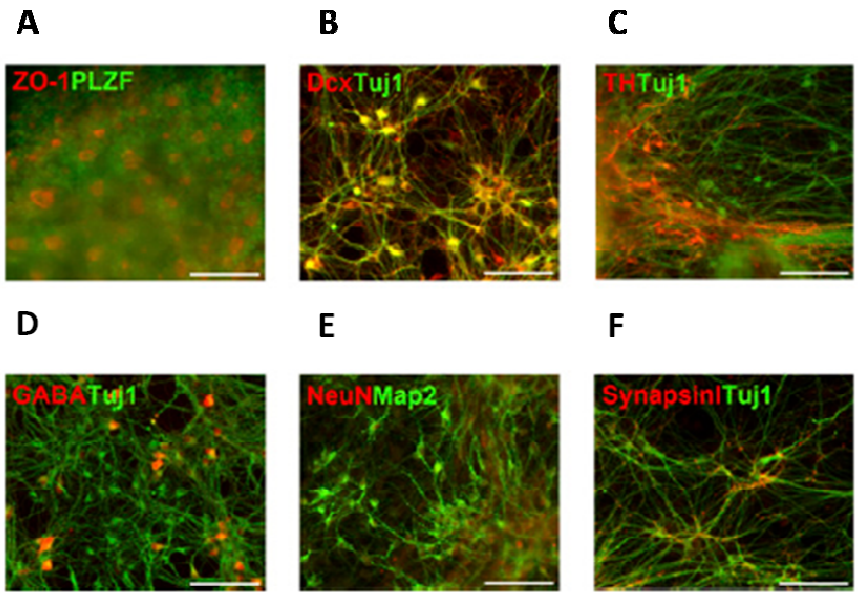

Figure 55. Neural progenitor induction from fibroblasts.
(Adapted from Kim et al., Proc Natl Acad Sci USA 108:7838–7843, 2011).

A further step onward was recently achieved by Lujan et al.who found that the combination of FoxG1 and Sox2 can induce NPCs ("iNPCs"). The most part of these cells were capable of generating clonal self-renewing, bipotent induced NPCs giving rise to functional neurons and astrocytes[197]. Moreover, the addition of the transcription factor Brn2 to Sox2 and FoxG1, induced tripotent NPCs, that could be differentiated into all three main derivatives of neural stem cells, neurons, astrocytes and oligodendrocytes. (**fig.56**).

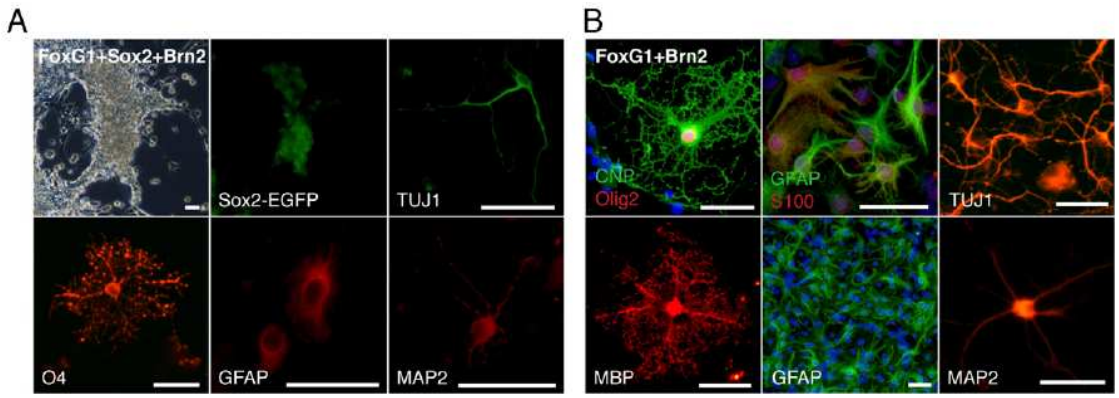

Figure 56. Tripotent NPC population derived from Sox2-EGFP MEFs(A) A Sox2-EGFP+ population that gives rise to O4+ oligodendrocytes, Tuj1+ and MAP2+ neurons, and GFAP+ astrocytes **(B)** FoxG1 and Brn2 alone induce a population that can give rise to mature CNP+, Olig2+, and MBP+ oligodendrocytes, GFAP+ and S100+ astrocytes, and TUJ1+ and MAP2+ neurons.(Adapted from Lujan, E., *Proc. Natl. Acad. Sci. U.S.A.***109**, 2527–2532, 2012).

These data demonstrate that direct lineage reprogramming based on target cell-type–specific transcription factors can be used to induce NPC-like cells, potentially useful for autologous cell transplantation-based therapies in the brain or spinal cord. Nevertheless, at date, an important issue is still far to be addressed: the generation of pure preparations of cortico-cerebral neurons.

CHAPTER 3.AIMS OF THESIS

As described above, specification of cerebral cortex is the result of two superimposed processes: pan-neural specification of the neural tube and regional sub-specification of its most rostro-dorsal part. The former largely relies on inhibition of Bmp signaling and active Fgf signalling. The latter requires the combinatorial activation of specific transcription factors (TFs) imparting distinct positional values along the rostro-caudal and the dorso-ventral axes.

Aim of this work was to assess if concerted co-expression of the main four TFs specifying rostro-dorsal identity, Foxg1, Pax6, Emx2 and Lhx2, is sufficient to convert somatic non neural cells, such as dermal fibroblasts, into neural-like precursors, regardless of previous activation of a pan-neural program.

This would allow to test the capability of positional identity machineries to trigger and sustain panneural programs. Reprogrammed cells originating from this procedure might represent on invaluable tool for patient-tailored cell therapy of brain diseases.

CHAPTER 4. RESULTS

4.1. Setting up the "FPd" reprogramming procedure.

We assayed the capability of distinct combinations of pallium-specifying genes (*Foxg1*, *Pax6*, *Emx2* and *Lhx2*, briefly: FPEL), to induce firing of the neural stem cell reporter *Sox1*^{EGFP} in derivatives of murine *Sox1*$^{EGFP/+}$ fibroblasts[198]. These four genes were delivered via lentiviral vectors, as doxycycline-activatable transgenes. To propitiate *Sox1*^{EGFP} activation, we used fibroblasts derived from embryos knock-out for *Trp53*[199] , an established promoter of histological homeostasis[200,201], and exposed them chronically to a specific drug cocktail promoting transcription. This cocktail included 1 µM BIX-01294 (an inhibitor of the H3K27-HMTase Ga9)[202], 2µM trans-2-Phenyl-cyclopropylamine hydrochloride (t2PCPA, an inhibitor of the H3K4m2-demethylase LSD1)[203] and 2 mM valproic acid (VPA, a HDAC inhibitor)[154,202]. [Actually, three additional drugs promoting transcription, the H3K9-HMTase inhibitor chaetocin [202], the DNA methylation antagonizer 5-azacytidine[154,202] and its functional synergizer dexamethasone [154]were also assayed. However, they resulted unacceptably toxic, at as less as 50 nM, 2µM and 1µM, respectively, and were early discarded]. 12 days post transgenes activation (d12), frequency of EGFP^{ON} cells was about 1% upon delivery of the FPEL set and arose to 1.8% for its FPL subset, pointing to a detrimental effect of *Emx2* against *Sox1* promoter activation. FP, FL and PL gave frequencies of 21.3, 0.1 and 0.7%, further suggesting the opportunity to exclude *Lhx2* from the reprogramming geneset and indicating the FP combination as the most promising one **(Fig. 57A-C)**. As for temporal progression of *Sox1*^{EGFP}activation, we found that, upon overexpression of the FP pair and in the presence of the VPA/BIX-01294/t2PCPA drug mix, frequency of *Sox1*$^{EGFP(ON)}$ cells, almost 17% at **d4**, reached its plateau (around 21%) at **d6,** whereas average fluorescence intensity within the EGFP^{ON} population continued to arise until at least d12 **(Fig. 57D)**.

Then, we systematically dissected functional relevance of the main ingredients of the previously assayed, best performing protocol (hereafter referred to as "the FPd protocol"): the *Foxg1*/*Pax6* pair (FP), the BIX-01294/t2PCPA/VPA drug mix (d) and the *Trp53*$^{-/-}$ genotype of substrate cells.

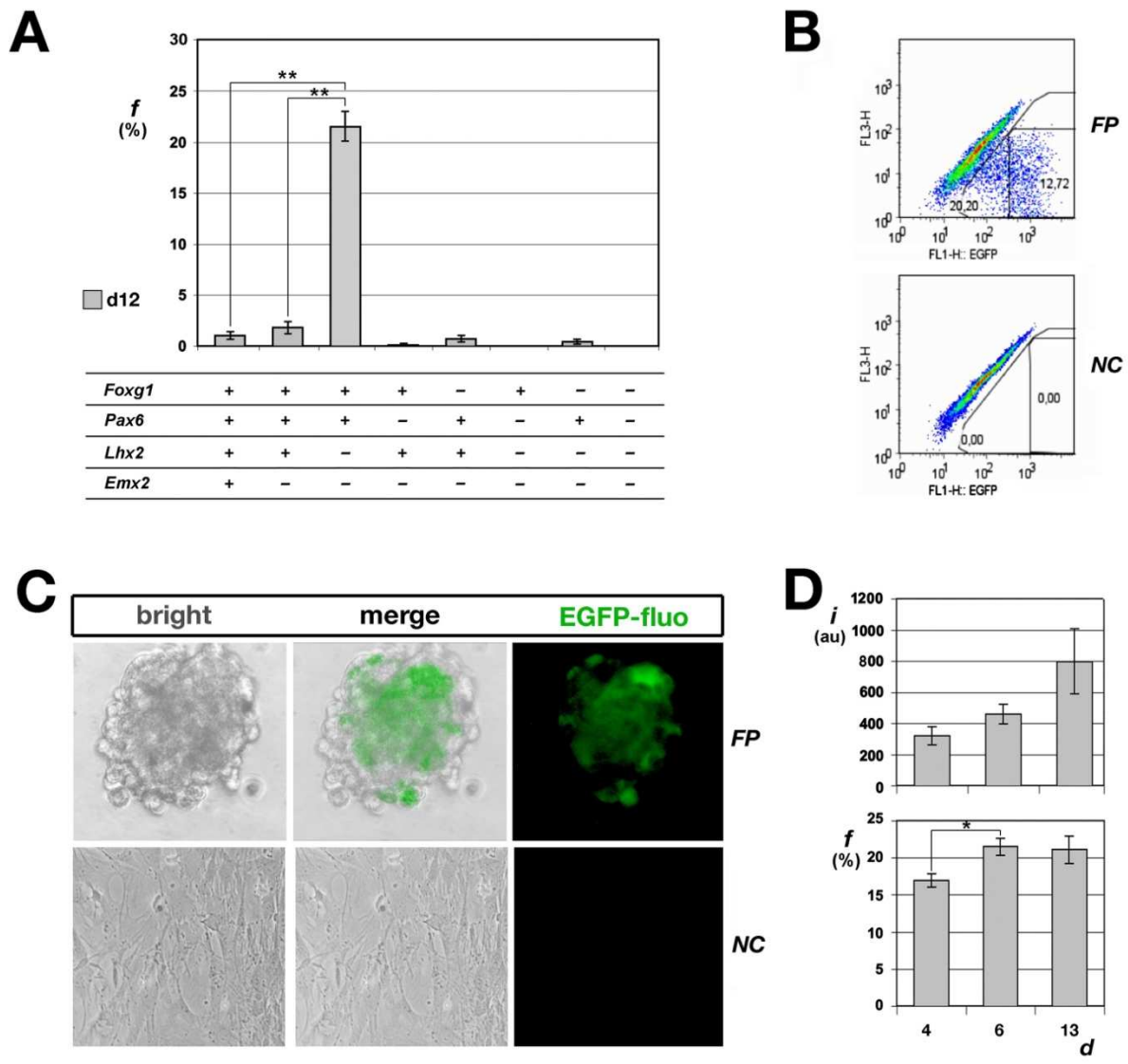

Figure 57. Setting-up the "FPd" protocol. (A) Frequencies of *Trp53*$^{-/-}$*Sox1*$^{EGFP/+}$ cells expressing EGFP, following lentiviral transduction with different combinations of doxy-activatable reprogramming factor genes, each at moi = 12, as evaluated by FAC sorting 12 days after transgenes activation. **(B)** Example of FACS plot, referring to *Trp53*$^{-/-}$*Sox1*$^{EGFP/+}$ fibroblasts transduced by *Foxg1/Pax6* (*FP*) or a negative control (*NC*). **(C)** *Sox1* promoter-driven EGFP fluorescence in neurosphere-like aggregates of *FP*-transduced cells and *NC* fibroblasts. **(D)** Time-course progression of frequency of *FP*-transduced cells expressing EGFP and the corresponding signal intensity. au = arbitrary units.

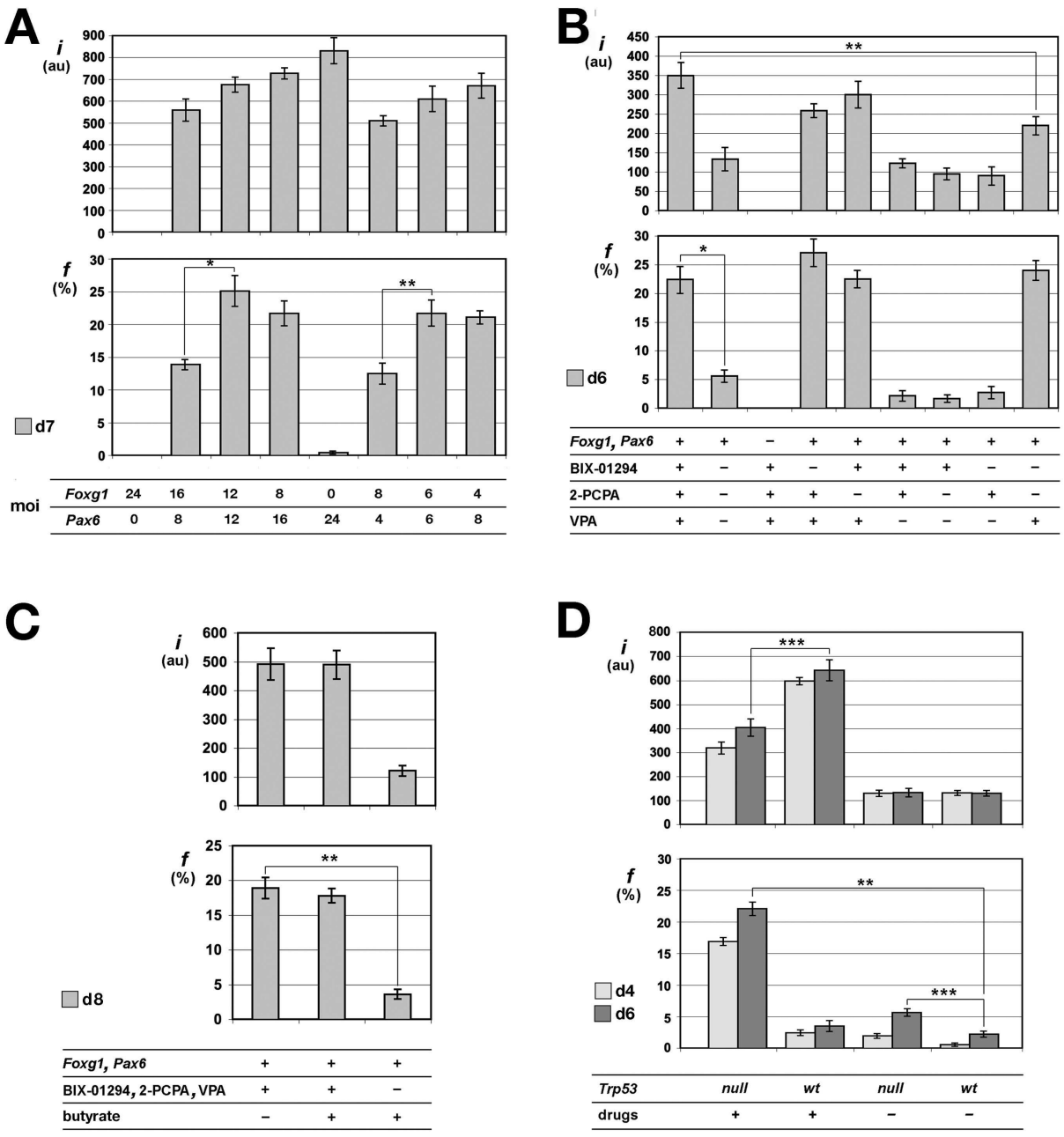

Figure 58. Dissecting contributions of TFs-ratio, drugs and Trp53 to fibroblasts reprogramming (A) Frequency of EGFP expressing cells and EGFP signal intensity, upon lentiviral delivery of *Foxg1* and Pax6 at different moi's, as evaluated by FACS, 7 days after transgenes activation. **(B)** Functional break-down of the drug mix promoting fibroblasts reprogramming. **(C)** Specificity of drugs effects. In (B,C), for each drug combination, frequency and signal intensity are reported as in (A). Cells were transduced by *Foxg1* and *Pax6* and monitored 6 of 8 days after transgenes activation. **(D)** Impact of *Trp53* genotype and drugs (BIX-01294, 2-PCPA, VPA) on the efficiency of the reprogramming process, at day 4 and day 6.

First, we found that *Sox1*^{EGFP} activation strictly requires over-expression of both *Foxg1* and *Pax6*. In fact, in the presence of the full drug mix and in a *Trp53*$^{-/-}$ environment, *Foxg1* alone did not give any appreciable fraction of *Sox1-EGFP*^{ON} cells, which conversely amounted to as little as 0.4% under *Pax6* only. Moreover, the protocol output resulted sensitive to relative dosages of *Foxg1*- and *Pax6*-expressing lentiviruses. At d7, the best result, 25.1%, was obtained with a 1:1 *Foxg1:Pax6* lentivirus stochiometry, whereas EGFP^{ON} cells were only 13.9% and 21.7% with 2:1 and 1:2 *F/P* ratios, respectively. Similar results were obtained when the total *FP* moi, 24, was halved, which also caused some slight frequencies dowregulation **(Fig. 58A)**.

Second, we found that the VPA/BIX-01294/t2PCPA drug mix, while not sufficient per se to trigger *Sox1*^{EGFP} expression, considerably enhanced the activity of the FP pair, expecially during early phases of the process. In a dedicated test, upon administration of *Foxg1*- and *Pax6*-expressor lentiviruses each at moi = 12, frequency of Sox1-EGFP^{ON} cells resulted 1.9% and 5.6% in the absence of drugs, at d4 and d7, respectively, and arose to 16.9 and 22.1% in their full presence. VPA was apparently the main contributor, as this frequency went back to 2.2% upon its selective removal from the drug mix and bounced to 24% under VPA only. However, as in this last case the average signal intensity was only 2/3 of that elicited by the full drug mix, we decided to retain BIX-01294 and t2PCPA in the standard "d" cocktail, to be emplyoyed in subsequent experiments **(Fig. 57F)**. Remarkably, effects of VPA resulted to be highly specific. In fact, when "d" was replaced by 0.5 mM Na-butyrate (another established HDAC inhibitor), frequency of Sox1-EGFP^{ON} cells at d8 dropped to as less as 3.6% **(Fig. 58C)**.

Third, as for *Trp53*, we found that itsinactivation makes substrate cells much more prone to get reprogrammed. Upon delivery of the "FPd" protocol, in fact, Sox1-EGFP^{ON} elements were 2.4% and 16.9% at d4, and 3.5% and 22.1% at d6, starting from *Trp53-wt* and *Trp53-null* fibroblasts, respectively. However, the intensity of Sox1-EGFP fluorescence was considerably higher in *Trp53-wt* than in *Trp53-ko* cells, further suggesting that, *after* recruitement of cells to the reprogramming process, Trp53 might help canalizing them into a NSC-like state. Remarkably, there was also some addition of drugs and genotype effects, as, in the absence of drugs, only 2.2% of d6 derivatives of infected *Trp53-wt* fibroblasts expressed EGFP **(Fig. 58D)**.

Finally, we tried to ameliorate NSC-like outputs of our "FPd" procedure by super-imposing to it select gene manipulations, supposed to help mimicking the dynamical transcriptional milieu of the early pallial field[204,205]**.** However, neither *delayed* overexpression of *Emx2* and *Lhx2*, nor *early* overexpression of two key hubs sustaining NSC programs[206–208], *Sox2* and *Brn2*, were successful **(Fig. S1A, B)**. Moreover, we tried to facilitate reprogramming, by counteracting the heat-shock machinery, known to promote phenotypic canalization within the ontogenetic and homeostatic domains[209,210].Three approaches were used. We: (a) kept *Sox1*$^{EGFP/+}$*;Trp53*$^{-/-}$ fibroblasts 2 hours at 41°C(13); (b) exposed them to 1µM 17-(allylamino)-17-demethoxygeldanamycin (17AAD, a powerful hsp90 inhibitor) [211] for 24 hours; (c) treated them by 1µM 17AAD/1µM CAY10603 (a HDAC6 inhibitor, synergyzing 17AAD[212]) again for 24 hours. When these treatments were combinatorially superimposed to our best performing protocol "FPd", 46 and 24 hous after transgenes activation, respectively, we did not elicit any upregulation of the *Sox1-EGFP*^{ON} fraction, which was conversely halved by the harshest, fully combined treatment. However, in such a case EGFP fluorescence intensity, as evaluated by FACS profiling, was upregulated by circa one quarter within the *Sox1-EGFP*^{ON} population. This suggests that knock-down of the heat shock machinery, albeit poorly useful to enroll more fibroblasts to get reprogrammed, might sustain the reprogramming process, once it has been triggered **(Fig. S1C)**.

4.2. Molecular characterization of NSC-like elements.

To confirm the conversion of fibroblasts into NSC-like elements, we inspected them for selected NSC markers. We found that at d13 about 20% of FP-treated cells were immunoreactive for Sox2, albeit at low level **(Fig. 59A)**. Moreover qRTPCR profiling of the same cells revealed that *Pax6* and *Hes5*, almost undetectable in negative control MEFs, were upregulated up to 40% and 25% of levels peculiar to derivatives of E12.5 cortico-cerebral precursors, respectively **(Fig. 59B,C)**.

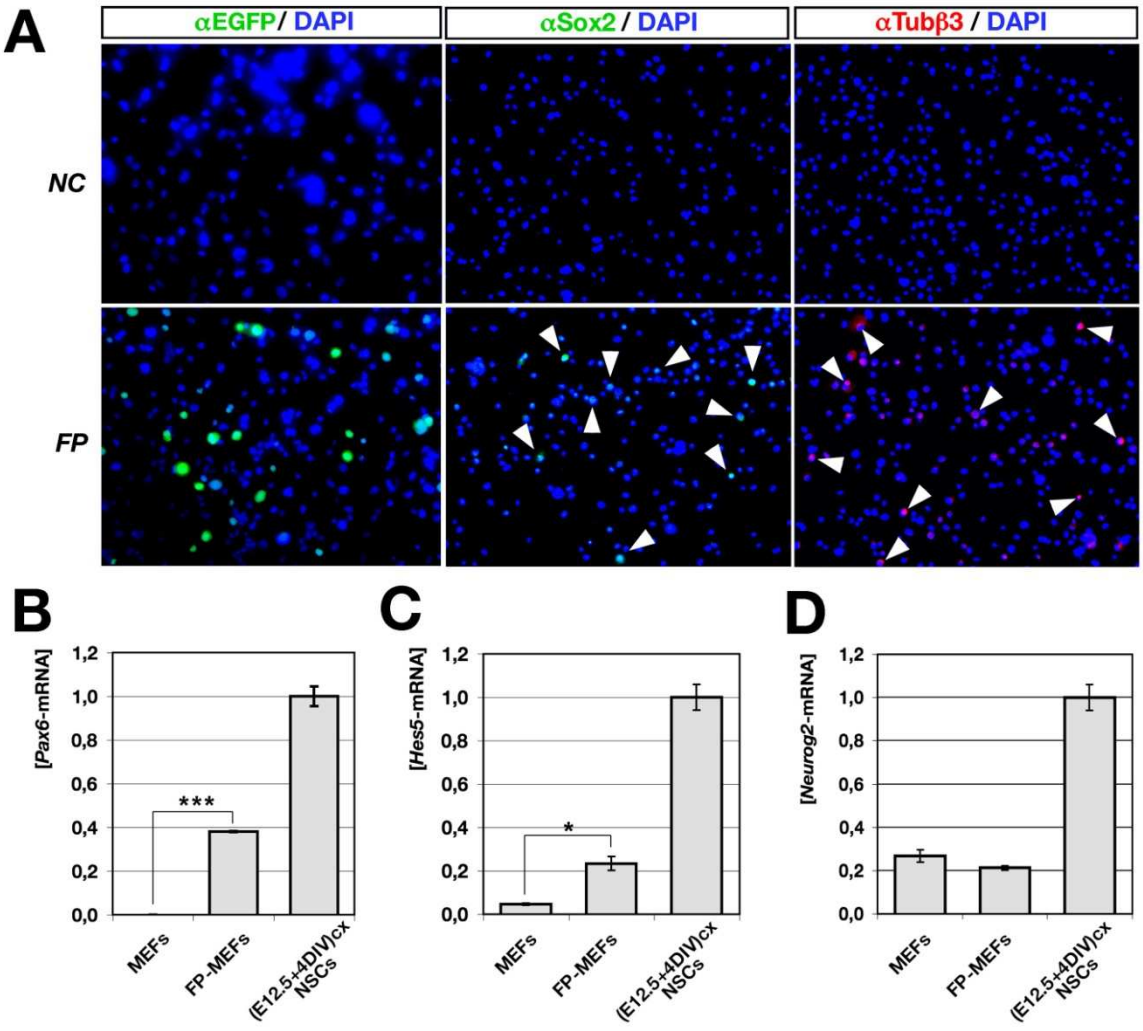

Figure 59. Molecular characterization of FPd-reprogrammed Sox1 $^{EGFP/+}$ **cells. (A)** Expression of *Sox1*-EGFP, Sox2 and Tubb3, in FP-treated and NC cells, as evaluated by immunofluorescence. **(B-D)** RTPCR quantitation of *Pax6*, *Hes5* and *Neurog2* mRNAs, in (1) FPd-treated fibroblasts at day 13, and (2) control neural stem cells (NSCs) from E12.5 cortico-cerebral precursors kept 4 days in vitro (E12.5+DIV4).

We also noticed a weak expression of Tubβ3 in about 15% of FP-treated cells **(Fig. 59A),** namely a promising index of neuronogenic potential. However, *Neurog2*, a key determinant of the glutamatergic lineage directly activated by *Pax6*, was expressed at similar low levels in both FP-treated and negative control MEFs **(Fig. 58D)**.

To preliminarly evaluate reprogramming advancement, we assayed cells resulting from this process for their capability to sustain firing of the NSC-specific Sox1 promoter, upon switching off the exogenous reprogramming geneset. For this purpose, we delivered the "FPd" protocol to two batches of *Trp53-ko* fibroblasts, harboring the *EGFP* cds alternatively under the control of the NSC-restricted *Sox1* promoter or the doxy-responsive *TREt* promoter **(Fig. 60A, i and ii, respectively)**, the latter further expressing the artificial transactivator rtTA^{2S}-M2. We removed doxycycline at d13 and scored subsequent decay of EGFP fluorescence. At d20, average EGFP intensity dropped to only 17% of the d13 value in *Sox1-wt/TREt-EGFP* samples, remaining above 65% in *Sox1*$^{EGFP/+}$ preparations **(Fig. 60C).** This suggests that, after switching the reprogramming transgenes off, some *Sox1*-promoter-driven neo-synthesis of EGFP occurred in reprogrammed *Sox1*$^{EGFP/+}$ cultures. However, in the same timeframe, the frequency of *Sox1-EGFP*^{ON} cells was reduced in these cultures about 12-fold, further suggesting that only a small subset of reprogrammed cells retained their new state **(Fig. 60B).**

4.3. Neuronogenic potential of Foxg1/Pax6-reprogrammed fibroblast derivatives.

Next, we wondered whether *neural*-like elements generated by combined *Foxg1/Pax6* overexpression were also able to activate *neuronal* markers. For this purpose, we delivered our best performing "FPd" protocol to *Tau-EGFP*$^{+/-}$*;Trp53*$^{-/-}$ fibroblasts[199,213]. At d6 we transferred the engineered cells to a B27/VPA-based medium ("neural differentiating medium"), in order to promote neuronal differentiation. Finally, 8 days later, we evaluated the frequency of EGFP expressing cells by FACS scanning. This frequency resulted to be 6.6%, suggesting that a subset

of the infected population could have acquired neuronal identity. No EGFP activation took conversely place in negative controls. We reasoned that the other two members of our original

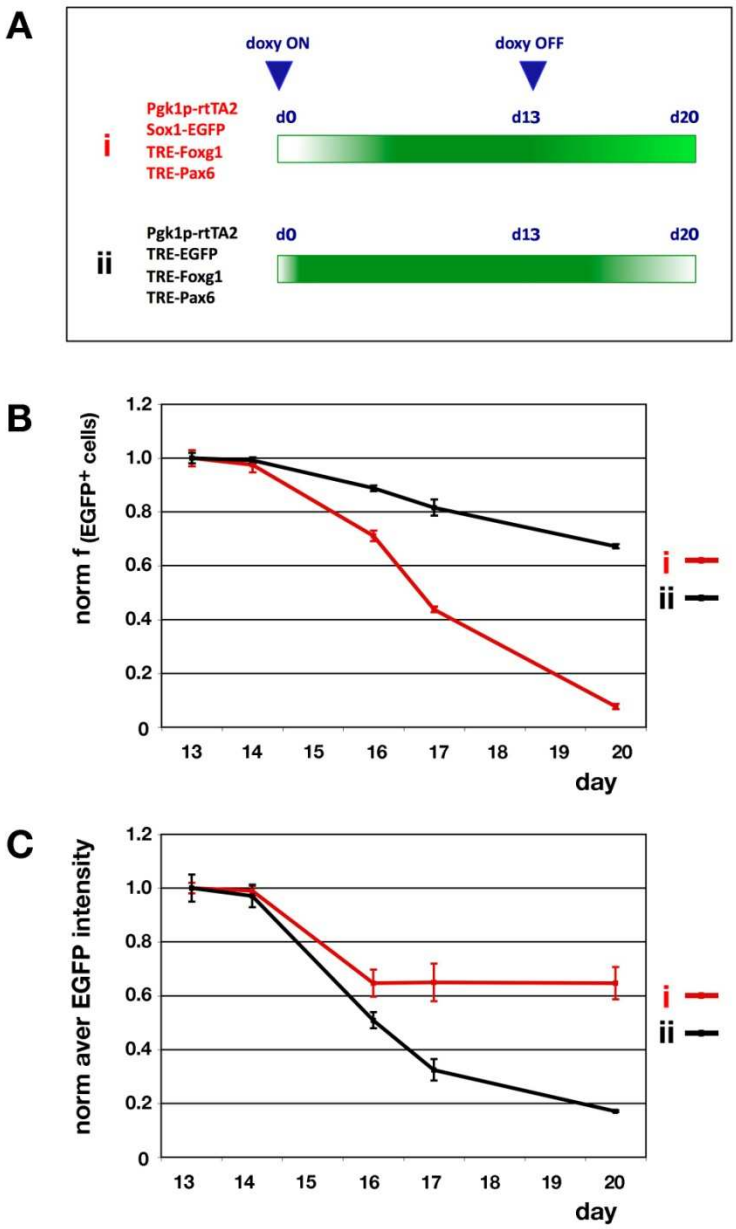

Figure 60. Assessing stability of NSC-like cells originating from FPd-treated fibroblasts. (A) Experimental design, including genotypes of the two cell preparations subject of analysis (i and II) and the doxycyclin administration schedule. **(B,C)** Frequencies of *Sox1*-EGFP-expressing cells and EGFP expression levels (within the expressing subpopulation) at days 13-20. For each cell preparation, frequencies and intensities are normalized against day 13 values.

geneset, *Emx2* and *Lhx2*, previously shown to promote neuronal differentiation in a variety of experimental contexts [214–217], might ameliorate the neuronal output of our manipulations. As expected, additional *Emx2/Lhx2* overexpression, from d7 to d14, increased the Tau-EGFP^{ON} fraction to 11.8% ("FPd/ELv" protocol). Moreover, the *EL* pair resulted far more neuronogenic than the established neuronogenic promoter *Ascl1*[185,187]. In fact, when *Ascl1* was added to the *EL* pair, the Tau-EGFP^{ON} fraction resulted only slightly upregulated (13.5%), when cells were superinfected by *Ascl1* alone, such fraction dropped back to 5.8%. Finally, as doxycyclin was removed from FPd/Ascl1-treated (FPd-A) samples at d7 (so resulting into a *Foxg1*^{OFF}*Pax6*^{OFF}*Ascl1*^{ON} configuration at d7-d14), the Tau-EGFP^{ON} fraction fell just above zero, further confirming the intrinsic *neuronogenic* activity of the FP pair **(Fig. 61A,B)**. As a control, FACS analysis of Tau-driven EGFP expression was backed by EGFP immunodetection, which gave consistent results **(Fig. 61C)**.

We tried to ameliorate the neuronal output of the above described two-steps "FPd/ELv" protocol, by exposing fibroblasts to four select drugs, known to promote their transdifferentiation into neuronal cell types [218] or synergize with VPA[219]**.** Remarkably, co-inhibition of BMP- and TGFβ-signalling by 10μM SB431542 and 0.7 μM LDN193189, from d2 to d13, almost doubled the frequency of Tau-EGFP$^{(ON)}$ cells. Therefore we included SB431542 and LDN193189 into an improved version of our protocol, we named "FPd/ELv^{+}". Conversely, stimulation of beta-catenin signaling by 0.7 μM BIO, in the same time window, as well as delivery of 25 μM vitamin C, from d2 to d14, approximately halved this frequency. Moreover, no advantage emerged from the addition to the "differentiating medium" of further drugs known to stimulate neuronal maturation (5μM forskolin, 5μM all-trans retinoic acid (atRA), 30mM KCl, 25μM glutamic acid, 200μM beta-hydroxyanisole (bHA) or 1mM beta-mercaptoethanol (bME)). Only 2% dimethyl-sulfoxide (DMSO) upregulated the TauEGFP$^{(ON)}$ cells frequency, however by only one third **(Fig. S2).**

Then to evaluate the extent of neuronal differentiation elicited with the FPd/ELv^{+} protocol, we immunoprofiled cells reprogrammed by this protocol for selected markers expressed in mature neurons. We confirmed high level expression of *Tau* promoter-directed EGFP. However, MAP2 and NeuN were not detectable, suggesting a severe defect of neuronal differentiation (Fig. S3). We speculated that exposing reprogrammed cells to histogenetic clues active in the developing brain might help fixing this issue. Therefore, we infected cells originating from *Trp53*$^{-/-}$*Tau*$^{EGFP/+}$ donors with *FP* viruses, made them *EL-GOF* ad d6 and transplanted them at d13 into the fronto-parietal cortex of P0 recipient mice. 1-3 weeks later, we monitored their distribution and profile. Differently from positive controls (i.e., *natural* cortico-cerebral precursors), which consistently shed around the injection point, reprogrammed elements preferably clustered in big subventricular clumps near the corpus callosum. Like in vitro, they activated Tau-EGFP, but not MAP2 or NeuN, so confirming the uncapability of the FPd/ELv^{+} protocol to sustain full neuronal differentiation **(Fig. S4).**

Finally, electrophysiological experiments were performed to assess whether FPd/ELv$^{(+)}$ cells exhibited a neuron-like phenotype. Comparison of Tau-EGFP positive and control cells *in vitro* revealed different characteristics in their passive and active membrane properties. We measured first the capacitance, the membrane input resistance, and the resting membrane potential (RMP), widely accepted indicators of the degree of cellular development and health in 19 controls and 25 FPd/ELv$^{(+)}$ cells. A significant more negative value of the RMP was detected in Tau-EGFP positive cells respect to control fibroblasts (-41 ± 2 mV and -22 ± 4 mV, respectively; $p<0.001$) **(Fig. 62A).**

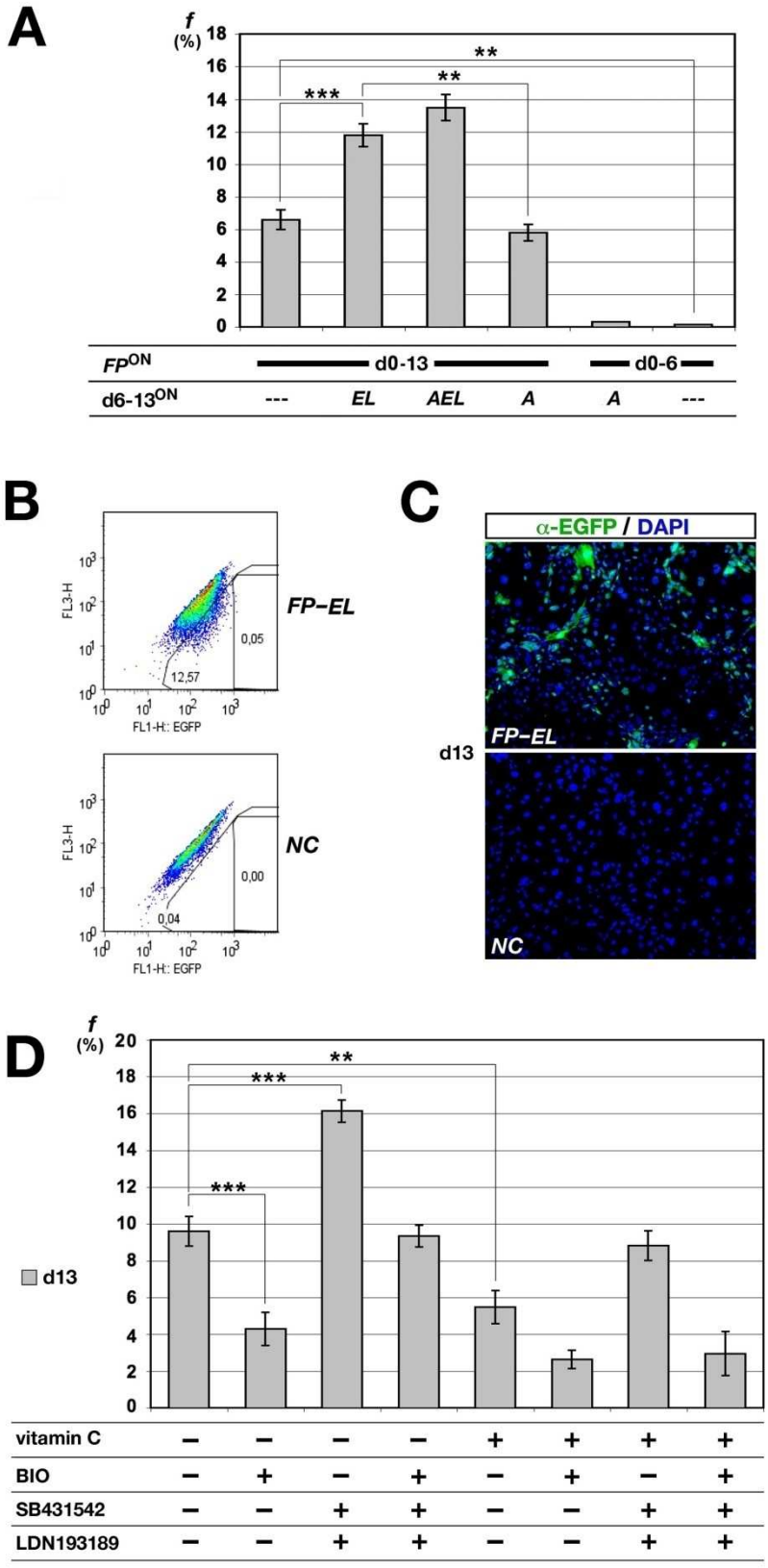

Figure 61. Setting-up and improving the FPd/ELv protocol. (A) Frequencies of *Trp53*$^{-/-}$ *Tau* $^{EGFP/+}$cells expressing EGFP, following lentiviral transduction of doxy-activatable *Foxg1* and *Pax6* and constitutively expressed Ascl1, each at moi = 6. Doxycyclin was administered in different time windows, between day 0 and day 13. Cells were analyzed by FAC sorting at day 13. **(B)** Example of FACS plot, referring to fibroblasts transduced by *Foxg1/Pax6* (*FP*) or a negative control (*NC*). **(C)** *Tau* promoter-driven EGFP fluorescence in *FP*-transduced and NC fibroblasts. **(D)** Effects of the combinatorial administration of four select drugs on the frequency of *Trp53*$^{-/-}$ *Tau*$^{EGFP/+}$ FPd/ELv-treated cells expressing EGFP, at day 13.

In addition, Tau-EGFP positive cells exhibited higher membrane capacitance (112 ± 16 pF versus 48 ± 8 pF; p=0.023) **(Fig. 62A)** which, as expected, was associated with a reduction in membrane input resistance (272 ± 55 MΩ and 340 ± 104 MΩ, in Tau-EGFP positive cells and control respectively; p>0.05), that did not reach a statistical value **(Fig. 62A).** Interestingly, while in control cells the voltage/current relationship was linear (n=18), in Tau-EGFP positive cells rectified in the depolarizing direction(Fig. 6B). Injection of a depolarizing current pulse of 200 pA, from a holding potential of -70 mV (subthreshold for spike activation) produced in Tau-EGFP positive cells a voltage deflection of -47 ± 3 mV instead of -26 mV, (expected value obtained by interpolating data at negative potentials; n=18). Moreover, while in control cells depolarizing current pulses failed to evoke spikes (18/18), in the majority of Tau-EGFP positive cells (19/25; 76%) they were able to evoke rudimentary action potentials, reminiscent of those observed in immature neurons **(Fig. 62B).** The difference between the two groups was statistically significant (p<0.001; Chi Square test). In three cases (out of six tested), the action potentials were blocked by TTX (1 μM), indicating that they were generated by the activation of voltage-dependent sodium channels. Overall these results suggest that the FPd/ELv(+) protocol channels fibroblasts towards a neuronal profile.

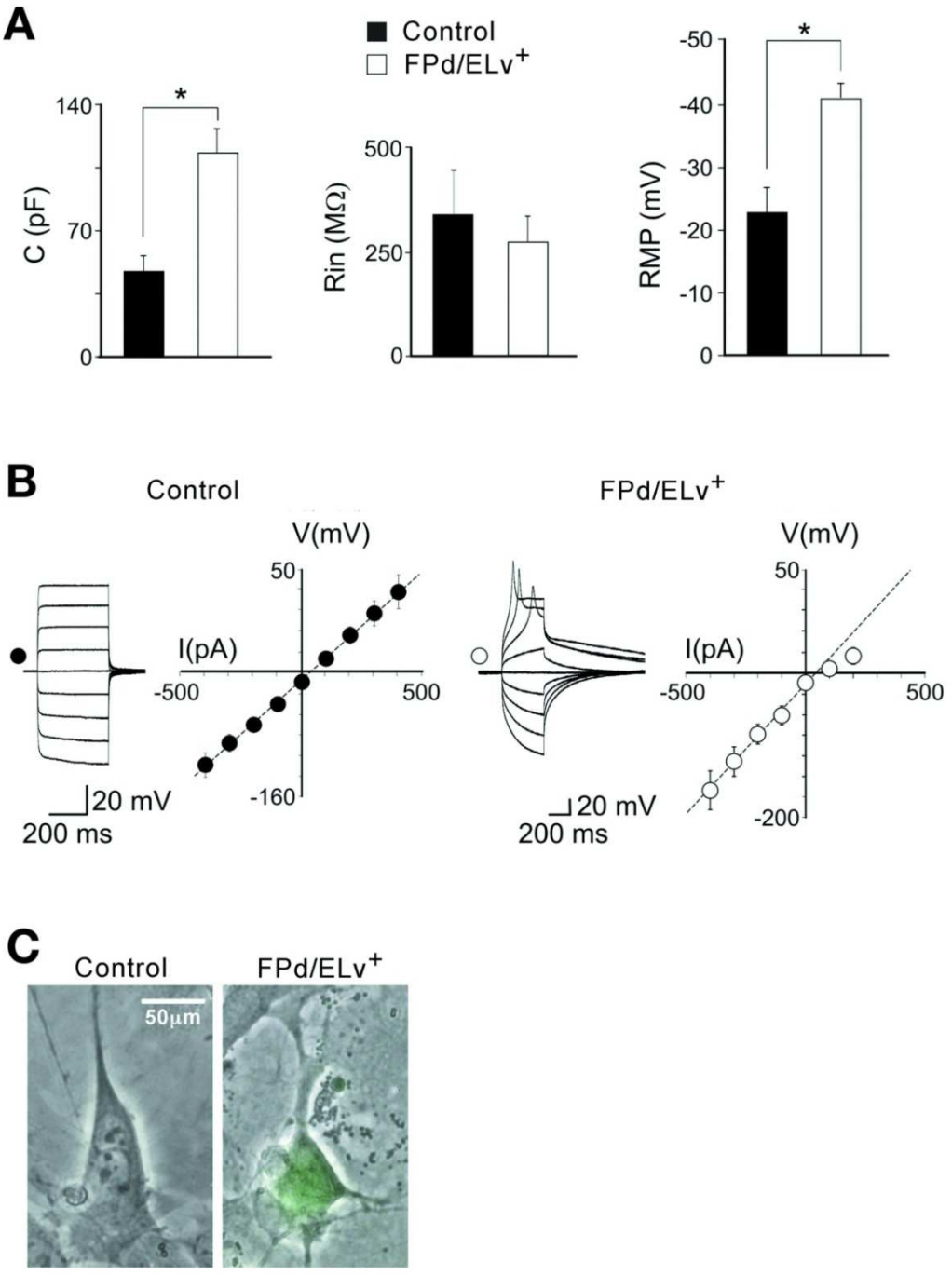

Figure 62. Neuron-like phenotype of FPd/ELv^{+} fibroblasts. (A) Each column represents the mean capacitance (C), input resistance (R_{in}) and resting membrane potential (RMP) values of control (black) and reprogrammed fibroblasts (white). **(B)** V/I relationship obtained by injecting depolarizing and hyperpolarizing current pulses of increasing amplitude from a holding potential of -70 mV (0 current) in controls (n=18; black symbols, left) and in FPd/ELv$^{(+)}$ cells (n=18; white symbols, right). Note rectification in the depolarizing direction in FPd/ELv$^{(+)}$ cells. On the left of of the V/I relationships, single sample from controls and FPd/ELv$^{(+)}$ cells **(C)** Examples of a single control and reprogrammed FPd/ELv$^{(+)}$ cell.

CHAPTER 5. DISCUSSION

We found that a selection of TFs dictating pancortical specification was able to convert non-neural somatic cells (fibroblasts) into neural stem cell-like (NSC-like) elements. The efficiency of this process was strongly increased by two classes of additional manipulations: (1) administration of drugs modulating the epigenetic state of chromatin and promoting transcription; (2) inactivation of the p53 pathway, stabilizing tissue identity. Inhibition of TGFβ and BMP pathways further upregulated NSC-like cells frequency, up to 30% (data not shown). A small fraction of NSC-like elements resulting from combined treatments (1) and (2) were able to maintain their identity, even after switching off the reprogramming transgenes**(fig. 60)**. These NSC-like elements, when cultured under pro-differentiative conditions, gave rise to neuron-like cells, expressing EGFP under the control of the Tau promoter. Frequency of neuron-like cells was enhanced by overexpression of the two TFs Emx2 and Lhx2 and tonic inhibition of TGFβ and BMP signallings. These Tau-EGFP(ON) cells showed a negative resting potential and displayed active electric responses, following injection of depolarizing currents. However their neuronal differentiation was largely defective, both in vitro and in vivo. Moreover no sign of glial differentiation was detected (data not shown).

The capability of Foxg1 and Pax6 to synergistically stimulate conversion of fibroblasts to neural precursor-like elements is consistent with the patterning activities displayed by these two genes in the developing neural tube: specifiction of telencephalic versus diencephalic identity by Foxg1[220]**,** and promotion of dorsal versus ventral telencephalic programs by Pax6 [221,222]. It is also consistent with the previously reported ability of these two genes to neuralize non neural tissues in vitro. In fact, Pax6 overexpression in HeLa cells induces a partial transdifferentiation towards a neuronal phenotype[223], combined overexpression of Foxg1 with Sox2 and Brn2 converts fibroblasts to tripotent neural precursors[197].

Moreover, we found that Foxg1 and Pax6 are further able to promote the generation of neuron-like elements, displaying active electrical properties **(Fig. 62).** Even this result reflects histogenetic activities already characterized in vivo. In fact, high levels of Pax6 trigger cortical neuronogenesis[224],Foxg1, strongly expressed in neocortical neurons, stimulates their

postmitotic maturation[225]. Notably, Emx2 and Lhx2, although promoting pancortical specification in vivo[221,222,226], were strongly detrimental to early steps of fibroblasts reprogramming, when overexpressed together with Foxg1 and Pax6 **(Fig. 57A)**. This could be related to their alternative involvement in mesenchymal development. For example, Emx2 specifies mesodermal structures, such as scapula and urogenital system [227–229], while Lhx2 channels ESCs and iPSCs towards the hematopoietic lineage[230]. Notably, however, delayed overexpression of these two genes in elements already reprogrammed by Foxg1 and Pax6 enhanced their neuron-like differentiation **(Fig. 61A)**. This parallels later promotion of neuronal differentiation elicited by both genes in vivo[215–217,231]**.** Remarkably, a specific mix of "epigenetic drugs" increased the NSC-like output of the FP protocol by 4- to 8-fold **(Fig. 58B)**. It has been proposed that stability of tissue identity largely relies on retention of specific epigenetic signatures, dictating differential gene availability to transcription and preventing improper gene expression [232]. We employed VPA, BIX-01294, and t2PCPA, hypothesizing that chromatin opening promoted by these drugs could facilitate the access of neuralizing TFs to target genes, usually hidden in non neural tissues. This concept is consistent with previous reports of VPA- and BIX-01294-dependent enhancement of iPSCs generation[233,152]. Interestingly the effects of VPA were highly specific, as this drug could not be vicariated by another established HDAC-inhibitor, Na-butyrate **(Fig. 58C)**. This might reflect the exquisite capability of VPA to upregulate bHLH neuronogenic genes [234]. On the other side, Na-butyrate might divert infected fibroblasts to iPSCs identities, by promoting the expression of endogenous pluripotency-associated genes[235].

Moreover, the NSC-like output of the FP protocol was also dramatically increased by genetic ablation of p53 **(Fig. 58D)**. This result echoes the effects of Trp53 knock-out on iPSCs generation[179,201] a phenomenon suggested to be underlain by two main mechanisms. First, p53 downregulation may be a key step of the chain of events leading to iPSC generation[236]. Second, p53 inactivation may prevent apoptosis induced by functional interaction between p53 itself and reprograming oncogenes[201]**.** Since Foxg1 itself may act as an oncogene[237], p53 knock-out might increase the frequency of $Sox1^{EGFP(ON)}$ elements, just preventing fibroblasts from cell death triggered by its sustained overexpression.

We found that combined inhibition of Tgfb and Bmp signalling doubled the neuronal-like output of our FPd/EL protocol, while stimulation of Wnt signalling and administration of vitamin C halved it. The first phenomenon is consistent with previously documented activities of these signalling systems in vivo and in vitro. In fact, within the developing embryo, Wnt, Tgfb and Bmp signalling promote epiblast conversion to endoderm and mesoderm[238,239], early activation of Wnt signalling and inhibition of Bmp4 promote neural at expenses of ectodermal fates[240,241]. Consistently, in vitro combined stimulation of Wnt pathway and inhibition of Bmp and Tgfb signalling strongly promote transdifferentiation of human fibroblasts to neurons[218].

Detrimental effects of Wnt signalling and vitamin C on neural transdifferentiation efficiency were conversely unexpected. It is possible that high Wnt signalling promoted fibroblasts self-renewal[242,243], so diluting reprogrammed cells. Moreover, Wnts, in the presence of residual Bmp/Tgfb signalling, might force transdifferentiating fibroblasts towards meso-endodermal fates. Finally, as for vitamin C, it was previously shown to enhance full reprogramming of fibroblasts to iPSCs[219], acting as key cofactor of histone demethylases which sustain the ESC master transcription factor Nanog[244]. As such, it might facilitate diversion of infected fibroblasts towards a pluripotent state.

Finally, it has to be underlined that, despite of activation of specific neuronal markers (Tubb3 and Tau-driven EGFP, see **Fig. 59 and 61**) and appearence of active electrical responses **(Fig. 62),** neuron-like differentiation elicited by the FPd/ELv+ protocol was highly defective, as the expression of established pan-neuronal markers (NeuN and MAP2) was completely missing. In this respect, we noticed that Neurog2, a key activator of the cortico-cerebral glutamatergic program[90], was not upregulated in reprogrammed fibroblasts cultures **(Fig. 59D)**, even in the presence of its direct activator Pax6[93]. We speculated that such missing upregulation might be responsible for defective neuronal differentiation. However, forced overexpression of Neurog2 (and its paralog Ascl1) in FPd-reprogrammed fibroblasts did not activate MAP2, even upon inclusion of forskolin into the differentiation medium (data not shown). This implies that further molecular defects prevented proper execution of the neuronogenic program in these cells. We further hypothesized that absence of p53 could be a major issue. In fact, p53 promotes conversion of early neural precursors to neuronal progenitor cells, by antagonizing

expression of Id1[245]. Moreover, it is required for advanced neuronal maturation, stimulating transcription of pro-neurite and axon-outgrowth genes *Coronin 1b*, *Rab13* and *GAP43*[246,247]. Finally, knock-down of p53 by RNAi redirects retinoic acid (RA)-induced ESCs differentiation from neuronal to mesenchymal [167]. For these reasons, we delivered the full FPd/EL+ protocol to Trp53 wild type fibroblasts. However, even in this case, no MAP2 activation was detected (data not shown).

In the light of these findings, an unbiased approach, based on comparative transcriptomic profiling of our FPd-induced elements and cortico-cerebral NSCs, seems necessary, to clarify molecular mechanisms underlying the histogenetic block undergone by such elements. This approach should provide a reasonable number of additional candidate genes, whose concerted modulation might fix defective neuronogenesis. We plan to implement this approach in dedicated follow-up study.

CHAPTER 6. CONCLUSIONS

In synthesis, we have shown that a subset of TFs specifying rostro-dorsal identity, including Foxg1 and Pax6, is sufficient to convert mouse embryonic dermal fibroblasts into neural-like precursors, even in the absence of previous activation of the pan-neural program.

These precursors express key NSC-markers, such as Sox1, Sox2, Hes5 and Pax6, and retain their new identity to some extent, even after switching off exogenous Foxg1/Pax6 expression. The same cells, following secondary overexpression of other two cortex-specifying genes, Emx2 and Lhx2, give rise to neuron-like elements, expressing the neuronal marker Tau and displaying active electrical properties. However, molecular and electrical profiles of these cells indicate that their neuronal differentiation is still rudimentary and incomplete. Comparative transcriptional profiling of these cells and their natural neural counterparts might help identifying molecular mechanisms underlying their defective differentiation. Such profiling will be subject of a dedicated follow-up study.

CHAPTER 7. MATERIALS AND METHODS

7.1. Animal handling, generation and genotyping of compound mutants.

Trp53$^{-/+}$ (a kind gift by G. Del Sal, CIB, Trieste, Italy), Tau$^{EGFP/+}$ (purchased from Jackson Laboratories, USA) and Sox1$^{EGFP/+}$ mice (a kind gift by A. Smith, University of Cambridge, UK) used in this study were maintained at the SISSA mouse facility. Embryos were staged by timed breeding and vaginal plug inspection. Double-mutant lines were generated by mating mice harboring Trp53^{-199},Tau^{EGFP248}, or Sox1^{EGFP198}mutant alleles, in different combinations. Trp53$^{-/-}$ females were ruled out from the breeding scheme, as sterile. The offspring genotype was determined by multiplex PCR. The following primers were employed : fwdX6: 5'-AGCGTGGTGGTACCTTATGAGC-3', RevX7: 5'-GGATGGTGGTATACTCAGAGCC-3', RevNeo19: 5'-GCTATCAGGACATAGCGTTGGC-3' for Trp53 line; PR385lu02 5' TGG TGA ACC GCA TCG AGC TGA AG 3', PR386lu02 5' AAC TCC AGC AGG ACC ATG TGA TGC 3', MG-S 5' CCC CCA AGT TGG TGT CAA AAG CC 3', MG-AS5' ATG CTC TCT GCT TTA AGG AGT CAG 3' for EGFP-reporter lines.

7.2. Primary cell cultures.

7.2.1. Mouse embryonic fibroblasts cultures.

Trp53KO;Sox1-EGFP and Trp53KO;Tau-EGFP MEFs were isolated from E14.5 embryos under a dissection microscope (Leica). The head, vertebral column (containing the spinal cord), dorsal root ganglia and all internal organs were removed and discarded to ensure the removal of all cells with neurogenic potential from the cultures. The remaining tissue was manually dissociated and incubated in 0,05 % trypsin (Sigma) for 10–15 min to create a single cell suspension. The cells from each embryo were plated onto a 10-cm tissue culture dish in MEF media (Dulbecco's Modified Eagle Medium; Invitrogen) containing 10% fetalbovine serum (FBS), and penicillin/streptomycin. Cells were grown at 37 °C for 3-4 days until confluent, and then split once before being frozen. After thawing, cells were cultured on 10-cm plates and allowed to become confluent before being split onto plates for infections using 0.05% trypsin.

7.2.2. Cortico-cerebral neuronal cultures.

The cortical tissue from E15.5-E18 mice was chopped to small pieces for 5-8 minutes, in the smallest volume of ice-cold 1X PBS-0,6% glucose-0,1% DNaseI. After digestion with 1mg/ml trypsin for 5 minutes, cortices were spinned down and resuspended in Neurobasal medium containing 1X B27, 0,5mM glutamine, 25µ□βMercaptoethanol,1X penicillin/ streptomycin. After pipetting 5-8 times with P1000 gilson pipette, undissociated tissue was left to sediment? for 2 minute at 1g, in ice. The supernatant was harvested and the living cells counted. Cells were resuspended at a concentration of 100-200/µl and plated on Poly-L-Lysine coated 24 Multiwell.

7.2.3. Cortico-cerebral precursors cultures.

NSCs were isolated from E12 embryonic cortices and plated onto uncoated 24 multiwell (BD Falcon) after gentle mechanical dissociation to single cells. 2.5*105 cPCs were plated for each well in 350 µl of serum free anti-differentiative medium [1:1 DMEM-F12, 1X Glutamax (Gibco), 1X N2 supplement (Invitrogen), 1 mg/ml BSA, 0.6% w/v glucose, 2 µg/ml heparin (Stemcell technologies), 20 ng/ml bFGF (Invitrogen), 20 ng/ml EGF (Invitrogen), 1X Pen/Strept (Gibco), 10 pg/ml fungizone (Gibco)] added with 2µg/µl doxycycline (Clontech).

7.3. Lentiviral transfer vectors construction.

Basic DNA manipulations (extraction, purification, ligation) as well as bacterial cultures and transformation, media and buffer preparations were performed according to standard methods. Plasmids were grown in E.Coli, Xl1-blue or TOP10 strains. A description of each transfer vector construction follows.

LV_Pgk1p-rtTA^{2S}-M2 is the "driver lentivirus"described in Fig. 1C of ref[249].

LV_TREt-Foxg1 was constructed by transferring the Foxg1-cds BamHI-HpaI fragment from LTV_TREt-Foxg1-IRES2EGFP[216] into BamHI-HpaI cut LV_TREt-Pax6-IRES2EGFP, followed by deletion of the IRESEGFP fragment via SalI-BamHI digestion, filling in and religation.

LV_TREt-Pax6 was generated in two steps: (1) The BamHI(filled)-XhoI 1.9kb fragment from the clone sc-35 (a kind gift by Anastassia Stoykova), corresponding to Pax6-cds (short

form) plus circa 570 bp from the 3'UTR (nt 813-2729 of Genbank # NM_013627.5), was transferred into the PmeI-XhoI cut LV_TREt-IRES2EGFP vector (which is the empty "expressor lentivirus" described in Fig. 1C of ref[249]), giving rise to LV_TREt-Pax6-IRES2EGFP; (2) then the IRESEGFP module was deleted via SalI digestion and religation.

LV_TREt-Lhx2 was generated in two steps: (1) The BamHI(filled)-XhoI 1.2kb fragment, corresponding to the Lhx2-cds (Genbank # NM_010710, nt192-1412) was transferred into the PmeI-XhoI cut LV_TREt-IRES2EGFP vector; (2) then the IRESEGFP module was deleted via SalI digestion and religation.

LV_TREt-Emx2 was a kind gift of Clara Grudina. It was generated by transferring the NotI(filled)-XhoI 0.8kb fragment, corresponding to the Emx2 cds (Genbank # NM_010132, nt 527-1288), into the PmeI-SalI cut LV_TREt-IRES2EGFP vector.

LV_TREt-luc was generated starting from LTV_TREt-luc-IRES2EGFP[216] by deleting the IRES2-EGFP fragment via SalI digestion and religation.

LV_TREt-Sox2 is the plasmid TetO-FUW-sox2 described in ref [250] and corresponds to plasmid #20326 of the Addgene collection.

LV_TREt-Brn2 is the plasmid Tet-O-FUW-Brn2 described in ref [185] and corresponds to plasmid # 27151 of the Addgene collection.

LV_Pgk1p-Ascl1 is the plasmid LV_pSIN-WP-mPGK-hMash1, a kind gift by E.Capowsky and Clive Svendsen.

LV_Pgk1p-Neurog2 is the plasmid "Ngn2" described in[188] and corresponds to plasmid #34999 of the Addgene collection.

7.4. Lentiviral vectors packaging and titration.

Third generation self-inactivating (SIN) lentiviral vectors (all except LV_TREt-Sox2) were produced as previously described (Follenzi and Naldini, 2002) with some modifications. Briefly, 293T cells were co-lipofected (Lipofectamine 2000, Invitrogen) with the transfer vector plasmid plus three auxiliary plasmids (pMD2 VSV.G; pMDLg/pRRE; pRSV-REV). In case of LV_TREt-Sox2, a 2nd generation lentivirus, the helper plasmids pMDLg/pRRE; pRSV-REV were replaced by

psPAX2. The conditioned medium was collected after 24 and 48hs, filtered and ultracentrifuged at 50000 RCF on a fixed angle rotor (JA 25.50 Beckmann Coulter) for 150 min at 4°C. Viral pellets were resuspended in PBS without BSA (Gibco).

Other LTVs were generally titrated by Real Time quantitative PCR after infection of HEK293T cells, as previously reported[251]. One end point fluorescence-titrated LTV was included in each PCR titration session and PCR- titers were converted into fluorescence-equivalent titers throughout the study.

7.5. Reprogramming protocol.

Depending on the experimental goal, passage 2 mouse embryonic fibroblasts (P2 MEFs), harboring different $Trp53^{+/+}$ vs $Trp53^{-/-}$, $Sox1^{+/+}$ vs $Sox1^{+/EGFP}$, and $Tau^{+/+}$ vs $Tau^{+/EGFP}$ genotypes, were reprogrammed as follows.

7.5.1.From fibroblasts to NSC-like cells.

Aliquots of $2*10^5$ MEFs were plated on 3.5cm∅ petri dishes (Nunc), as single cell suspensions in MEF medium (90% DMEM, 10% FBS, 1X Glutamax), at 200 cells/µl. Cells were acutely infected by LV_Pgk1p-rtTA^{2S}-M2 and different combinations of LV_TREt-Xi (where Xi = Foxg1, Pax6, Emx2, Lhx2, Brn2 and Sox2), or, alternatively, by LV_Pgk1p-Ascl1. Each lentivirus was used at m.o.i. = 6 when not otherwise specified, in the presence of 9 µg/ml polybrene. 16-20 hours after infection, the medium was replaced by fresh MEF medium, containing 2µg/ml doxycyclin (for TetON system activation) plus different combinations of "epigenetic drugs" [1µM BIX-01294, 2µM trans-2-Phenyl-cyclopropylamine hydrochloride (t2PCPA), 2 mM valproic acid (VPA) and 0.5 mM Na-butyrate](we refer to this TetON activation time point as day 0). 48 hours after doxycyclin addition (day 2), MEF medium was replaced by "neural proliferative medium"(1:1 DMEM-F12, 1X Glutamax, 1X N2 supplement, 6 mg/ml glucose, 1 mg/ml BSA, 2.0 µg/ml heparin, 20 ng/ml Fgf2, 20 ng/ml Egf) supplemented with 2µg/ml doxycyclin (when not otherwise required), previously listed "epigenetic drugs" and different combinations of "signalling pathways modulators" (10µM SB431542, 0.7µM LDN193189, 25µM vitamin C, 0.7µM BIO). Depending on cases, cells were kept in these conditions for 4 up to 15 days. During

this time, drugs-supplemented "neural proliferative medium" was changed every 48 hours. For each experimental session, appearence of NSC-like cells and reprogramming efficiency were assayed by FACs analysis of a dedicated batch of $Sox1^{+/EGFP}$ fibroblasts.

7.5.2.From NSC-like cells to neuron-like cells.

At day ≥6 onward, cultures containing NSC-like cells were trypsinized. When required, they were infected by LV_TREt-Emx2 and LV_TREt-Lhx2, or, alternatively by LV_Pgk1p-Neurog2 and LV_Pgk1p-Ascl1. Infections were performed at m.o.i.'s and cell densities described above, Cells were transferred into 2.0cm∅ wells of 12-well plates (Nunc), pre-coated with 200 µg/ml poly-L-lysine (mw=30,000-70,000). $2,5*10^5$ cells were plated in each well, at a concentration of 500 cells/µl. Cells were kept under "neural differentiative medium" (1:1 DMEM-F12, 1X Glutamax, 1X N2 supplement, 1X B27 supplement, 6 mg/ml glucose, 1 mg/ml BSA, 2.0 µg/ml heparin, 5% heat inactivated FBS), supplemented with 2µg/ml doxycyclin (when not otherwise required), 2 mM VPA and "signalling pathways modulators". Limited to the FPd/N protocol, an alternative neural differentiative medium was employed (1:1 mix of DMEM/F12/N2 and neurobasal/B27, supplemented with 1X glutamax, 1% FBS, 5 µM forskolin, 10□M SB431542 and 0.7µM LDN193189). For each experimental session, appearence of neuron-like cells and reprogramming efficiency were assayed by FACs analysis of a dedicated batch of $Tau^{+/EGFP}$ fibroblasts.

7.6. FACS Sorting and Analysis.

Cultures were dissociated in 0,05% trypsin–EDTA diluted in 1X PBS, for 10 min at 37 °C, pelleted and resuspended in 1X PBS. FACS analysis and sorting of dissociated cells were conducted on a three lasers-equipped Cyan ADP flow cytometer (Dakocytomation, Denmark). Multivariate data analysis was performed by using Flowjo TM software (Tree Star, Ashland, OR). Forward scatter (FSC) and side scatter (SSC) were used to gate nucleated cells and to exclude debris and cell aggregates (live gate) in every analysis. Cells belonging to the live gate were then

further evaluated for the expression of the fluorochromes in use. Cells were categorized on the basis of their EGFP fluorescence profiles.

7.7. Transplantations.

Day 13 FPd/ELv^{+}-fibroblasts were dissociated by 0,05% trypsin (Invitrogen) digestion for 10 min at 37°C. Trypsin was inhibited by addition of 1 volume of DMEM/F12 containing soybean inhibitor (SIGMA), according to manifacturer's instructions. Cell suspension was centrifuged at 100g for 7 min at RT and cells were resuspended in DMEM/F12, containing 1X pen/strept. 50,000 cells (in 1-3µl) were injected by free-hands, with a pulled borosilicate pipette, into the fronto-parietal parenchyma of P0 CD1 wild-type mouse pups, preanasthetized by hypothermia. As a positive control, an equal amount of E12.5 cortico-cerebral precursors form *Tau*^{EGFP} donors, pre-expanded in vitro in DMEM/F12/N2/Fgf2/Egf for 7 days, were injected into recipient pups, in the same transplantation session. Operated recipients were returned to mothers and allowed to develop up to P7 or P14. Their brains were fixed, crioprotected, and sliced at 10 µm, according to standard procedures.

7.8. Immunofluorescence.

For immunocytofluorescence on reprogrammed fibroblasts and cortico-cerebral neurons, cells were fixed directly on poly-L-lysine coated 12 or 24 multiwell plates in 4% paraformaldehyde (PFA) for 20 min at 4°C. Subsequently, cells were washed 3 times in 1X PBS. Alternatively, for immunocytofluorescence analysis on proliferating NSC-like elements, cell clumps were dissociated to single cells as already described and transferred 24 multiwell plates, previously coated with 20µg/µl poly-D-lysine. Cells were left to attach to the well bottom one hour at 37°C, then they were fixed and washed 3 times in 1X PBS. Finally, as for immunofluorescence on brain sections, slices were allowed to dry for at least one hour at RT, they were post-fixed 5 minutes in 4% paraformaldeyde at RT, followed by three washes in 1X PBS. In all three cases, samples were subsequently treated with blocking mix (1X PBS; 10% FBS;

1mg/ml BSA; 0.1% Triton X100) for at least 1 hour at RT. Then, incubation with primary antibody was performed in blocking mix, overnight at 4°C. The day after, samples were washed in 1X PBS and 0,1% Triton X-100 4 times and incubated with a secondary antibody in blocking mix, for 2 hours at RT. Samples were finally washed in PBS for 5 minutes, 4 times, and counterstained with DAPI (4', 6'-diamidino-2-phenylindole). When appropriate, they were and mounted in VECTASHIELD Mounting Medium (Vector).

The following primary antibodies were used: anti-Tubb3, mouse monoclonal, (clone Tuj1, Covance, MMS-435P, 1:1200); anti-GFP, chicken polyclonal (AbCam, ab 13970, 1:600); anti-NeuN mouse monoclonal (clone A60, Millipore, MAB 377, 1:100); anti-MAP2, rabbit polyclonal (Abcam, ab 32454, 1:500); anti-Sox2, rabbit polyclonal (Abcam, ab 97959,1:1000). Secondary antibodies were conjugates of Alexa Fluor 488, and Alexa Fluor 594 (Invitrogen, 1:500).

7.9. Quantitative RT-PCR.

In each experimental session, 500,000 FPd, day 13 cells were trypsinized, centrifuged at 200g for 7min and processed for RNA extraction by TrizolTM (Invitrogen), according to manufacturer's instructions. RNA preparations were treated by DNAseI (2U/mg of RNA) 1 hour at 37°C, and processed by RNeasy Mini Kit (Qiagen). At least 3.0µg of genomic DNA-free total RNA from each sample was retrotranscribed by SuperScriptIII™ (Invitrogen) in the presence of random hexamers, according to manifacturer's instructions. 1/100 of the resulting cDNA was used as substrate of any subsequent qPCR reaction. Limited to intronless amplicons, negative control PCRs were run on RT- RNA preparations. PCR reactions were performed by the SsoAdvanced SYBR Green Supermix™ platform (Biorad), according to manifacturer's instructions. Per each transcript under examination and each sample, cDNA was PCR-analyzed at least in technical triplicate and results averaged. Averages were further normalized against *Gapdh.* Experiments were performed in biological triplicate and analyzed by Student's t test.

Oligos were as follows: Hes5/F 5' GCT CAG TCC CAA GGA GAA AAA CCG ACT GCG 3'; Hes5/R 5' CGC GGC GAA GGC TTT GCT GTG TTT CAG 3'; Neurog2/F 5' GCG ACA CAT CTG GAG

CCG CGT AGG AT 3'; Neurog2/R 5' GCA GCT CCT CGT CCT CCT CCT CGT 3'; Pax6/ForM 5' CCA AGG GCG GTG AGC AGA TGT GTG AGA TCT TCT ATT CTA G 3'; Pax6/RevM 5' CCC GTT GAC AAA GAC ACC ACC AAG CTG ATT CAC TC 3'; Gapdh5/F 5'ATC TTC TTG TGC AGT GCC AGC CTC GTC 3'; Gapdh5/R 5'GAA CAT GTA GAC CAT GTA GTT GAG GTC AAT GAA GG 3'.

7.10. Electrophysiological recordings and data analysis

Whole cell patch clamp recordings (mainly in current-clamp mode) were performed from control and FPd/ELv+ cells 13-19 days after transgenes activation, at 22–24 °C, using a Multiclamp 700A amplifier (Axon Instruments, Foster City, CA).

Patch electrodes were pulled from borosilicate glass capillaries (Hilgenberg, Malsfeld, Germany). They had a resistance of 5-7 MΩ when filled with an intracellular solution containing (in mM): $KMeSO_4$, 135; KCl, 10; EGTA, 0.5; ATP, 2; GTP 0.4 and HEPES 10 (the pH was adjusted to 7.3–7.4 with KOH). During the experiments, cultured cells were superfused with an external solution containing (in mM): NaCl, 140; KCl, 5; $CaCl_2$, 2; $MgCl_2$, 2; glucose 10 and HEPES 10 (pH 7.4 with NaOH). The stability of the patch was checked by repetitively monitoring the input and series resistance during the experiments. Cells exhibiting 15-20% changes were excluded from the analysis. The series resistance was 5–7 MΩ, and it was not compensated.

We first measured the passive membrane properties of control and reprogrammed cells. The latter were recognized by their EGFP fluorescent signals. The resting membrane potential (RMP) was estimated immediately upon break-in by setting the clamp current equal to 0 and was corrected for a liquid junction potential of 10 mV. Membrane capacitance was measured by dividing the area underlying the capacitative transients of current evoked by a 5 mV, 100 ms, voltage step by the voltage step amplitude. The membrane input resistance (R_{in}) was measured by the linear part of the slope of the voltage/current (V/I) relationship obtained by applying hyperpolarizing and depolarizing voltage steps (400 ms duration) of increasing amplitude from a holding potential of -60 mV. The depolarizing voltage steps were sub-threshold for spike generation.

Single action potentials were evoked in current-clamp mode by depolarizing current pulses of increasing amplitude (400 ms duration) delivered at the frequency of 0.05 Hz from a holding potential of -70 mV. In some cases, tetrodotoxin (TTX, purchased from Latoxan, France) was used to block the spikes. Signals were sampled at 10 kHz, low pass-filtered with a Butterworth filter at 3 kHz and stored on a computer hard disk. The analysis of traces was performed with Clampfit 10.1 software (Axon Instruments, Foster City, CA). Data are expressed as mean ± SEM. Unless otherwise stated, significance of differences was assessed by Student's *t* test. The differences were considered significant for $p < 0.05$.

7.11.Images acquisitions

Immunoprofiled cultured reprogrammed cells were photographedon a Nikon TI-E microscope, equipped with 20X or 40X objectives and a Hamamtsu C4742-95 camera.

Immunoprofiled slices of transplanted brains were photographed on a 80i Nikon microscope equipped with a 4X objective and a DS-2MBWC digital microscope camera, as well as on aTCS SP2 Leica confocal microscope equipped with a 20X objective. In the latter case, they were collected as 6µm Z-stacks of 1024*1024 pixel images.

All images were processed using Adobe Photoshop CS3 software.

7.12. Statistical analysis of results.

Generally, when not otherwise stated, experiments were performed at least in biological triplicate. Results were averaged and their statistical significance was evaluated by one-way and two-ways ANOVA (* p<0.5; ** p<0.01; *** p<0.001).

SUPPLEMENTARY MATERIALS

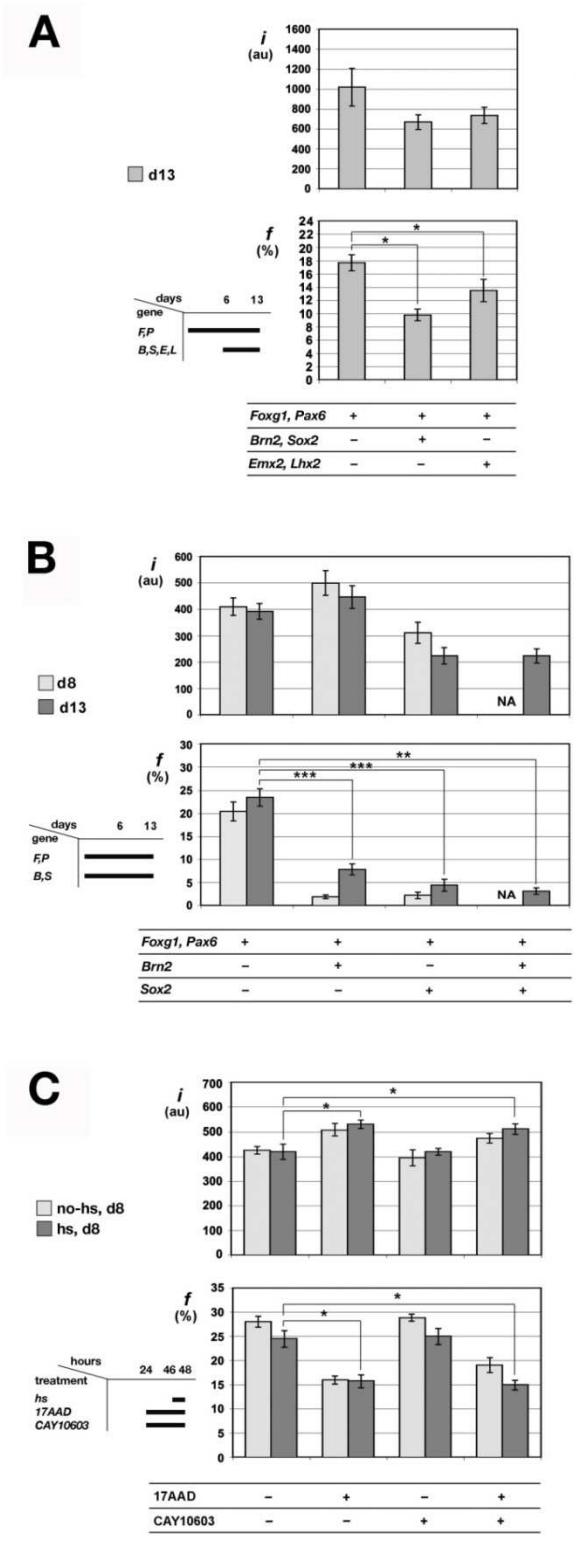

Figure S1. Setting-up the "FPd" protocol: auxiliary tests. (A,B) FACs evaluation of EGFP activation (signal intensity and frequency of positive cells) in cultures of *Trp53*$^{-/-}$*Sox1*^{EGFP} fibroblasts, following lentiviral transduction with different combinations of doxy-activatable reprogramming factor genes. Each lentivirus was delivered at moi = 6. Foxg1 and Pax6 (F and P, respectively) were activated at day 0; Brn2, Sox2, Emx2 and Lhx2 were co-activated with the former ones (A) or, alternatively, transduced at day 6 (B). Frequencies and intesities were evaluated by FAC sorting at day 8 (B) or 13 (A and B). NA, not available. **(C).** FACs evaluation of EGFP activation (signal intensity and frequency of positive cells) in cultures of *Trp53*$^{-/-}$ *Sox1*^{EGFP} fibroblasts, upon delivery of the "FPd" protocol and inibition of the hsp90 machinery. Such inhibition was achieved by keeping cells 24 hours under different combinations of 1μM 17-(allylamino)-17-demethoxygeldanamycin and 1μM CAY10603, and/or exposing them at 41°C for 2 hours. FACs analysis was performed at day 8. au, arbitrary units.

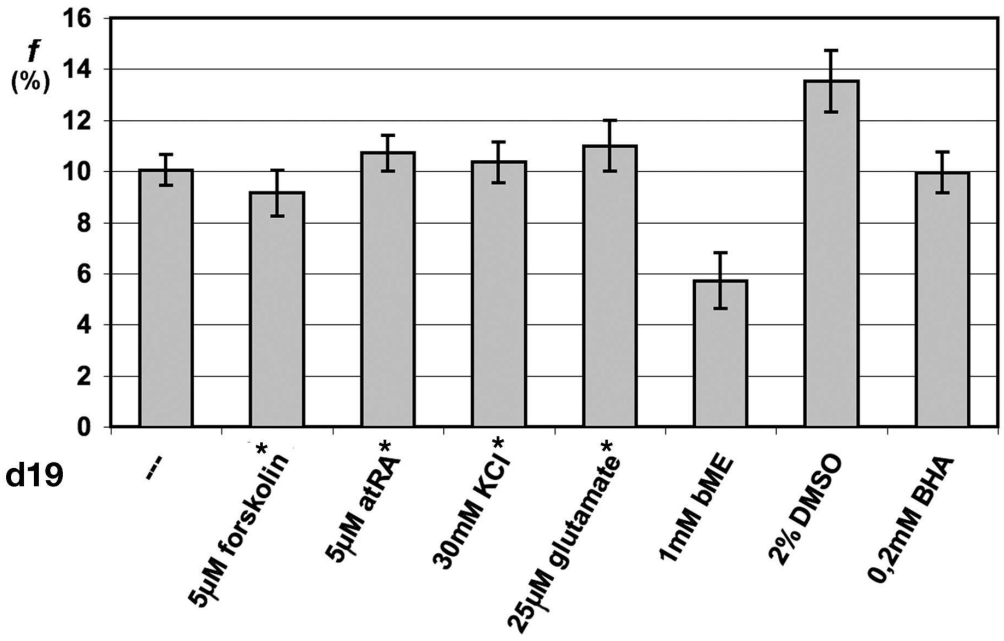

Figure S2. Testing neuronogenic activities of additional drugs on FPd/ELv+ - treated fibroblasts. Plotted are frequencies of TauEGFP(ON) cells, evaluated at day 19, upon inclusion of neuronogenic drugs into the "neural prodifferentiative medium". Cells were exposed to these drugs from day 7 to day 19, or from day 7 -to day 11 (asterisks).

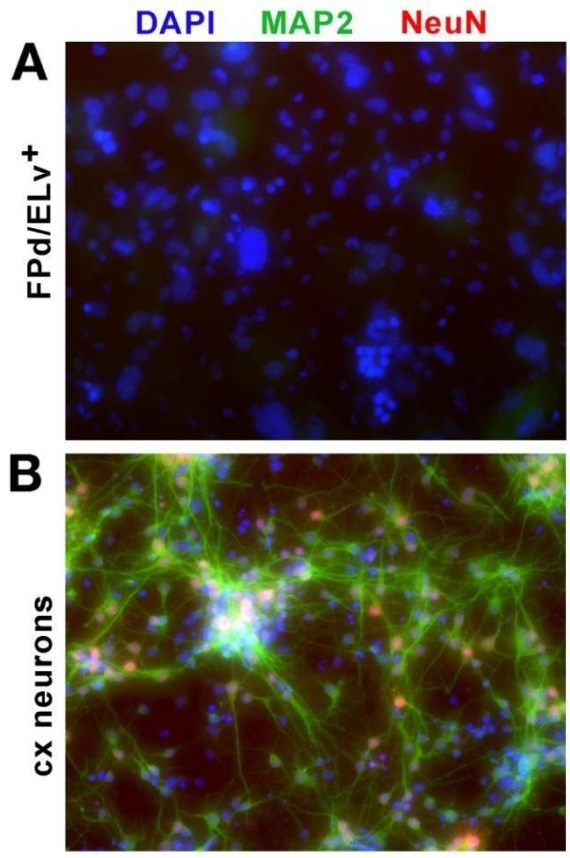

Figure S3. Defective neuronal differentiation of reprogrammed fibroblasts in vitro. MAP2/NeuN immunoprofiling of FPd/ELv+ day 13 fibroblasts **(A)** and control E14.5 cortico-cerebral precursors, differentiated in vitro for 7 days **(B)**.

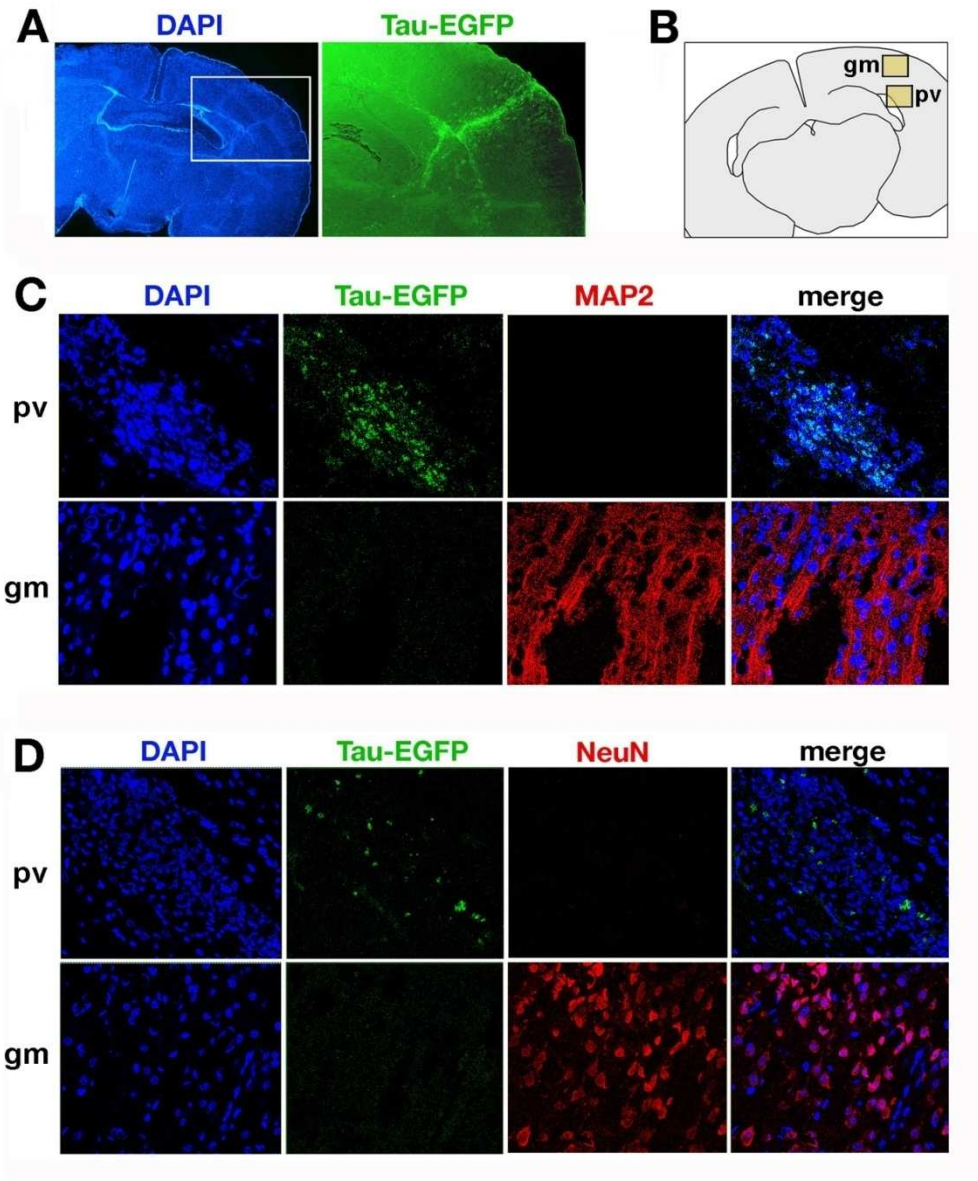

Figure S4. Defective neuronal differentiation of reprogrammed fibroblasts in vivo. (A) In vivo distribution of derivatives of E12.5 cortico-cerebral precursors, originating from *Tau*^{EGFP} donors, cultured 7 days in vitro under "neural proliferative medium" and transplanted into parietal cortex of P0 wild type recipients. Brains were fixed 7 days after transplantation. **(B).** Silhouette representing a midfrontal section of a wild type brain transplanted at P0 with derivatives of FPd/ELv^{+}-treated, IVD14 *Tau*^{EGFP} fibroblasts, fixed 7 days after transplantation. gm, grey matter; pv, periventricular region. (C, D). Distribution of -EGFP, -MAP2 and -NeuN immunoreactivities, as detected by confocal microscopy in the two boxed regions of panel **(B)**.

ACKNOWLEDGMENTS

It would not have been possible to write this doctoral thesis without the help and support of so many beautiful people around me. However, only to some of them it is possible to give particular mention here.

First, I would like to thanks my supervisor, Antonello Mallamaci, for his patience, scientific support and for giving me the opportunity to join his group and to work on such a fascinating topic. His guidance helped me in all the time of research and writing of this thesis.

I am most grateful to my previous and actual labmates, for helping and supporting me during these years of PhD, for the stimulating discussions , for all the fun we have had in the last four years and, above all, for their friendship. I consider myself very lucky to have met them. I know that, in the future, I hardly will have the opportunity to work surrounded by such a beautiful and reassuring atmosphere.

I would like to thank my dear friend Andrea Tomicich for his kindness, friendship and support, Beatrice Pastore for technical assistance in cell cultures and all the SISSA staff people.

Special thanks to Cristina and Minh, for their precious and irreplaceable help in molecular and in vivo characterization of my experiments, to Marilena for her substantial contribution to this project, for her patience and for the accuracy in analysis of FACS data.

I would like to express my gratitude to prof. Enrico Cherubini and Giada Cellot for electrophysiological recordings, proficient interpretation of data and for their important suggestions.

I am eternally grateful to Ludwig for being always a source of inspiration and strength.

Finally, my deepest thankfulness goes to Francis, for bringing joy into my days since the first moment he came into my life, for his love, for sharing with me so many dreams and beautiful experiences and for supporting me in the darkest moments.

Last but not the least, I would like to thank my parents, my brother and all close members of my family, for their esteem and for supporting me spiritually throughout my life.

REFERENCES

1. Rhinn, M., Picker, A. & Brand, M. Global and local mechanisms of forebrain and midbrain patterning. *Curr. Opin. Neurobiol.***16**, 5–12 (2006).
2. Gamse, J. & Sive, H. Vertebrate anteroposterior patterning: the Xenopus neurectoderm as a paradigm. *Bioessays***22**, 976–986 (2000).
3. Thomas, P. & Beddington, R. Anterior primitive endoderm may be responsible for patterning the anterior neural plate in the mouse embryo. *Curr. Biol.***6**, 1487–1496 (1996).
4. Sasai, Y. & De Robertis, E. M. Ectodermal patterning in vertebrate embryos. *Dev. Biol.***182**, 5–20 (1997).
5. Altmann, C. R. & Brivanlou, A. H. Neural patterning in the vertebrate embryo. *Int. Rev. Cytol.***203**, 447–482 (2001).
6. Ciani, L. & Salinas, P. C. WNTs in the vertebrate nervous system: from patterning to neuronal connectivity. *Nat. Rev. Neurosci.***6**, 351–362 (2005).
7. Shimamura, K. & Rubenstein, J. L. Inductive interactions direct early regionalization of the mouse forebrain. *Development***124**, 2709–2718 (1997).
8. Fuccillo, M., Rutlin, M. & Fishell, G. Removal of Pax6 partially rescues the loss of ventral structures in Shh null mice. *Cereb. Cortex***16 Suppl 1**, i96–102 (2006).
9. Garcia-Lopez, R., Vieira, C., Echevarria, D. & Martinez, S. Fate map of the diencephalon and the zona limitans at the 10-somites stage in chick embryos. *Dev. Biol.***268**, 514–530 (2004).
10. Paek, H., Gutin, G. & Hébert, J. M. FGF signaling is strictly required to maintain early telencephalic precursor cell survival. *Development***136**, 2457–2465 (2009).
11. Liem, K. F., Jr, Tremml, G., Roelink, H. & Jessell, T. M. Dorsal differentiation of neural plate cells induced by BMP-mediated signals from epidermal ectoderm. *Cell***82**, 969–979 (1995).
12. Liem, K. F., Jr, Tremml, G. & Jessell, T. M. A role for the roof plate and its resident TGFbeta-related proteins in neuronal patterning in the dorsal spinal cord. *Cell***91**, 127–138 (1997).
13. Pierani, A., Brenner-Morton, S., Chiang, C. & Jessell, T. M. A sonic hedgehog-independent, retinoid-activated pathway of neurogenesis in the ventral spinal cord. *Cell***97**, 903–915 (1999).
14. Roelink, H. *et al.* Floor plate and motor neuron induction by different concentrations of the amino-terminal cleavage product of sonic hedgehog autoproteolysis. *Cell***81**, 445–455 (1995).
15. Briscoe, J. *et al.* Homeobox gene Nkx2.2 and specification of neuronal identity by graded Sonic hedgehog signalling. *Nature***398**, 622–627 (1999).
16. Rallu, M., Corbin, J. G. & Fishell, G. Parsing the prosencephalon. *Nat. Rev. Neurosci.***3**, 943–951 (2002).
17. Hoch, R. V., Rubenstein, J. L. R. & Pleasure, S. Genes and signaling events that establish regional patterning of the mammalian forebrain. *Semin. Cell Dev. Biol.***20**, 378–386 (2009).
18. Hébert, J. M. & Fishell, G. The genetics of early telencephalon patterning: some assembly required. *Nat. Rev. Neurosci.***9**, 678–685 (2008).
19. Martynoga, B., Morrison, H., Price, D. J. & Mason, J. O. Foxg1 is required for specification of ventral telencephalon and region-specific regulation of dorsal telencephalic precursor proliferation and apoptosis. *Dev. Biol.***283**, 113–127 (2005).
20. Yun, K. *et al.* Modulation of the notch signaling by Mash1 and Dlx1/2 regulates sequential specification and differentiation of progenitor cell types in the subcortical telencephalon. *Development***129**, 5029–5040 (2002).

21. Fode, C. *et al.* A role for neural determination genes in specifying the dorsoventral identity of telencephalic neurons. *Genes Dev.***14**, 67–80 (2000).
22. Hébert, J. M. & McConnell, S. K. Targeting of cre to the Foxg1 (BF-1) locus mediates loxP recombination in the telencephalon and other developing head structures. *Dev. Biol.***222**, 296–306 (2000).
23. Tao, W. & Lai, E. Telencephalon-restricted expression of BF-1, a new member of the HNF-3/fork head gene family, in the developing rat brain. *Neuron***8**, 957–966 (1992).
24. Storm, E. E. *et al.* Dose-dependent functions of Fgf8 in regulating telencephalic patterning centers. *Development***133**, 1831–1844 (2006).
25. Danesin, C. *et al.* Integration of telencephalic Wnt and hedgehog signaling center activities by Foxg1. *Dev. Cell***16**, 576–587 (2009).
26. Bourguignon, C., Li, J. & Papalopulu, N. XBF-1, a winged helix transcription factor with dual activity, has a role in positioning neurogenesis in Xenopus competent ectoderm. *Development***125**, 4889–4900 (1998).
27. Dou, C. *et al.* BF-1 interferes with transforming growth factor beta signaling by associating with Smad partners. *Mol. Cell. Biol.***20**, 6201–6211 (2000).
28. Li, J., Chang, H. W., Lai, E., Parker, E. J. & Vogt, P. K. The oncogene qin codes for a transcriptional repressor. *Cancer Res.***55**, 5540–5544 (1995).
29. Seoane, J., Le, H.-V., Shen, L., Anderson, S. A. & Massagué, J. Integration of Smad and Forkhead Pathways in the Control of Neuroepithelial and Glioblastoma Cell Proliferation. *Cell***117**, 211–223 (2004).
30. Yao, J., Lai, E. & Stifani, S. The winged-helix protein brain factor 1 interacts with groucho and hes proteins to repress transcription. *Mol. Cell. Biol.***21**, 1962–1972 (2001).
31. Seoane, J., Le, H.-V., Shen, L., Anderson, S. A. & Massagué, J. Integration of Smad and forkhead pathways in the control of neuroepithelial and glioblastoma cell proliferation. *Cell***117**, 211–223 (2004).
32. Hanashima, C., Shen, L., Li, S. C. & Lai, E. Brain factor-1 controls the proliferation and differentiation of neocortical progenitor cells through independent mechanisms. *J. Neurosci.***22**, 6526–6536 (2002).
33. Sonderegger, C. K. & Vogt, P. K. Binding of the corepressor TLE1 to Qin enhances Qin-mediated transformation of chicken embryo fibroblasts. *Oncogene***22**, 1749–1757 (2003).
34. Tan, K. *et al.* Human PLU-1 Has transcriptional repression properties and interacts with the developmental transcription factors BF-1 and PAX9. *J. Biol. Chem.***278**, 20507–20513 (2003).
35. Chen, G., Fernandez, J., Mische, S. & Courey, A. J. A functional interaction between the histone deacetylase Rpd3 and the corepressor groucho in Drosophila development. *Genes Dev.***13**, 2218–2230 (1999).
36. Yamane, K. *et al.* PLU-1 is an H3K4 demethylase involved in transcriptional repression and breast cancer cell proliferation. *Mol. Cell***25**, 801–812 (2007).
37. Marçal, N. *et al.* Antagonistic Effects of Grg6 and Groucho/TLE on the Transcription Repression Activity of Brain Factor 1/FoxG1 and Cortical Neuron Differentiation. *Mol Cell Biol***25**, 10916–10929 (2005).
38. Roth, M. *et al.* FoxG1 and TLE2 act cooperatively to regulate ventral telencephalon formation. *Development***137**, 1553–1562 (2010).
39. Toresson, H., Potter, S. S. & Campbell, K. Genetic control of dorsal-ventral identity in the telencephalon: opposing roles for Pax6 and Gsh2. *Development***127**, 4361–4371 (2000).
40. Stoykova, A., Treichel, D., Hallonet, M. & Gruss, P. Pax6 modulates the dorsoventral patterning of the mammalian telencephalon. *J. Neurosci.***20**, 8042–8050 (2000).

41. Sussel, L., Marin, O., Kimura, S. & Rubenstein, J. L. Loss of Nkx2.1 homeobox gene function results in a ventral to dorsal molecular respecification within the basal telencephalon: evidence for a transformation of the pallidum into the striatum. *Development***126**, 3359–3370 (1999).
42. Grove, E. A., Tole, S., Limon, J., Yip, L. & Ragsdale, C. W. The hem of the embryonic cerebral cortex is defined by the expression of multiple Wnt genes and is compromised in Gli3-deficient mice. *Development***125**, 2315–2325 (1998).
43. Furuta, Y., Piston, D. W. & Hogan, B. L. Bone morphogenetic proteins (BMPs) as regulators of dorsal forebrain development. *Development***124**, 2203–2212 (1997).
44. Monuki, E. S., Porter, F. D. & Walsh, C. A. Patterning of the dorsal telencephalon and cerebral cortex by a roof plate-Lhx2 pathway. *Neuron***32**, 591–604 (2001).
45. Assimacopoulos, S., Grove, E. A. & Ragsdale, C. W. Identification of a Pax6-dependent epidermal growth factor family signaling source at the lateral edge of the embryonic cerebral cortex. *J. Neurosci.***23**, 6399–6403 (2003).
46. Simeone, A. *et al.* Two vertebrate homeobox genes related to the Drosophila empty spiracles gene are expressed in the embryonic cerebral cortex. *EMBO J.***11**, 2541–2550 (1992).
47. Mallamaci, A. *et al.* EMX2 protein in the developing mouse brain and olfactory area. *Mech. Dev.***77**, 165–172 (1998).
48. Gulisano, M., Broccoli, V., Pardini, C. & Boncinelli, E. Emx1 and Emx2 show different patterns of expression during proliferation and differentiation of the developing cerebral cortex in the mouse. *Eur. J. Neurosci.***8**, 1037–1050 (1996).
49. Walther, C. & Gruss, P. Pax-6, a murine paired box gene, is expressed in the developing CNS. *Development***113**, 1435–1449 (1991).
50. Stoykova, A. & Gruss, P. Roles of Pax-genes in developing and adult brain as suggested by expression patterns. *J. Neurosci.***14**, 1395–1412 (1994).
51. Briata, P. *et al.* EMX1 homeoprotein is expressed in cell nuclei of the developing cerebral cortex and in the axons of the olfactory sensory neurons. *Mech. Dev.***57**, 169–180 (1996).
52. Bulfone, A. *et al.* Expression pattern of the Tbr2 (Eomesodermin) gene during mouse and chick brain development. *Mech. Dev.***84**, 133–138 (1999).
53. Roelink, H. & Nusse, R. Expression of two members of the Wnt family during mouse development--restricted temporal and spatial patterns in the developing neural tube. *Genes Dev.***5**, 381–388 (1991).
54. Lee, S. M., Tole, S., Grove, E. & McMahon, A. P. A local Wnt-3a signal is required for development of the mammalian hippocampus. *Development***127**, 457–467 (2000).
55. Ragsdale, C. W. & Grove, E. A. Patterning the mammalian cerebral cortex. *Current Opinion in Neurobiology***11**, 50–58 (2001).
56. Monuki, E. S., Porter, F. D. & Walsh, C. A. Patterning of the dorsal telencephalon and cerebral cortex by a roof plate-Lhx2 pathway. *Neuron***32**, 591–604 (2001).
57. Ivaniutsin, U., Chen, Y., Mason, J. O., Price, D. J. & Pratt, T. Adenomatous polyposis coli is required for early events in the normal growth and differentiation of the developing cerebral cortex. *Neural Dev***4**, 3 (2009).
58. Crossley, P. H., Martinez, S., Ohkubo, Y. & Rubenstein, J. L. Coordinate expression of Fgf8, Otx2, Bmp4, and Shh in the rostral prosencephalon during development of the telencephalic and optic vesicles. *Neuroscience***108**, 183–206 (2001).
59. Garel, S., Huffman, K. J. & Rubenstein, J. L. R. Molecular regionalization of the neocortex is disrupted in Fgf8 hypomorphic mutants. *Development***130**, 1903–1914 (2003).
60. Machon, O. *et al.* A dynamic gradient of Wnt signaling controls initiation of neurogenesis in the mammalian cortex and cellular specification in the hippocampus. *Dev. Biol.***311**, 223–237 (2007).

61. Ivaniutsin, U., Chen, Y., Mason, J. O., Price, D. J. & Pratt, T. Adenomatous polyposis coli is required for early events in the normal growth and differentiation of the developing cerebral cortex. *Neural Dev***4**, 3 (2009).
62. Bulchand, S., Subramanian, L. & Tole, S. Dynamic spatiotemporal expression of LIM genes and cofactors in the embryonic and postnatal cerebral cortex. *Dev. Dyn.***226**, 460–469 (2003).
63. Bishop, K. M., Goudreau, G. & O'Leary, D. D. Regulation of area identity in the mammalian neocortex by Emx2 and Pax6. *Science***288**, 344–349 (2000).
64. Muzio, L. *et al.* Emx2 and Pax6 control regionalization of the pre-neuronogenic cortical primordium. *Cereb. Cortex***12**, 129–139 (2002).
65. Kimura, J. *et al.* Emx2 and Pax6 function in cooperation with Otx2 and Otx1 to develop caudal forebrain primordium that includes future archipallium. *J. Neurosci.***25**, 5097–5108 (2005).
66. Theil, T., Alvarez-Bolado, G., Walter, A. & Rüther, U. Gli3 is required for Emx gene expression during dorsal telencephalon development. *Development***126**, 3561–3571 (1999).
67. Frotscher, M. *et al.* Role of Reelin in the development and maintenance of cortical lamination. *J Neural Transm***116**, 1451–1455 (2009).
68. Takiguchi-Hayashi, K. *et al.* Generation of reelin-positive marginal zone cells from the caudomedial wall of telencephalic vesicles. *J. Neurosci.***24**, 2286–2295 (2004).
69. Yoshida, M., Assimacopoulos, S., Jones, K. R. & Grove, E. A. Massive loss of Cajal-Retzius cells does not disrupt neocortical layer order. *Development***133**, 537–545 (2006).
70. Tan, S. S. & Breen, S. Radial mosaicism and tangential cell dispersion both contribute to mouse neocortical development. *Nature***362**, 638–640 (1993).
71. Soriano, E., Dumesnil, N., Auladell, C., Cohen-Tannoudji, M. & Sotelo, C. Molecular heterogeneity of progenitors and radial migration in the developing cerebral cortex revealed by transgene expression. *Proc. Natl. Acad. Sci. U.S.A.***92**, 11676–11680 (1995).
72. O'Rourke, N. A., Sullivan, D. P., Kaznowski, C. E., Jacobs, A. A. & McConnell, S. K. Tangential migration of neurons in the developing cerebral cortex. *Development***121**, 2165–2176 (1995).
73. Wonders, C. P. & Anderson, S. A. The origin and specification of cortical interneurons. *Nat. Rev. Neurosci.***7**, 687–696 (2006).
74. Anderson, S. A., Eisenstat, D. D., Shi, L. & Rubenstein, J. L. R. Interneuron Migration from Basal Forebrain to Neocortex: Dependence on Dlx Genes. *Science***278**, 474–476 (1997).
75. Marin-Padilla, M. Early prenatal ontogenesis of the cerebral cortex (neocortex) of the cat (Felis domestica). A Golgi study. I. The primordial neocortical organization. *Z Anat Entwicklungsgesch***134**, 117–145 (1971).
76. Marin-Padilla, M. Structural abnormalities of the cerebral cortex in human chromosomal aberrations: a Golgi study. *Brain Res.***44**, 625–629 (1972).
77. Bayer, S. A. & Altman, J. Development of the endopiriform nucleus and the claustrum in the rat brain. *Neuroscience***45**, 391–412 (1991).
78. Englund, C. *et al.* Pax6, Tbr2, and Tbr1 are expressed sequentially by radial glia, intermediate progenitor cells, and postmitotic neurons in developing neocortex. *J. Neurosci.***25**, 247–251 (2005).
79. Götz, M. & Huttner, W. B. The cell biology of neurogenesis. *Nat. Rev. Mol. Cell Biol.***6**, 777–788 (2005).
80. Gal, J. S. *et al.* Molecular and Morphological Heterogeneity of Neural Precursors in the Mouse Neocortical Proliferative Zones. *J Neurosci***26**, 1045–1056 (2006).
81. Götz, M. & Huttner, W. B. The cell biology of neurogenesis. *Nat. Rev. Mol. Cell Biol.***6**, 777–788 (2005).
82. Kriegstein, A., Noctor, S. & Martínez-Cerdeño, V. Patterns of neural stem and progenitor cell division may underlie evolutionary cortical expansion. *Nat. Rev. Neurosci.***7**, 883–890 (2006).
83. Sawamoto, K. *et al.* Direct isolation of committed neuronal progenitor cells from transgenic mice coexpressing spectrally distinct fluorescent proteins regulated by stage-specific neural promoters. *J. Neurosci. Res.***65**, 220–227 (2001).

84. Hartfuss, E., Galli, R., Heins, N. & Götz, M. Characterization of CNS precursor subtypes and radial glia. *Dev. Biol.***229**, 15–30 (2001).
85. Hatakeyama, J. *et al.* Hes genes regulate size, shape and histogenesis of the nervous system by control of the timing of neural stem cell differentiation. *Development***131**, 5539–5550 (2004).
86. Heins, N. *et al.* Emx2 promotes symmetric cell divisions and a multipotential fate in precursors from the cerebral cortex. *Mol. Cell. Neurosci.***18**, 485–502 (2001).
87. Muzio, L., Soria, J. M., Pannese, M., Piccolo, S. & Mallamaci, A. A mutually stimulating loop involving emx2 and canonical wnt signalling specifically promotes expansion of occipital cortex and hippocampus. *Cereb. Cortex***15**, 2021–2028 (2005).
88. Roy, K. *et al.* The Tlx gene regulates the timing of neurogenesis in the cortex. *J. Neurosci.***24**, 8333–8345 (2004).
89. Quinn, J. C. *et al.* Pax6 controls cerebral cortical cell number by regulating exit from the cell cycle and specifies cortical cell identity by a cell autonomous mechanism. *Dev Biol***302**, 50–65 (2007).
90. Schuurmans, C. *et al.* Sequential phases of cortical specification involve Neurogenin-dependent and -independent pathways. *EMBO J.***23**, 2892–2902 (2004).
91. Schwab, M. H. *et al.* Neuronal basic helix-loop-helix proteins (NEX, neuroD, NDRF): spatiotemporal expression and targeted disruption of the NEX gene in transgenic mice. *J. Neurosci.***18**, 1408–1418 (1998).
92. Götz, M., Stoykova, A. & Gruss, P. Pax6 controls radial glia differentiation in the cerebral cortex. *Neuron***21**, 1031–1044 (1998).
93. Scardigli, R., Bäumer, N., Gruss, P., Guillemot, F. & Le Roux, I. Direct and concentration-dependent regulation of the proneural gene Neurogenin2 by Pax6. *Development***130**, 3269–3281 (2003).
94. Evans, M. J. & Kaufman, M. H. Establishment in culture of pluripotential cells from mouse embryos. *Nature***292**, 154–156 (1981).
95. Martin, G. R. Isolation of a pluripotent cell line from early mouse embryos cultured in medium conditioned by teratocarcinoma stem cells. *Proc. Natl. Acad. Sci. U.S.A.***78**, 7634–7638 (1981).
96. Thomson, J. A. *et al.* Embryonic stem cell lines derived from human blastocysts. *Science***282**, 1145–1147 (1998).
97. Takahashi, K. & Yamanaka, S. Induction of Pluripotent Stem Cells from Mouse Embryonic and Adult Fibroblast Cultures by Defined Factors. *Cell***126**, 663–676 (2006).
98. Wilmut, I., Schnieke, A. E., McWhir, J., Kind, A. J. & Campbell, K. H. S. Viable offspring derived from fetal and adult mammalian cells. *, Published online: 27 February 1997; | doi:10.1038/385810a0***385**, 810–813 (1997).
99. French, A. J. *et al.* Development of human cloned blastocysts following somatic cell nuclear transfer with adult fibroblasts. *Stem Cells***26**, 485–493 (2008).
100. Chung, Y. *et al.* Reprogramming of human somatic cells using human and animal oocytes. *Cloning Stem Cells***11**, 213–223 (2009).
101. Kim, D. *et al.* Generation of human induced pluripotent stem cells by direct delivery of reprogramming proteins. *Cell Stem Cell***4**, 472–476 (2009).
102. Miller, R. A. & Ruddle, F. H. Pluripotent teratocarcinoma-thymus somatic cell hybrids. *Cell***9**, 45–55 (1976).
103. Tada, M., Tada, T., Lefebvre, L., Barton, S. C. & Surani, M. A. Embryonic germ cells induce epigenetic reprogramming of somatic nucleus in hybrid cells. *EMBO J.***16**, 6510–6520 (1997).
104. Tada, M., Takahama, Y., Abe, K., Nakatsuji, N. & Tada, T. Nuclear reprogramming of somatic cells by in vitro hybridization with ES cells. *Current Biology***11**, 1553–1558 (2001).
105. Tada, M. *et al.* Pluripotency of reprogrammed somatic genomes in embryonic stem hybrid cells. *Developmental Dynamics***227**, 504–510 (2003).

106. Cowan, C. A., Atienza, J., Melton, D. A. & Eggan, K. Nuclear Reprogramming of Somatic Cells After Fusion with Human Embryonic Stem Cells. *Science***309**, 1369–1373 (2005).
107. Hochedlinger, K. & Jaenisch, R. Nuclear reprogramming and pluripotency. *Nature***441**, 1061–1067 (2006).
108. Maherali, N. *et al.* Directly reprogrammed fibroblasts show global epigenetic remodeling and widespread tissue contribution. *Cell Stem Cell***1**, 55–70 (2007).
109. Okita, K., Ichisaka, T. & Yamanaka, S. Generation of germline-competent induced pluripotent stem cells. *Nature***448**, 313–317 (2007).
110. Wernig, M. *et al.* In vitro reprogramming of fibroblasts into a pluripotent ES-cell-like state. *Nature***448**, 318–324 (2007).
111. Yu, J. *et al.* Induced Pluripotent Stem Cell Lines Derived from Human Somatic Cells. *Science***318**, 1917–1920 (2007).
112. Takahashi, K. *et al.* Induction of Pluripotent Stem Cells from Adult Human Fibroblasts by Defined Factors. *Cell***131**, 861–872 (2007).
113. Aasen, T. & Belmonte, J. C. I. Isolation and cultivation of human keratinocytes from skin or plucked hair for the generation of induced pluripotent stem cells. *Nature Protocols***5**, 371–382 (2010).
114. Aasen, T. *et al.* Efficient and rapid generation of induced pluripotent stem cells from human keratinocytes. *Nat. Biotechnol.***26**, 1276–1284 (2008).
115. Loh, Y.-H. *et al.* Generation of induced pluripotent stem cells from human blood. *Blood***113**, 5476–5479 (2009).
116. Giorgetti, A. *et al.* Generation of induced pluripotent stem cells from human cord blood using OCT4 and SOX2. *Cell Stem Cell***5**, 353–357 (2009).
117. Haase, A. *et al.* Generation of Induced Pluripotent Stem Cells from Human Cord Blood. *Cell Stem Cell***5**, 434–441 (2009).
118. Utikal, J., Maherali, N., Kulalert, W. & Hochedlinger, K. Sox2 is dispensable for the reprogramming of melanocytes and melanoma cells into induced pluripotent stem cells. *J Cell Sci***122**, 3502–3510 (2009).
119. Kim, J. B. *et al.* Direct reprogramming of human neural stem cells by OCT4. *Nature***461**, 649–643 (2009).
120. Li, C. *et al.* Pluripotency can be rapidly and efficiently induced in human amniotic fluid-derived cells. *Hum. Mol. Genet.***18**, 4340–4349 (2009).
121. Ye, Z. *et al.* Human-induced pluripotent stem cells from blood cells of healthy donors and patients with acquired blood disorders. *Blood***114**, 5473–5480 (2009).
122. Sun, N. *et al.* Feeder-free derivation of induced pluripotent stem cells from adult human adipose stem cells. *Proceedings of the National Academy of Sciences***106**, 15720–15725 (2009).
123. Yan, X. *et al.* iPS Cells Reprogrammed From Human Mesenchymal-Like Stem/Progenitor Cells of Dental Tissue Origin. *Stem Cells Dev***19**, 469–480 (2010).
124. Cai, J. *et al.* Generation of Human Induced Pluripotent Stem Cells from Umbilical Cord Matrix and Amniotic Membrane Mesenchymal Cells. *J Biol Chem***285**, 11227–11234 (2010).
125. Nakagawa, M. *et al.* Generation of induced pluripotent stem cells without Myc from mouse and human fibroblasts. *Nature Biotechnology***26**, 101–106 (2008).
126. Kim J, et al. Direct reprogramming of mouse fibroblasts to neural progenitors. Proc Natl Acad Sci USA 108:7838–7843 (2011).
127. Yu, J. *et al.* Induced Pluripotent Stem Cell Lines Derived from Human Somatic Cells. *Science***318**, 1917–1920 (2007).
128. Kim, J. B. *et al.* Pluripotent stem cells induced from adult neural stem cells by reprogramming with two factors. *Nature***454**, 646–650 (2008).

129. Zhao, H. *et al.* Rapid and efficient reprogramming of human amnion-derived cells into pluripotency by three factors OCT4/SOX2/NANOG. *Differentiation***80**, 123–129 (2010).
130. Huangfu, D. *et al.* Induction of pluripotent stem cells from primary human fibroblasts with only Oct4 and Sox2. *Nat. Biotechnol.***26**, 1269–1275 (2008).
131. Giorgetti, A. *et al.* Generation of induced pluripotent stem cells from human cord blood cells with only two factors: Oct4 and Sox2. *Nat Protoc***5**, 811–820 (2010).
132. Tsai, S.-Y. *et al.* Oct4 and klf4 reprogram dermal papilla cells into induced pluripotent stem cells. *Stem Cells***28**, 221–228 (2010).
133. Picanço-Castro, V. *et al.* Pluripotent reprogramming of fibroblasts by lentiviral mediated insertion of SOX2, C-MYC, and TCL-1A. *Stem Cells Dev.***20**, 169–180 (2011).
134. Feng, B. *et al.* Reprogramming of fibroblasts into induced pluripotent stem cells with orphan nuclear receptor Esrrb. *Nat. Cell Biol.***11**, 197–203 (2009).
135. Heng, J.-C. D. *et al.* The nuclear receptor Nr5a2 can replace Oct4 in the reprogramming of murine somatic cells to pluripotent cells. *Cell Stem Cell***6**, 167–174 (2010).
136. Maherali, N. & Hochedlinger, K. Guidelines and techniques for the generation of induced pluripotent stem cells. *Cell Stem Cell***3**, 595–605 (2008).
137. Okita, K., Nakagawa, M., Hyenjong, H., Ichisaka, T. & Yamanaka, S. Generation of mouse induced pluripotent stem cells without viral vectors. *Science***322**, 949–953 (2008).
138. Yamanaka, S. Strategies and new developments in the generation of patient-specific pluripotent stem cells. *Cell Stem Cell***1**, 39–49 (2007).
139. Wernig, M. *et al.* A drug-inducible transgenic system for direct reprogramming of multiple somatic cell types. *Nat. Biotechnol.***26**, 916–924 (2008).
140. Hong, H. *et al.* Suppression of induced pluripotent stem cell generation by the p53–p21 pathway. *Nature***460**, 1132–1135 (2009).
141. Loh, Y.-H. *et al.* The Oct4 and Nanog transcription network regulates pluripotency in mouse embryonic stem cells. *Nature Genetics***38**, 431–440 (2006).
142. Loh, Y.-H., Zhang, W., Chen, X., George, J. & Ng, H.-H. Jmjd1a and Jmjd2c histone H3 Lys 9 demethylases regulate self-renewal in embryonic stem cells. *Genes Dev***21**, 2545–2557 (2007).
143. Meissner, A., Wernig, M. & Jaenisch, R. Direct reprogramming of genetically unmodified fibroblasts into pluripotent stem cells. *Nat. Biotechnol.***25**, 1177–1181 (2007).
144. Bestor, T. H. Activation of mammalian DNA methyltransferase by cleavage of a Zn binding regulatory domain. *EMBO J.***11**, 2611–2617 (1992).
145. Li, E., Bestor, T. H. & Jaenisch, R. Targeted mutation of the DNA methyltransferase gene results in embryonic lethality. *Cell***69**, 915–926 (1992).
146. Okano, M., Bell, D. W., Haber, D. A. & Li, E. DNA methyltransferases Dnmt3a and Dnmt3b are essential for de novo methylation and mammalian development. *Cell***99**, 247–257 (1999).
147. Lyko, F., Beisel, C., Marhold, J. & Paro, R. Epigenetic regulation in Drosophila. *Curr. Top. Microbiol. Immunol.***310**, 23–44 (2006).
148. Hsieh, C. L. In vivo activity of murine de novo methyltransferases, Dnmt3a and Dnmt3b. *Mol. Cell. Biol.***19**, 8211–8218 (1999).
149. Burgers, W. A., Fuks, F. & Kouzarides, T. DNA methyltransferases get connected to chromatin. *Trends Genet.***18**, 275–277 (2002).
150. Mikkelsen, T. S. *et al.* Dissecting direct reprogramming through integrative genomic analysis. *Nature***454**, 49–55 (2008).
151. Mikkelsen, T. S. *et al.* Dissecting direct reprogramming through integrative genomic analysis. *Nature***454**, 49–55 (2008).
152. Shi, Y. *et al.* Induction of pluripotent stem cells from mouse embryonic fibroblasts by Oct4 and Klf4 with small-molecule compounds. *Cell Stem Cell***3**, 568–574 (2008).

153. Meissner, A., Wernig, M. & Jaenisch, R. Direct reprogramming of genetically unmodified fibroblasts into pluripotent stem cells. *Nat. Biotechnol.***25**, 1177–1181 (2007).
154. Huangfu, D. *et al.* Induction of pluripotent stem cells by defined factors is greatly improved by small-molecule compounds. *Nat. Biotechnol.***26**, 795–797 (2008).
155. Feldman, N. *et al.* G9a-mediated irreversible epigenetic inactivation of Oct-3/4 during early embryogenesis. *Nat. Cell Biol.***8**, 188–194 (2006).
156. Epsztejn-Litman, S. *et al.* De novo DNA methylation promoted by G9a prevents reprogramming of embryonically silenced genes. *Nat. Struct. Mol. Biol.***15**, 1176–1183 (2008).
157. Willis, B. C. & Borok, Z. TGF-beta-induced EMT: mechanisms and implications for fibrotic lung disease. *Am. J. Physiol. Lung Cell Mol. Physiol.***293**, L525–534 (2007).
158. Thiery, J. P. & Sleeman, J. P. Complex networks orchestrate epithelial-mesenchymal transitions. *Nat. Rev. Mol. Cell Biol.***7**, 131–142 (2006).
159. Chou, Y.-F. *et al.* The growth factor environment defines distinct pluripotent ground states in novel blastocyst-derived stem cells. *Cell***135**, 449–461 (2008).
160. Maherali, N. & Hochedlinger, K. Tgfbeta signal inhibition cooperates in the induction of iPSCs and replaces Sox2 and cMyc. *Curr. Biol.***19**, 1718–1723 (2009).
161. Marson, A. *et al.* Wnt Signaling Promotes Reprogramming of Somatic Cells to Pluripotency. *Cell Stem Cell***3**, 132–135 (2008).
162. Cole, M. F., Johnstone, S. E., Newman, J. J., Kagey, M. H. & Young, R. A. Tcf3 is an integral component of the core regulatory circuitry of embryonic stem cells. *Genes Dev***22**, 746–755 (2008).
163. Tam, W.-L. *et al.* T-cell factor 3 regulates embryonic stem cell pluripotency and self-renewal by the transcriptional control of multiple lineage pathways. *Stem Cells***26**, 2019–2031 (2008).
164. Yi, F., Pereira, L. & Merrill, B. J. Tcf3 functions as a steady-state limiter of transcriptional programs of mouse embryonic stem cell self-renewal. *Stem Cells***26**, 1951–1960 (2008).
165. Lane, D. & Levine, A. p53 Research: the past thirty years and the next thirty years. *Cold Spring Harb Perspect Biol***2**, a000893 (2010).
166. Armstrong, J. F., Kaufman, M. H., Harrison, D. J. & Clarke, A. R. High-frequency developmental abnormalities in p53-deficient mice. *Curr. Biol.***5**, 931–936 (1995).
167. He, Z., Li, J., Zhen, C., Feng, L. & Ding, X. Knockdown of p53 by RNAi in ES cells facilitates RA-induced differentiation into muscle cells. *Biochem. Biophys. Res. Commun.***335**, 676–683 (2005).
168. Lee, K.-H. *et al.* A genomewide study identifies the Wnt signaling pathway as a major target of p53 in murine embryonic stem cells. *Proc. Natl. Acad. Sci. U.S.A.***107**, 69–74 (2010).
169. Lin, T. *et al.* p53 induces differentiation of mouse embryonic stem cells by suppressing Nanog expression. *Nat. Cell Biol.***7**, 165–171 (2005).
170. Vogelstein, B., Lane, D. & Levine, A. J. Surfing the p53 network. *Nature***408**, 307–310 (2000).
171. Jin, S. & Levine, A. J. The p53 functional circuit. *J. Cell. Sci.***114**, 4139–4140 (2001).
172. Lane, D. P. Cancer. p53, guardian of the genome. *Nature***358**, 15–16 (1992).
173. Rowland, B. D., Bernards, R. & Peeper, D. S. The KLF4 tumour suppressor is a transcriptional repressor of p53 that acts as a context-dependent oncogene. *Nat. Cell Biol.***7**, 1074–1082 (2005).
174. Zhao, Y. *et al.* Two supporting factors greatly improve the efficiency of human iPSC generation. *Cell Stem Cell***3**, 475–479 (2008).
175. Hong, H. *et al.* Suppression of induced pluripotent stem cell generation by the p53–p21 pathway. *Nature***460**, 1132–1135 (2009).
176. Kawamura, T. *et al.* Linking the p53 tumour suppressor pathway to somatic cell reprogramming. *Nature***460**, 1140–1144 (2009).
177. Marión, R. M. *et al.* A p53-mediated DNA damage response limits reprogramming to ensure iPS cell genomic integrity. *Nature***460**, 1149–1153 (2009).

178. Utikal, J. *et al.* Immortalization eliminates a roadblock during cellular reprogramming into iPS cells. *Nature***460**, 1145–1148 (2009).
179. Krizhanovsky, V. & Lowe, S. W. Stem cells: The promises and perils of p53. *Nature***460**, 1085–1086 (2009).
180. Davis, R. L., Weintraub, H. & Lassar, A. B. Expression of a single transfected cDNA converts fibroblasts to myoblasts. *Cell***51**, 987–1000 (1987).
181. Xie, H., Ye, M., Feng, R. & Graf, T. Stepwise Reprogramming of B Cells into Macrophages. *Cell***117**, 663–676 (2004).
182. Cobaleda, C., Jochum, W. & Busslinger, M. Conversion of mature B cells into T cells by dedifferentiation to uncommitted progenitors. *Nature***449**, 473–477 (2007).
183. Yechoor, V. *et al.* Neurogenin3 is Sufficient for in vivo Transdetermination of Hepatic Progenitor Cells into Islet-like cells but not Transdifferentiation of Hepatocytes. *Dev Cell***16**, 358–373 (2009).
184. Zhou, Q., Brown, J., Kanarek, A., Rajagopal, J. & Melton, D. A. In vivo reprogramming of adult pancreatic exocrine cells to beta-cells. *Nature***455**, 627–632 (2008).
185. Vierbuchen, T. *et al.* Direct conversion of fibroblasts to functional neurons by defined factors. *Nature***463**, 1035–1041 (2010).
186. Ambasudhan, R. *et al.* Direct reprogramming of adult human fibroblasts to functional neurons under defined conditions. *Cell Stem Cell***9**, 113–118 (2011).
187. Pang, Z. P. *et al.* Induction of human neuronal cells by defined transcription factors. *Nature***476**, 220–223 (2011).
188. Pfisterer, U. *et al.* Direct conversion of human fibroblasts to dopaminergic neurons. *Proc Natl Acad Sci U S A***108**, 10343–10348 (2011).
189. Son, E. Y. *et al.* Conversion of mouse and human fibroblasts into functional spinal motor neurons. *Cell Stem Cell***9**, 205–218 (2011).
190. Yoo, A. S. *et al.* MicroRNA-mediated conversion of human fibroblasts to neurons. *Nature***476**, 228–231 (2011).
191. Caiazzo, M. *et al.* Direct generation of functional dopaminergic neurons from mouse and human fibroblasts. *Nature***476**, 224–227 (2011).
192. Marchetto, M. C. N. *et al.* A model for neural development and treatment of Rett syndrome using human induced pluripotent stem cells. *Cell***143**, 527–539 (2010).
193. Zhou, Q. & Tripathi, P. How to Remake a Fibroblast into a Neural Stem Cell. *Cell Stem Cell***10**, 347–348 (2012).
194. Thier, M. *et al.* Direct Conversion of Fibroblasts into Stably Expandable Neural Stem Cells. *Cell Stem Cell***10**, 473–479 (2012).
195. Han, D. W. *et al.* Direct reprogramming of fibroblasts into neural stem cells by defined factors. *Cell Stem Cell***10**, 465–472 (2012).
196. Kim, J. B. *et al.* Pluripotent stem cells induced from adult neural stem cells by reprogramming with two factors. *Nature***454**, 646–650 (2008).
197. Lujan, E., Chanda, S., Ahlenius, H., Südhof, T. C. & Wernig, M. Direct conversion of mouse fibroblasts to self-renewing, tripotent neural precursor cells. *Proc. Natl. Acad. Sci. U.S.A.***109**, 2527–2532 (2012).
198. Aubert, J. *et al.* Screening for mammalian neural genes via fluorescence-activated cell sorter purification of neural precursors from Sox1-gfp knock-in mice. *Proc. Natl. Acad. Sci. U.S.A.***100 Suppl 1**, 11836–11841 (2003).
199. Donehower, L. A. *et al.* Mice deficient for p53 are developmentally normal but susceptible to spontaneous tumours. *Nature***356**, 215–221 (1992).
200. Krizhanovsky, V. & Lowe, S. W. Stem cells: The promises and perils of p53. *Nature***460**, 1085–1086 (2009).

201. Puzio-Kuter, A. M. & Levine, A. J. Stem cell biology meets p53. *Nat. Biotechnol.***27**, 914–915 (2009).
202. Ellis, L., Atadja, P. W. & Johnstone, R. W. Epigenetics in cancer: targeting chromatin modifications. *Mol. Cancer Ther.***8**, 1409–1420 (2009).
203. Lee, M. G., Wynder, C., Schmidt, D. M., McCafferty, D. G. & Shiekhattar, R. Histone H3 lysine 4 demethylation is a target of nonselective antidepressive medications. *Chem. Biol.***13**, 563–567 (2006).
204. Bell, E., Ensini, M., Gulisano, M. & Lumsden, A. Dynamic domains of gene expression in the early avian forebrain. *Dev. Biol.***236**, 76–88 (2001).
205. Uchikawa, M. *et al.* B1 and B2 Sox gene expression during neural plate development in chicken and mouse embryos: universal versus species-dependent features. *Dev. Growth Differ.***53**, 761–771 (2011).
206. Tanaka, S. *et al.* Interplay of SOX and POU factors in regulation of the Nestin gene in neural primordial cells. *Mol. Cell. Biol.***24**, 8834–8846 (2004).
207. Catena, R. *et al.* Conserved POU binding DNA sites in the Sox2 upstream enhancer regulate gene expression in embryonic and neural stem cells. *J. Biol. Chem.***279**, 41846–41857 (2004).
208. Iwafuchi-Doi, M. *et al.* The Pou5f1/Pou3f-dependent but SoxB-independent regulation of conserved enhancer N2 initiates Sox2 expression during epiblast to neural plate stages in vertebrates. *Dev. Biol.***352**, 354–366 (2011).
209. Taipale, M., Jarosz, D. F. & Lindquist, S. HSP90 at the hub of protein homeostasis: emerging mechanistic insights. *Nat. Rev. Mol. Cell Biol.***11**, 515–528 (2010).
210. Ruden, D. M. The (new) new synthesis and epigenetic capacitors of morphological evolution. *Nat. Genet.***43**, 88–89 (2011).
211. Lang, S. A. *et al.* Inhibition of heat shock protein 90 impairs epidermal growth factor-mediated signaling in gastric cancer cells and reduces tumor growth and vascularization in vivo. *Mol. Cancer Ther.***6**, 1123–1132 (2007).
212. Rao, R. *et al.* HDAC6 inhibition enhances 17-AAG--mediated abrogation of hsp90 chaperone function in human leukemia cells. *Blood***112**, 1886–1893 (2008).
213. Tucker, K. L., Meyer, M. & Barde, Y. A. Neurotrophins are required for nerve growth during development. *Nat. Neurosci.***4**, 29–37 (2001).
214. Gangemi, R. M. *et al.* Emx2 in adult neural precursor cells. *Mech. Dev.***109**, 323–329 (2001).
215. Galli, R. *et al.* Emx2 regulates the proliferation of stem cells of the adult mammalian central nervous system. *Development***129**, 1633–1644 (2002).
216. Brancaccio, M., Pivetta, C., Granzotto, M., Filippis, C. & Mallamaci, A. Emx2 and Foxg1 inhibit gliogenesis and promote neuronogenesis. *Stem Cells***28**, 1206–1218 (2010).
217. Subramanian, L. *et al.* Transcription factor Lhx2 is necessary and sufficient to suppress astrogliogenesis and promote neurogenesis in the developing hippocampus. *Proc. Natl. Acad. Sci. U.S.A.***108**, E265–274 (2011).
218. Ladewig, J. *et al.* Small molecules enable highly efficient neuronal conversion of human fibroblasts. *Nature Methods* (2012).doi:10.1038/nmeth.1972
219. Esteban, M. A. *et al.* Vitamin C enhances the generation of mouse and human induced pluripotent stem cells. *Cell Stem Cell***6**, 71–79 (2010).
220. Hanashima, C., Fernandes, M., Hebert, J. M. & Fishell, G. The role of Foxg1 and dorsal midline signaling in the generation of Cajal-Retzius subtypes. *J. Neurosci.***27**, 11103–11111 (2007).
221. Muzio, L. *et al.* Emx2 and Pax6 control regionalization of the pre-neuronogenic cortical primordium. *Cereb. Cortex***12**, 129–139 (2002).
222. Muzio, L. *et al.* Conversion of cerebral cortex into basal ganglia in Emx2(-/-) Pax6(Sey/Sey) double-mutant mice. *Nat Neurosci***5**, 737–45 (2002).

223. Cartier, L. *et al.* Pax6-induced alteration of cell fate: shape changes, expression of neuronal alpha tubulin, postmitotic phenotype, and cell migration. *J. Neurobiol.***66**, 421–436 (2006).
224. Sansom, S. N. *et al.* The level of the transcription factor Pax6 is essential for controlling the balance between neural stem cell self-renewal and neurogenesis. *PLoS Genet***5**, e1000511 (2009).
225. Miyoshi, G. & Fishell, G. Dynamic FoxG1 expression coordinates the integration of multipolar pyramidal neuron precursors into the cortical plate. *Neuron***74**, 1045–1058 (2012).
226. Mangale, V. S. *et al.* Lhx2 Selector Activity Specifies Cortical Identity and Suppresses Hippocampal Organizer Fate. *Science***319**, 304–309 (2008).
227. Pröls, F. *et al.* The role of Emx2 during scapula formation. *Developmental Biology***275**, 315–324 (2004).
228. Miyamoto, N., Yoshida, M., Kuratani, S., Matsuo, I. & Aizawa, S. Defects of urogenital development in mice lacking Emx2. *Development***124**, 1653–64 (1997).
229. Pellegrini, M., Pantano, S., Lucchini, F., Fumi, M. & Forabosco, A. Emx2 developmental expression in the primordia of the reproductive and excretory systems. *Anat. Embryol***196**, 427–433 (1997).
230. Kitajima, K., Minehata, K., Sakimura, K., Nakano, T. & Hara, T. In vitro generation of HSC-like cells from murine ESCs/iPSCs by enforced expression of LIM-homeobox transcription factor Lhx2. *Blood***117**, 3748–3758 (2011).
231. Mariani, J. *et al.* Emx2 is a dose-dependent negative regulator of Sox2 telencephalic enhancers. *Nucleic Acids Res.***40**, 6461–6476 (2012).
232. Lanzuolo, C. & Orlando, V. Memories from the Polycomb Group Proteins. *Annu. Rev. Genet.* (2012).doi:10.1146/annurev-genet-110711-155603
233. Huangfu, D. *et al.* Induction of pluripotent stem cells by defined factors is greatly improved by small-molecule compounds. *Nat. Biotechnol.***26**, 795–797 (2008).
234. Hsieh, J., Nakashima, K., Kuwabara, T., Mejia, E. & Gage, F. H. Histone deacetylase inhibition-mediated neuronal differentiation of multipotent adult neural progenitor cells. *Proc. Natl. Acad. Sci. U.S.A.***101**, 16659–16664 (2004).
235. Mali, P. *et al.* Butyrate Greatly Enhances Derivation of Human Induced Pluripotent Stem Cells by Promoting Epigenetic Remodeling and the Expression of Pluripotency-Associated Genes. *STEM CELLS***28**, 713–720 (2010).
236. Li, H. *et al.* The Ink4/Arf locus is a barrier for iPS cell reprogramming. *Nature***460**, 1136–1139 (2009).
237. Banerjee-Basu, S. & Baxevanis, A. D. Molecular modeling of mutations in the DNA-binding domain of the oncoprotein Qin. *Mol. Cancer Ther.***1**, 1237–1241 (2002).
238. Gadue, P., Huber, T. L., Paddison, P. J. & Keller, G. M. Wnt and TGF-beta signaling are required for the induction of an in vitro model of primitive streak formation using embryonic stem cells. *Proc. Natl. Acad. Sci. U.S.A.***103**, 16806–16811 (2006).
239. Sumi, T., Tsuneyoshi, N., Nakatsuji, N. & Suemori, H. Defining early lineage specification of human embryonic stem cells by the orchestrated balance of canonical Wnt/beta-catenin, Activin/Nodal and BMP signaling. *Development***135**, 2969–2979 (2008).
240. Baker, J. C., Beddington, R. S. & Harland, R. M. Wnt signaling in Xenopus embryos inhibits bmp4 expression and activates neural development. *Genes Dev.***13**, 3149–3159 (1999).
241. Sasal, Y., Lu, B., Steinbelsser, H. & De Robertis, E. M. Regulation of neural induction by the Chd and Bmp-4 antagonistic patterning signals in Xenopus. *Nature***378**, 419 (1995).
242. Young, C. S., Kitamura, M., Hardy, S. & Kitajewski, J. Wnt-1 induces growth, cytosolic beta-catenin, and Tcf/Lef transcriptional activation in Rat-1 fibroblasts. *Mol. Cell. Biol.***18**, 2474–2485 (1998).

243. Galli, L. M. *et al.* Differential inhibition of Wnt-3a by Sfrp-1, Sfrp-2, and Sfrp-3. *Developmental Dynamics***235**, 681–690 (2006).
244. Cloos, P. A. C., Christensen, J., Agger, K. & Helin, K. Erasing the methyl mark: histone demethylases at the center of cellular differentiation and disease. *Genes Dev.***22**, 1115–1140 (2008).
245. Aranha, M. M., Solá, S., Low, W. C., Steer, C. J. & Rodrigues, C. M. P. Caspases and p53 modulate FOXO3A/Id1 signaling during mouse neural stem cell differentiation. *J. Cell. Biochem.***107**, 748–758 (2009).
246. Di Giovanni, S. *et al.* The tumor suppressor protein p53 is required for neurite outgrowth and axon regeneration. *EMBO J.***25**, 4084–4096 (2006).
247. Tedeschi, A., Nguyen, T., Puttagunta, R., Gaub, P. & Di Giovanni, S. A p53-CBP/p300 transcription module is required for GAP-43 expression, axon outgrowth, and regeneration. *Cell Death Differ.***16**, 543–554 (2009).
248. Tucker, K. L., Meyer, M. & Barde, Y.-A. Neurotrophins are required for nerve growth during development. *Nature Neuroscience***4**, 29–37 (2001).
249. Spigoni, G., Gedressi, C. & Mallamaci, A. Regulation of Emx2 expression by antisense transcripts in murine cortico-cerebral precursors. *PLoS ONE***5**, e8658 (2010).
250. Brambrink, T. *et al.* Sequential expression of pluripotency markers during direct reprogramming of mouse somatic cells. *Cell Stem Cell***2**, 151–159 (2008).
251. Sastry, L., Johnson, T., Hobson, M. J., Smucker, B. & Cornetta, K. Titering lentiviral vectors: comparison of DNA, RNA and marker expression methods. *Gene Ther***9**, 1155–62 (2002).
252. Wolff, G. Entwicklungsphysiologische Studien. I. Die Regeneration der. Urodelenlinse. *Wilhelm Roux' Arch. Entwickl-Mech. Org.* **1**, 380–390 (1895).